UNIVERSITY OF SOUTHAMPTON

FACULTY OF ENGINEERING AND APPLIED SCIENCE

Submitted for the degree of Doctor of Philosophy

STUDIES BY EXPERIMENTAL SIMULATION OF ROLLOVER AND SURFACE VAPORISATION OF CRYOGENS

by Martin Charles Morton Atkinson-Barr

Institute of Cryogenics
Southampton
England
June 1989

Table of Contents

UNIVERSITY OF SOUTHAMPTON

ABSTRACT

FACULTY OF ENGINEERING

INSTITUTE OF CRYOGENICS

Doctor of Philosophy

STUDIES BY EXPERIMENTAL SIMULATION OF ROLLOVER AND SURFACE VAPORISATION OF CRYOGENS

by
Martin C M Atkinson-Barr

Investigations have been carried out on stratified and unstratified cryogens, on a laboratory scale, to relate the rate of vapour generation to the liquid behaviour. Experimental simulations of rollover using liquid nitrogen and liquid argon were used to elucidate the process of enhanced vapour generation (EVG) in commercial liquid natural gas tanks.

Temperature profiles in cryogens near the liquid vapour interface reveal a sublayer with a high temperature gradient in which thermal conduction is dominant and convection processes are intermittent. Measurements of the bulk superheat of the cryogens are correlated to the rate of vapour generation and values are given for LIN, LAr, LOX, LCH_4 and LNG.

A schlieren technique has been developed for the observation of temperature gradients in cryogens. Observations have been made on the surface layer and on the interfacial region between compositionally stably stratified cryogens destabilised by heating from below.

Microthermocouple arrays have been used to obtain temperature profiles during the mixing process in stratified cryogenic systems heated from below.

A new technique has been found and developed that allows cryogenic flows to be visualised with minimal experimental complexity.

On the basis of these observations a new mechanism is suggested for EVG events in large vessels and recommendations are made on the handling of stratified LNG and the design of cryogenic storage tanks.

NOMENCLATURE

Boldface indicates vector notation.

a	Radius of tank m
A	Cross-sectional area of tank m^2
b	Plume diameter m
c_i	Constant
C_p	Specific heat $J\,Kg^{-1}\,K^{-1}$
D_{ij}	Mass diffusivity of solute i through fluid j $m^2\,s^{-1}$
D_m	Mass diffusivity $m^2\,s^{-1}$
f	Focal length of lens m
F_S	Transfer of solute through interface $kg\ m^{-2}hr^{-1}$
F_T	Transfer of heat through interface $m\,K\ hr^{-1}$
g	Acceleration due to gravity $m\,s^{-2}$
g'	Reduced gravitational acceleration $g\rho'/\rho\ m^2 s^{-1}$
Gr	Grashof number $\left(\beta_T \Delta T h^3 g\right)/\nu^2$
h_i	Layer depth m
hT	Heat transfer coefficient $J\,m^{-2}\,s^{-1}\,K^{-1}$
H_i	Enthalpy of component i $J\,kgmol^{-1}$
Ho_i	Enthalpy at saturation for component i $J\,kgmol^{-1}$
I	Light intensity
K_T	Thermal conductivity $W\,m^{-1}\,K^{-1}$
l	Length m
l_e	Eddy length m
L	Latent heat of vapourisation $J\,Kg^{-1}$
LAr	Liquid Argon
LIN	Liquid Nitrogen
LNG	Liquid Natural Gas

LOX	Liquid Oxygen
Le	Lewis number $K_T/(\rho C_p D_{ij})$
$\dot{m}$	Mass flux $Kg\ m^{-2} s^{-1}$
n	Unit vector normal to a surface
n	Refractive index
N	Nusselt number $(Q h)/(K_T \Delta T)$
p	Pressure $N m^{-2}$
Pr	Prandtl number ν/α
Q	Heat flux $W m^{-2}$
r	Cylindrical polar coordinate
r_{curv}	Radius of curvature m
R	Reynolds number ul/ν
Rc	Critical Reynolds number
Ra	Rayleigh number $(g \beta_T \Delta T h^3)/(\alpha\nu)$
Ri	Gradient Richardson number $-g(\partial\rho/\partial z)/(\rho(\partial u/\partial z)^2)$
Ri_o	Overall Richardson number $g' l/u^2$
Rs	Solutal Rayleigh number $(g \beta_s \Delta S h^3)/(\alpha\nu)$
$R\rho$	Stability ratio $(\beta_s \Delta S/\beta_T \Delta T)$
ΔS	Concentration difference $kg\ m^{-3}$
t	time s
T	Temperature K
T_b	Bulk liquid temperature K
T_{sat}	Saturation temperature K
ΔT	Temperature difference K
TO	Thermal overfill $J\ kgmol^{-1}$
u	Velocity of flow $m\ s^{-1}$
$\mathbf{u}_e$	Entrainment velocity $m\ s^{-1}$
U_S	Solute transfer velocity $m\ hr^{-1}$
U_T	Heat transfer velocity $m\ hr^{-1}$
z	Vertical coordinate
α	Thermal diffusivity ($\alpha = K_T/\rho Cp$) $m^2 s^{-1}$

β_T	Thermal expansion coefficient K^{-1}
β_s	Solutal expansion coefficient $m^3 kg^{-1}$
δ	The depth of a thin layer m
ε	Angular deflection
η	Dynamic viscosity $kg\, m^{-1} s^{-1}$
ξ	Vorticity
φ	Velocity potential
ψ	Stream function
ρ	Density $Kg\, m^{-3}$
σ_{ii}	Stress tensor $kg\ m^{-1} s^{-2}$
σ	Surface tension (N/m)
τ	Diffusivity ratio $\left(D_m/\alpha\right)$
θ	Angular coordinate
υ	Light absorbtion coefficient
ν	Kinematic viscosity $\left(\nu = \eta/\rho\right)$ $m^2 s^{-1}$
ζ	Height of displaced surface m

1. INTRODUCTION

Storage at Equilibrium Under Commercial Conditions

Commercial volumes of natural gas are stored most conveniently in a liquefied, unpressurised state near 112 K in insulated tanks. In the case of LNG tanks connected to supply lines the boiloff gas due to heat inleak can be directed to the user however in peak-shaving plants and storage tanks the boiloff is reliquefied and reenters the vessel. Minimising the heat inleak to reduce operating costs is a major goal of tank designers. Pressure relief valves are built into the dome of the tank to safeguard against overpressurisation but at a cost of increased heat inleak and therefore the number and size of the relief valves is kept to a minimum consistent with the anticipated maximum flow. Venting natural gas to the atmosphere is in itself a hazardous procedure especially near populated areas and the capacity of a reliquefaction cycle is balanced to the tank design such that normal variations in boiloff can be accommodated. An overlarge reliquefaction compressor will reduce the pressure in the tank and increase the operating costs[5] as well as the capital cost.

In an LNG tank under equilibrium conditions there is a constant boiloff caused by heat inleak into the tank.The insulation in the flat bottom of the tank must provide the required structural strength; this leads to a high basal heat flux. In all LNG storage tanks of industrial size the base heat flow dominates the total heat inleak. Filled to an operational maximum level half of the total heat flow is through the floor of the tank. The total heat inleak causes vapourisation of ~0.05% of the full tank contents per day.

Since LNG is a mixture the boiloff gas has a different composition from the liquid in the tank and over a period of time the composition of the tank liquid changes. This process is called weathering, a term which is also used to describe any change of composition over time including the condensation of less volatile components from the vapour phase above the liquid.

In the normal LNG tank under equilibrium conditions there is sufficient sidewall heat flux to sustain boundary layer convective flow. The boundary layer liquid is warmed only marginally and there is no boiling. This liquid rises to the surface where it flashes, cools and sinks to the bulk. The convective flow so generated is sufficient to maintain a uniformity of temperature, density and composition throughout the vessel[52].

Enhanced Vapour Generation

Stable density stratification of LNG in a storage tank has been observed when a new load of differing density is added to an existing heel. Enhanced vapour generation (EVG)

following the stratification has been ascribed to migration of the superheated lower layer to the surface [1] or the subsequent mixing of the layers [2,4]. Rollover is the term which has been used to describe this phenomenon but this may be misleading as it suggests a mechanism of the lower layer displacing the upper layer at the surface rather than a mixing process. However common usage of the term rollover forces its use here in the sense of the events of mixing in the tank and subsequent EVG. EVG leading to the operation of the relief valves are not well documented but operators report regular episodes of EVG from tanks and occurrences of anomalous losses of tank contents. On the basis of considerable experience tank operators generally reject the notion that EVG is associated with boiling in the tank.

Tank designers and operators need to know the initial conditions leading to EVG, the maximum vapour generation that could occur and how to identify a potentially dangerous situation. Ultimately they require a course of actions that can avoid EVG even after the development of an unstable configuration of tank contents .

Many of the earlier studies on rollover used data obtained with ambient temperature liquids in experiments that sought to gain an understanding of basic fluid mechanics of the liquid-liquid interface rather then the rollover process itself. The success of the rollover models have been mixed and given the paucity of rollover data this does not inspire confidence in the projections.

This is the record of a study of the behaviour of cryogenic liquids under simulated storage conditions both in stable and unstable configurations. The experimental simulations were done on a small scale under laboratory conditions. We sought to gain an understanding of the behaviour of cryogens within tanks to guide and clarify the simplifying assumptions that can lead to more general rules and predict tank behaviour. Progress in using the framework of fluid mechanics for clarification and prediction can only come from observations such as this since theory cannot describe the simplest of fluid flows.

For laboratory safety reasons the simulations of EVG from stratified tanks used LIN and LIN/LAr layers rather than LNG. Experiments on unstratified liquids, where there are lower limits of boiloff gas generation, also used LOX and LNG.

The stratified contents of a tank were analysed as these connected systems:

- The free surface or liquid-vapour interface.
- One or more liquid-liquid interfaces separating bulk layers of differing composition and temperature.
- Bulk liquid layers.
- A boundary layer flow at the tank wall.

The experiments were designed to observe the above systems and how they are interconnected. Some elements of the real tank, such as the relationship of the boundary layer to the heated wall and the behaviour of the bulk adjacent to the tank floor, are not included since earlier investigators have studied ambient fluids and their results have been usefully applied to cryogenic liquids in the design of heat exchangers. This does not mean that there is no need for further work, in fact quite the opposite as better heat exchanger design offers significant savings in operating costs to the cryogenic industry. It does mean that the degree of understanding of the liquid-vapour and liquid-liquid interfaces is much inferior to the knowledge of cryogenic boundary layers.

The Liquid-Vapour and Liquid-Liquid Interfaces

It will be shown in the next chapter that earlier considerations of rollover have focussed on the liquid-liquid interface as the key element in EVG from stratified systems. In this work it will be shown that a better approach to a solution comes from an examination of the connections between the elements. In chapters 7 and 8 an experimental observation leads directly to a great simplification in the analysis of the connection of the bulk liquid and the liquid-vapour interface. The connection is by way of a thin, predominately conducting sublayer. Assuming conductive heat transfer across the sublayer gives a correlation of the rate of boiloff gas generation to the bulk temperature which has been verified for a number of cryogens.

It should be noted that laboratory sized dewars do demonstrate an uneven boiloff pattern with frequent puffs of vapour interspersed with longer periods of inactivity and vapour explosions have been observed, presumably associated with boiling in the vessel. These instabilities in vapour generation may arise from:

- Failure to maintain a steady convective pattern within the liquid such that the liquid contents are not well mixed and a higher level of superheat is attained in the bulk. The convective flow then initiates, bringing hot bulk near the surface and puffs of vapour are generated.

- Either a thermal or compositional stratification develops in the bulk liquid leading to convective cells that eventually mix. In the case of moderately large compositional density differences, nucleate boiling can take place without mixing.

- An external event provides sufficient energy for homogeneous nucleate boiling to occur at superheat temperatures well below the ~ 40K temperature excess over saturation normally required. The external event may be a sound wave, a cosmic ray or some other energetic input to the bulk. It has been speculated that this can lead to homogeneous boiling and vapour explosions at temperatures near the

normal bulk superheat, that is 3-4K above saturation temperature. This hypothesis has been termed 'quasi homogeneous nucleate boiling'[1].

- Impurities from the environment will condense onto the surface of the cryogen, diffuse into and stabilise the thin surface sublayer against convection, and establish a greater bulk superheat. This hypothesis is made the more tenable by the discovery of the high solubility of water and carbon dioxide in cryogens[19]. It is also noted that filled dewars that have been allowed to remain undisturbed are particularly subject to more severe vapour generation instabilities.

- In a similar way to the last hypothesis the impurity may not diffuse into the cryogen but may remain on the surface effectively inhibiting evaporation until bulk processes are sufficiently energetic to disrupt the impurity layer.

In contrast to LNG tanks the laboratory sized dewars have conduction down the inner neck of the vessel as the major heat inleak and are often spherical. This may quantitatively change the scale of EVG however the hypothesised mechanisms remain the same.

Chapters 4 and 5 discuss the liquid-vapour and liquid-liquid interfaces respectively and in chapter 7 it can be seen that other, earlier experimental results can now be explained in a straightforward way by direct observation of the effect of the boundary layer on the liquid-liquid interface. It is also apparent from this study why the models of rollover succeed in predicting the time history up to the onset of EVG as a result of the mixing of stratified layers but fail to describe the development of EVG after this point which is the prediction of prime interest to the gas industry. From these results it is now clear that progress in modelling rollover induced EVG will come from an understanding of the behaviour of the liquid-vapour interface as it is perturbed from its equilibrium state rather than a change in perception of the dynamics of the liquid-liquid boundary.

1 Private communication from Professor R. Scurlock

2. REVIEW OF ROLLOVER

ROLLOVER EVENTS

Apart from the La Spezia event quoted, there are two other examples of rollover in full size LNG tanks cited in the open literature. They are less well documented than the La Spezia incident and therefore less useful in assessing the performance of rollover models. A very brief summary is given here.

Boiloff tests were being carried out at the Fos-Sur-Mer LNG terminal in 1978 when the evaporation rate suddenly increased to 12000m^3/hr, 20 times the normal rate[10]. The 36m diameter tank contained 26000m^3 of LNG and, from the boiloff-time plot of this event, the total boiloff loss was 160000 m^3 of vapour, equivalent to 500m^3 of LNG or 2% of the tank contents.

Chatterjee & Geist[8] quote the second of the two events. A peak-shaving plant exhibited a rollover 40 days after the end of the liquefaction season. A high nitrogen bearing LNG cargo was bottom filled into a heel with a density some 10 kg/m^3 lighter due to preferential loss of nitrogen by weathering. The 42m diameter tank contained 44000m^3 of LNG and lost 1% during the 24hrs of the rollover compared to a normal evaporation of 0.06% per day.

Analysis of the mechanisms of rollover in LNG storage vessels has been based upon the behaviour of multi-component liquid systems at ambient temperatures and in particular on saline/water stratification. Some observations of rollover have been carried out with freons on the laboratory scale [7] and one actual LNG tank test has been reported [7]. In reviewing the published work on LNG rollover it is appropriate first to examine the models of LNG rollover and then proceed to discuss the more general findings which have formed the foundation for predictions of stratified LNG behaviour.

The La Spezia Rollover

There are few documented cases of rollover. The most often quoted event is the La Spezia case which was reported by Sarsten[3] and subsequently revised[1]. This event and the figures provided by Sarsten have formed the basis for much of the analysis of rollover models published in the intervening years. Accordingly the events and data are reproduced here for reference and to define the scope of the application of further research.

	RESIDUAL HEEL		SHIP CARGO	
	SARSTEN	REVISED	SARSTEN	REVISED
Tank vapour space pressure N/m^2 gauge	2452	3433	10971	9810
Bulk liquid vapour pressure N/m^2 gauge	3924	4905	16284	15303
Equilibrium temperature K	114.9	117.1	118.9	119.2
Density at equilibrium temperature Kg/m^3	536.6	532.3	541.1	541.6
Amount of LNG m^3	9600	9600	33500	35000

Table 1 LNG Parameters at La Spezia

	RESIDUAL HEEL		SHIP CARGO	
	SARSTEN	REVISED	SARSTEN	REVISED
N_2	0.35	-	0.02	0.02
CH_4	63.62	64.10	62.26	62.03
C_2H_6	24.16	24.32	21.85	21.99
C_3H_8	9.36	9.29	12.66	12.78
C_4H_{10}	2.35	2.16	3.14	3.12
C_5H_{12}	0.16	0.13	0.07	0.06
Total	100.00	100.00	100.00	100.00

Table 2 Composition of LNG at La Spezia

1 Private communication from Sarsten to British Gas.

TANK DIAMETER	49.1	m
TANK HEIGHT	26.8	m
HEAT FLUX BASE	20.82	W/m^2
HEAT FLUX SIDEWALL	6.94	W/m2
INITIAL HEEL DEPTH	5.0	m
CARGO DEPTH	17.8	m

Table 3 The Tank at La Spezia

EVENT	DURATION(hrs)	BOILOFF(00kgs)	MEAN RATE (00kgs/hr)
Normal	-	-	4.5
During Filling	11	567	49.9
Before Rollover	18	159	9.1
Rollover	1.25	1361	1185
After Valve Closure	2	499	250

Table 4 Record of Vapour Generation at La Spezia

At the time of the incident the 49m diameter, 26.8m high tank at La Spezia, Italy contained a light heel of LNG. The tanker Esso Brega had been in the harbour for more than one month during which time the cargo had weathered becoming denser than the tank heel.

The tank was bottom filled with the cargo and the less dense heel did not mix but was displaced upwards leaving the denser cargo on the bottom of the tank. According to the published report it was presumed that there was little mixing of the cargo and heel.

The transfer continued for 13hrs and during this period 125,000lb of vapour was generated. Of this total vapour 100,000lb is accounted for by the displacement volume of the liquid. The remaining is presumed to have originated from the partial mixing of heel and cargo and from some flashing of the cargo as it reached tank pressure.

If the transfer had resulted in total mixing it would be expected that a total of 600,000lb of vapour would be generated. That is 100,000lb of displaced volume and 500,000lb of vapour generated as the cargo flashed to tank pressure.

The normal boiloff for this tank would have been 1000lbs/hr. After the filling period had finished the tank performed apparently normally for 18hrs with a mean boiloff of 2000lbs/hr. Note that there was no depression of normal boiloff probably because the tank was returning to an equilibrium state.

The rollover event then occurred. In a period of 75mins 300,000lbs of vapour was vented from the tank itself and a further 30,000lbs was vented from a connected tank over a 15min period. At the end of the rollover the emergency valves closed. In a subsequent 2hr period a further 110,000lbs of vapour was generated before the tank returned to equilibrium pressure

It is of particular interest that the tank operators reported 'sloshing' noises from the tank during the rollover event. We must presume that these noises indicated large scale fluid motion.

MODELS OF LNG ROLLOVER

In any mathematical model of LNG rollover the most important parameters to predict are the time from stratification to rollover, the quantity of vapour generated and the rate of boiloff. Of course, from the point of view of tank design and safety, a good prediction of peak boiloff is required. Fig 48 shows a typical LNG storage tank and fig 1 demonstrates the conceptual model adopted by most of the authors of rollover models.

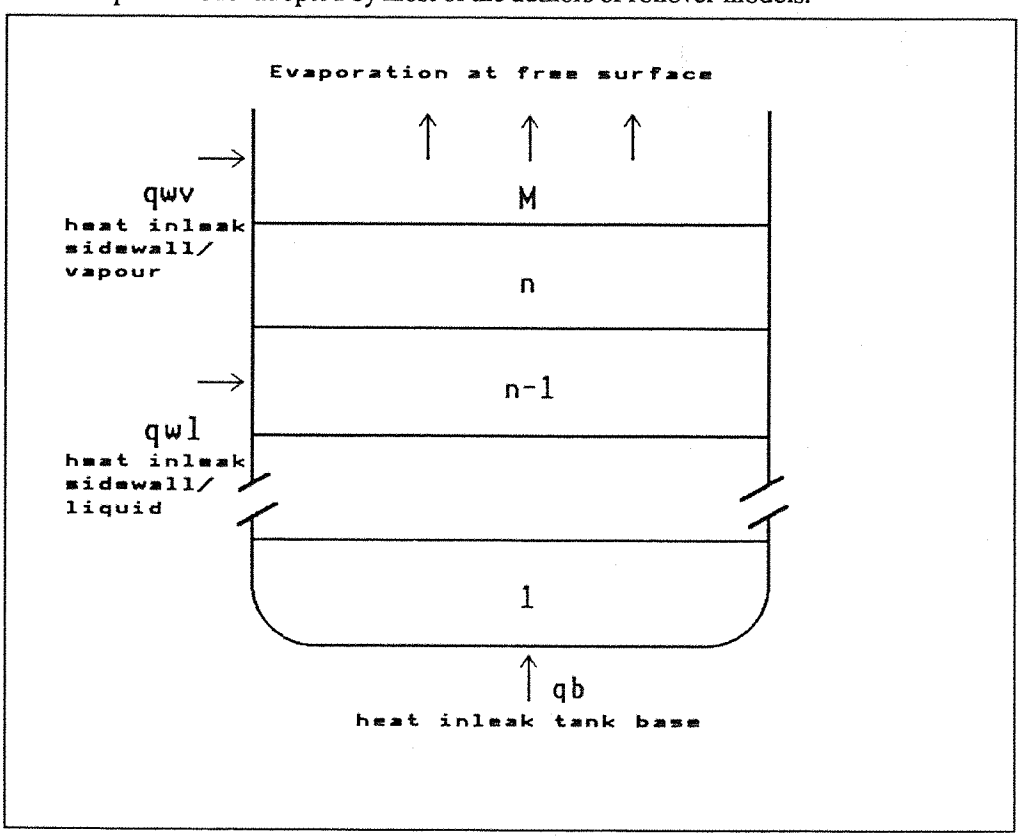

Fig.1 The conceptual model of an LNG tank

Maher & Van Gelder (1972)

In this discussion of the thermodynamics of stored cryogens[50] much of the data from rollover events was not available to the authors. The authors point out that the term rollover is probably quite inappropriate in the context of LNG storage since the convection currents will produce agitation of the tank contents and hence mixing. They support this view with the observation that the heating value of LNG removed from well-weathered tanks is constant as the tank is pumped out, indicating a uniformity in the tank contents.

Instead of a mechanism whereby a large mass of superheated liquid is transported to the surface of the liquid[1] it is suggested that the enhanced vapour generation is a result of superheated bulk liquid with a surface layer which is cooler than the bulk and in equilibrium with vapour. An hypothesis is put forward that if the surface layer is destroyed by agitation, the rate of vapour generation will increase in proportion to the degree of superheat of the bulk liquid.

To support this view some calculations are presented that show that if an 2.7m thick superheated layer were flashed by a true rollover phenomenon the total vapour generated would be 363,000 kg. Assuming a time scale of two minutes this gives a peak vapour generation rate of the order of 10 million kg/hr. If a new surface layer forms before all the superheat is released then the peak vapour rate would be less than this theoretical maximum. The authors then reject the view of events as a disturbance in, and hence destruction of, the surface layer on the basis of the huge vapour generation.

The paper quotes, but wrongly uses, the Hashemi-Wesson formula[5] for the surface layer effect. The vapour withdrawal is taken as pound-moles per hour; in fact Hashemi-Wesson predicts lb/hr. These calculations lead the authors to conclude that the enhanced vapour generation can be explained as the effect of valve opening and suddenly reducing the tank pressure rather than due to rollover. However their conclusion that the Hashemi-Wesson formula cannot account for the high boiloff at La Spezia remains sound despite the inaccuracy.

In light of the subsequent data on La Spezia these conclusions are untenable. In particular this model would predict similar instabilities in single-component cryogenic fluids. These effects are seen quite commonly but are of a different scale to the La Spezia rollover event. The crude calculations on a true rollover, rejected in this paper, do approach the vapour generation seen in Sarsten's report[3]. They therefore support the view that a large quantity of liquid was flashed at the surface, though over a longer period than the 2

1 This type of rollover is seen in some lakes where stratification is a result of dissolved salts. At certain times of the year the water warms to a point where the liquid layers literally 'roll over' on eachother

minutes presumed in the calculation. The premise that a surface layer exists in the undisturbed storage vessel is valid[5,6] and the concept that this surface layer can be destroyed is an important one that is ignored in later models of rollover.

Chatterjee & Geist (1972)

An *n*-layer stratification is considered; each layer having a different density and a sharp interface with its neighbours. The density of a layer is taken to be a function of the methane mole fraction and the temperature only, with known initial values. A heat and methane mass balance is considered for each layer.

The bottom layer receives heat from the base and the walls, exchanges mass with the layer above and passes heat to the layer above. The uppermost layer receives heat from the walls, heat and mass from the underlying layer and loses heat and mass to the vapour. All other layers exchange heat and mass with their adjacent layers and receive heat from the walls. Heat and mass transfer coefficients between layers are inferred from Turner's work[10] on thermohaline systems.

Mass transfer is by equimolar counterdiffusion so that, with the exception of the bottom layer, the total number of moles in each layer is constant. The boiloff is considered to be pure methane. The composition of the top layer is therefore considered to be methane and other less volatile hydrocarbons. This model cannot easily be adapted for nitrogen rich LNG where a significant mole fraction is more volatile than methane.

The topmost cell is assumed to be at saturation temperature, a premise at variance with later investigations[4,6] which demonstrate a thin surface layer with a high temperature gradient.

The balance equations are solved simultaneously on a computer as an initial value problem. When two adjacent layers have a compositional difference of less than 0.002 mole fraction methane and a temperature difference of less than 0.03 K they are considered to mix and form one layer. This process is repeated until just one layer remains. In this model final mixing will only occur after the peak in boiloff since the last two layers can only be mixed once temperature and composition is nearly uniform throughout the tank. In fact, as will be discussed later, the sufficiency condition for two layers to mix is not straightforward. Rayleigh[55] demonstrated that a viscous liquid can have a density that increases upwards and be stable. In later models of rollover the mixing condition is taken to be equal densities; as discussed below this is not a sufficient condition for mixing for the conditions pertaining to a stratified LNG tank.

Three rollover cases are used to test the performance of the model including La Spezia. In the La Spezia case they assume a three layer stratification, the middle layer being the result of partial mixing of the heel and cargo. The assumed heat leaks are lower than those used in later papers and are inconsistent with the quoted normal boiloff of 1100 lb/hr.The model predicts a time from end of filling to rollover of 30hr as compared to an actual time of 18hr. The peak boiloff rate is poorly predicted at 50000 lb/hr compared with the average

La Spezia rollover rate of 248000 lb/hr; it must be assumed that the actual peak rate at La Spezia was of the order of 500000 lb/hr, that is 10 times the figure predicted by the Chatterjee-Geist model.

No references are given in the Chatterjee-Geist paper to give further details of the other instances of rollover that are used to test the model.

Germeles (1975)

The model of rollover due to Germeles[2] is similar to that presented by Chatterjee & Geist. The differences are as follows:

1 Equimolal counter diffusion is not assumed and hence the number of moles per layer is free to change.

2 The top cell is assumed to have a thin surface layer following the Hashemi-Wesson model[5] except that this layer is stable through out the rollover event. This model ignores the effects of surface agitation discussed in Maher & Van Gelder[50]

3 The criterion for mixing is equal densities.

The LNG is modelled as a two component fluid of methane and an impurity component whose molecular weight is a weighted mean of the all the other components. It is assumed that the impurity component is non-volatile and heavy, effectively this eliminates the effect of nitrogen in the LNG mixture. Heat and mass transfer across the interfaces follows the thermohaline double diffusive investigations reported by Turner[10] in a similar way to the Chatterjee & Geist model.

The results of the model are not very sensitive to the initial number and sizes of the layers for reasonable values.

A time to rollover is computed for the La Spezia data at 34hr compared to the observed time of 31hr. Germeles admits that this must be partly fortuitous in light of the assumptions made. This view must also then be taken of the Chatterjee & Geist predictions of time to rollover.

The Germeles model fails to predict the peak boiloff rate. A value of 32000 lb/hr is obtained which is at least a factor of ten too low.

Other notable results of the modelling are:

- Both the upper and lower layer densities increase with time. The upper layer warms but the density increases as a result of the enrichment of the LNG by methane evaporation. The lower layer cools by heat transfer to the upper layer.

- The composition of the lower layer changes little showing that the effect of mass diffusion is slight.

- Boiloff before rollover and boiloff at rollover are seriously at variance with the available data since the peak boiloff before rollover is overestimated by a factor of 5 and the model also fails to predict peak rollover boiloff. This is not noted in the text of the paper.

Chatterjee & Geist (1976)

The second model[8] by these authors attempts to modify that presented in their 1972 paper in order to include the effects of nitrogen in LNG. The paper is entitled 'Spontaneous Stratification in LNG Tanks Containing Nitrogen' but also modifies the original assumptions of the 1972 model. The paper considers fill-induced stratification and introduces the concept of stratification due to weathering of nitrogen rich LNG where the flashing of the hot liquid reaching the surface produces a less dense mixture which can remain as a surface layer. The less dense layer, formed as a result of flashing the liquid, grows downward from the surface until a point is reached where the hot boundary flow fails to reach the free surface and the heat inleak due to base and lower wall heating then superheats the lower layer in the manner of a fill-induced stratification and rollover.

1 The LNG is considered to be a three component mixture of methane, ethane and nitrogen rather than a simple methane/ethane mix.

2 Equimolar counter-diffusion is replaced by mass transfer rates for each component obtained from thermohaline experiments due to Turner[10]. The Turner data includes the effect of enhanced mass transfer by entrainment at low stability ratios.

3 The boiloff from the tank has to include the boiloff of nitrogen since this is more volatile than methane. The boil off rate is obtained from a flash calculation. The Hashemi-Wesson[5] formula for the liquid-vapour interface is not used in the model, instead the top layer flashes at each time step.

4 In the 1972 model the necessary condition for two layers to mix was .002 mole fraction of methane and .03 K difference between adjacent layers. In this later model the rollover phenomenon is a consequence of the heat and mass transfer, a function of the stability parameter, as reported by Turner[10]. Some consideration is given to the penetration of the boundary layer through an interface though it is clear that criterion of boundary layer penetration to the top of the overlaying layer is not used to determine mixing of adjacent layers. The necessary condition for the boundary layer to reach the free surface is considered as a requirement for nitrogen-induced spontaneous stratification and determines the minimum height for the top layer to prevent the wall-heated boundary layer fluid from flashing at the surface. The authors consider the effect of entrainment of the boundary layer flow on the degree to which the boundary layer will penetrate a layer of lower density, however this is not considered as a mechanism for heat and mass transfer.

The La Spezia event is not modelled in this paper. Another, unidentified rollover is referred to and some data quoted against which the mathematical model is tested. In this case the normal boiloff of the tank was 0.06% per day. In a 40 day period after filling the

boiloff was lower than normal; a rollover then occurred and the tank lost 1% of its contents in a 24 hr period. Following this several further incidents of enhanced vapour generation were experienced at 20-25 day intervals when the peak boiloff was two to three times the normal boiloff.

In the major incident a peak rate of vapour evolution is not quoted but, by similar arguments to those of the La Spezia incident, it must be anticipated that the peak must have considerably exceeded the 16-fold enhancement reported as an average over the 24 hours of the main incident.

As with previous models the calculated time to rollover agrees well with the data but the peak of vapour generation predicted is the same as the boiloff rate averaged over the 24hr period. Furthermore the scale of rollover is an order of magnitude less than that at La Spezia and the assumptions made in this model may be inappropriate in considering worst-case situations.

Takao & Suzuki (1982)

This work[32] models rollover in a similar way to Germeles[2]. Mass, solute and energy balances are taken for each layer. Equalisation of density is the condition of mixing for adjacent layers and the boiloff from the top layer is evaluated from the Hashemi-Wesson[5]. Instead of using Turner's results[33] obtained on saline/water systems, the authors evaluate the heat and mass transfer through the double-diffusive interface from experimental results obtained by Takao & Narusawa[31] on $CuSO_4$, NaCl and HCl as solute in water systems.

The stratified tank is considered as a number of cells and the initial properties and sizes of the cells are computed from results based on cell formation due to lateral heating of a linear solute gradient. The initial condition is then not a linear solute and temperature gradient or a single sharp interface. The cell sizes are based on saline/water experiments reported in this paper and by other workers[34,35] when a linear solute gradient is laterally heated. The density profile of the tank at the start of simulation is strongly nonlinear with the largest gradients near the surface of the tank. The cell size decreases as the solute gradient increases.

The model so derived is not tested against La Spezia nor against experimental rollovers. The boiloff computed has several peaks corresponding to layers mixing as their densities equalise and the peak value is of the order of seven times the normal vapourisation rate.

Heestand, Shipman & Meader (1983)

This work[4] aims to overcome some of the objections to the earlier models that are itemised above. The LNG is considered to be a mixture of five components: methane, ethane, propane, n-butane and nitrogen. Mass balances are taken for each cell and for each component.

The major change in the description of the behaviour of LNG is the basis for heat and mass transfer between cells. It is apparent that the mass transfers arising from double-diffusive convection are insufficient to account for the vapour evolution reported at La Spezia. In particular double-diffusive convection almost eliminates mass transfer between cells until the interface is unstable. On this basis the mechanism of double-diffusive convection is abandoned and it is assumed that there are two fully turbulent free convective films at each liquid/liquid interface and that the density of this intermediate section is intermediate between the densities of the cells. Two alternative correlations are then considered for the heat transfer coefficient. Firstly each film is considered to be equivalent to a single heated plate and a correlation based on air is used. Secondly the heat transfer is modelled with a correlation for transfer through a fluid placed between two horizontal plates and heated from below.

A common mass transfer coefficient is adopted: the product of this coefficient and the difference in mole fractions between the cells describes the mass transfer rate. This is similar to the high-stability ratio data of Turner[9] previously used by Chatterjee & Geist[8] and later by Sugawara *et al*[7] but does not include entrainment effects at low stability ratios.

In both of the heat transfer correlations used retention of the Prandtl number term leads to times to rollover which are too short and a boiloff which is too large in the pre-rollover period. These inaccuracies can be removed by ignoring the Prandtl number term. In effect this means that, in contrast to the situations involving horizontal plates and fluid bounded above and below by horizontal plates, the molecular level of thermal and viscous diffusion can be ignored in comparison to longer length scale effects. In fact the Prandtl number for air, which is close to 1.0, is used in both correlations and an average of the two constant terms taken. As a corollary this implies that the velocity and temperature distributions in the liquid/liquid interface will be similar.

The data is fitted to the time to rollover and the vapour evolution prior to rollover. It is claimed that the total vapour evolution is within 14% of Sarsten's theoretical estimate however the peak vapour generation is predicted to be 12700 kg/hr which is conservatively a factor of ten less than the La Spezia incident and worse than the predictions of the earlier two models. The model also predicts a much longer time constant for the decrease in boiloff following the peak of vapour evolution. As in the Germeles model the thin surface layer at saturation temperature is assumed to be stable throughout the simulation.

Sugawara, Kubota & Muraki (1983)

The new features of this model[7] arise from observations of laboratory scale tests with freons and an actual LNG tank test. It is claimed that the resulting model is a modification of that of Germeles[2] however the transport of heat and mass through the liquid/liquid layer is considered as a fundamentally different mechanism.

1 In contrast to the sharp interface between layers assumed by Germeles this model allows the formation of an intermediate mixing layer with a temperature and concentration gradient.

2 Whereas in the Germeles model the thickness of all the layers except the uppermost is fixed, here the interface level does change as a result of convective flow within the layers.

3 Three mechanisms of heat and mass transfer at the interface are considered. Firstly a diffusive transfer as in Germeles, secondly penetration from the lower layer to the upper, and lastly entrainment mixing at the interface. In the actual LNG tank test the authors believe that the test results indicate that entrainment is the dominant factor in the movement of the interface level. The data points do not span the low stability region where entrainment would be exhibited; however measurement of the speed of movement of the interface layer, u, and calculations of the interfacial radial velocity do show a correlation between a Richardson number and the ratio of u to the interfacial radial velocity. This dependency is examined by Turner[11]. On this basis the entrainment mechanism is considered to be the mechanism for movement in the interfacial layer in the LNG tank test.

4 The heat transfer coefficient was experimentally determined as a function of the stability parameter and these points lie broadly in the range experimentally determined by Turner[9]. A curve is presented which follows that presented by Turner however the points at low stability ratios deviate strongly from the fitting curve and insufficient measurements are available to confirm the Turner results obtained from thermohaline systems.

5 In the case of small temperature gradients or large density gradients when there is a high stability ratio, $R\rho$, the entrainment is small and diffusive heat and mass transfer is dominant. This is evident from the experimental data quoted by the authors. For $R\rho \geq 2$ the product of the stability ratio and the mass transfer velocity is a constant multiple of the heat transfer velocity and the experimental data provides a reasonable confirmation of this. For $R\rho < 2$ a curve is extrapolated from the experimental data points relating the Richardson number to the experimentally observed velocity of the interface layer as it moves through the liquid. The applied fit to these data points follows closely the analysis of thermohaline heat and mass transfer due to Turner[9] however there are only two or three points for the region $R\rho < 2$ and these do not fall on the fitting curve.

This paper covers both mathematical and experimental modelling of rollover events. In both sets of results the peak boiloff is of the order of three or four times the normal boiloff. The mathematical model is applied to La Spezia and although the time to rollover is reasonably well predicted the peak boiloff is underestimated in a similar way to other models.

Summary of LNG Rollover Models

All the models achieve similar success in predicting the course of events at La Spezia. In all cases the time to roll over agrees quite closely with Sarsten's reports. No model is capable of explaining the peak boiloff. Laboratory scale tests and one LNG tank test have not revealed similar rates of vapour evolution to those at La Spezia. Only the explanation rejected by Maher and Van Gelder[12], namely destroying the surface layer effect, appears to account for the magnitude of boiloff.

In these models the process of rollover is a function of the heat and mass transfer across the liquid-liquid interface and the condition for instability leading to large scale mixing of the tank contents. Most models use the Turner[10] saline/water data for the former and equalisation of densities as the end point for mixing.

As the stratification approaches instability there is some evidence from thermohaline studies to suggest that the mechanism of heat and mass transfer is at longer length scales and particularly entrainment and boundary layer penetration are important. The models discussed above offer reasonable solutions to the first part of rollover but fail to account for the behaviour when mixing occurs. All the models consider the heat and mass transfer at an interface. Only Chatterjee & Geist[8] and Sugawara et al[7] include in the models the effect of the large scale convective flows on interfacial behaviour, the former in terms of boundary layer penetration and the latter as the effect of velocity shear on entrainment at the liquid-liquid interface as a two dimensional problem.

Since the surface layer and bulk superheat are phenomena of saturated liquids the thermohaline experimental results are not useful in modelling the outcome of large-scale mixing in cryogens.

It can be seen from these models that the fundamental questions yet to be answered are:

1. What are the heat and mass transfer coefficients across the interface?

2. What are the conditions for instability of the liquid/liquid interface?

3. What are the modes of instability in the liquid/liquid interface?

4. How does the surface layer respond to changes in the bulk of the liquid?

5. Can the surface layer become unstable?

3. BASIC FLUID DYNAMICS

DEFINITIONS OF TERMS AND SCOPE

This research was prompted by the real problems faced by the natural gas industry on an everyday basis. The scope of the investigation is circumscribed by the real nature of the vessels and the fluids. It is important to cast these limits in terms of a scientific framework to draw from the extensive body of knowledge pertinent to the problem.

There are many facets to the operation of an LNG storage facility and there are aspects that are far beyond the scope of the rollover problem which can effect the outcome of a rollover type incident. The mechanism of rollover itself is not well understood and the fluid behaviour of cryogens in vessels is only now beginning to be elucidated. It seems appropriate to examine the behaviour of the fluid itself and to minimise the complexity of the system to be analysed. For example no consideration is given to the behaviour of a fluid jet entering the heel of fluid in the tank nor for the conditions for stratification in that case. In fact the starting point for the analysis is an existing stratified fluid.

In operational terms consider a cylindrical vessel containing a two or more fluids which are horizontally homogeneous but are vertically separated by comparatively thin regions with high concentration and temperature gradients. The system is initially stable by virtue of increasing density with depth. The only body force is gravity. At the top of the uppermost layer there is a free surface. There is an evaporative mass flux through this surface into the vessel vapour space and it is initially in saturated equilibrium with the vapour. There is a heat inleak through the base and walls of the vessel. The total heat inleak into the bottom layer exceeds the heat flux through the liquid-liquid interface at the top of the lower layer with the result that the lower layer warms. The fluid become less dense with increasing temperature. The opposing effects of temperature, which is increasing in the lower layer, and composition, which is effectively constant up until mixing, drive the systems towards a condition where the density of the lower cell approaches, or equals, that of its neighbour. When the densities become equal the layers are marginally stable.

The discussion in this chapter will form the framework for consideration of the conditions for stability, the modes of instability and development of mixing processes.

BASIC THEORY AND ASSUMPTIONS

Much of this theory is standard and can be found in almost any text on fluid dynamics. It is reproduced here for the purpose of elucidating later experimental results and to act as a framework for the assumptions and discussion.

Incompressible Fluid

Gravity is the only external force acting upon the system. It exerts a force ρg per unit volume. The effects on the fluid arise from variations in the density of the fluid due to thermal and compositional differences. The fluids are assumed to be incompressible. As the density varies

$$p = p_o - g\int_o^z \rho\left(z\right)\, dz \tag{3-1}$$

and the condition for stable stratification in an inviscid fluid is that the density increases with depth where x and y are in the horizontal plane and z vertically upwards.

When the fluid is considered non diffusive we have the condition

$$\frac{D\rho}{Dt} = 0 \tag{3-2}$$

with the differentiation following the motion and the continuity equation is

$$\nabla \cdot u = 0 \tag{3-3}$$

The Navier-Stokes momentum equations can be expressed as

$$\rho\frac{Du}{Dt} = \rho\left(\frac{\partial u}{\partial t} + u\cdot\nabla\cdot u\right) = -\nabla p + \rho g + \mu\nabla^2 u \tag{3-4}$$

Since all the flow patterns of normal liquids and gases are solutions of (3-4) the actual flows are distinguished by the boundary and initial conditions and by flow parameters such as the Reynolds number.

In the standard manner the curl of the Navier-Stokes equation gives an expression for the vorticity ξ where the vorticity is related to the velocity:

$$\xi = \nabla \times u \tag{3-5}$$

$$\frac{D\xi}{Dt} = \xi \nabla u + \nu \nabla^2 \xi + \nabla p \times \nabla \left(\frac{1}{\rho} \right) \tag{3-6}$$

where the kinematic viscosity $\nu = \eta / \rho_0$ has been taken to be constant.

Now the important part of this relation is the independence of the vorticity on variation of density except in the third term. It follows that, whenever the cross product of the density gradient and the pressure gradient is non-zero, vorticity will be generated; that is whenever the gradients are not parallel. If the pressure gradient is considered solely a function of gravity acting purely in the vertical direction then any displacement of the density gradient away from the vertical due to compositional differences or variations in temperature will result in the generation of vorticity. Conversely if the density gradient becomes zero, as it may with stratified layers and an applied temperature gradient, the flow will become irrotational.

Viscous Incompressible Fluids in Cylindrical Polar Coordinates

In an axisymmetric system like the LNG tank it is appropriate to use cylindrical polar coordinates (r, θ, z).

For a viscous incompressible liquid:

The continuity condition becomes

$$\frac{1}{r} \frac{\partial}{\partial r} \left(r u_r \right) + \frac{1}{r} \frac{\partial u_\theta}{\partial \theta} + \frac{\partial u_z}{\partial z} = 0 \tag{3-7}$$

The three components of the Navier-Stokes equations are

$$\frac{\partial u_r}{\partial t} + \left(\mathbf{u} \cdot \nabla \right) u_r - \frac{u_\theta^2}{r} = -\frac{1}{\rho} \frac{\partial P}{\partial r} + \nu \left(\Delta u_r - \frac{2}{r^2} \frac{\partial u_\theta}{\partial \theta} - \frac{u_r}{r^2} \right) \tag{3-8}$$

$$\frac{\partial u_\theta}{\partial t} + \left(\mathbf{u} \cdot \nabla \right) u_\theta + \frac{u_r u_\theta}{r} = -\frac{1}{\rho r} \frac{\partial P}{\partial \theta} + \nu \left(\Delta u_\theta + \frac{2}{r^2} \frac{\partial u_r}{\partial \theta} - \frac{u_\theta}{r^2} \right) \tag{3-9}$$

$$\frac{\partial u_z}{\partial t} + \left(\mathbf{u} \cdot \nabla \right) u_z = -\frac{1}{\rho} \frac{\partial P}{\partial z} + \nu \Delta u_z \tag{3-10}$$

Approximations to Achieve Solutions

The approximations that are normally made may be relevant to the whole system, parts of the system or not appropriate at all. Here the possible simplifications are considered in order that the experimental data can be used to clarify the possible assumptions.

For the inviscid case the Navier-Stokes equations reduce to the Euler equations. If the pressure and the density are written as deviations from a reference state of equilibrium $p = p_o + p'$ and $\rho = \rho_o + \rho'$ the Euler equations reduce to

$$\rho \frac{Du}{Dt} = -\nabla p' + \rho' g \tag{3-11}$$

so that only ρ' is relevant to the effect of gravity on the fluid element. In a stratified fluid of two layers Prandtl[61] has shown that the standard density ρ_o can be considered as zero and the second layer is acted upon by a reduced body force of $g\rho'/\rho$ or, equivalently, subject to a reduced gravitational acceleration g'.

In the incompressible case considered here Boussinesq introduces a further simplification possible when ρ' is small compared to ρ_o. The above Euler equation is rewritten as

$$\left(1 + \frac{\rho'}{\rho_o}\right) \frac{Du}{Dt} = -\frac{1}{\rho_o} \nabla p' + \frac{\rho'}{\rho_o} g \tag{3-12}$$

and the ρ'/ρ_o appears in the inertial term and in the body force term. The assumption is that the effect on the inertia can be ignored compared to the effect on buoyancy. The net result of this approach is to ignore inertial density variations and keep the density variations where they affect buoyancy.

The Euler equations can be linearised in certain situations by making the assumption that $u\ \partial u/\partial x$ is small compared to $\partial u/\partial t$ and this linearised form can in some cases be applied with the Boussinesq approximation and then the continuity equation is also linearised to give this pair.

$$\frac{\partial u}{\partial t} = -\frac{1}{\rho_o} \nabla p' + \frac{\rho'}{\rho_o} g \tag{3-13}$$

$$\frac{\partial \rho'}{\partial t} + u_z \frac{\partial \rho_o}{\partial t} = 0$$

To arrive at this point there have been a number of assumptions that it is instructive to reiterate. The validity of these assumptions for regions of the tank will help analyse the total problem.

- The fluid is incompressible. ($\nabla \cdot \mathbf{u} = 0$)
- The fluid is non-diffusive.
- The fluid is inviscid.
- The density variations from point to point are small. (Boussinesq)
- The motions and velocities are of small amplitude. (Linearisation)

For most of the regions of interest in a tank it will not be valid to make some of these approximations though the liquid in the tank will always be considered incompressible.

Boundary Conditions

The boundary condition at a fixed solid surface in a viscid liquid (i.e. the walls and base of the tank) are non-slip so that the fluid velocity vanishes $u_{\text{wall}} = 0$. In an inviscid liquid only the normal component of the fluid velocity at the wall is zero.

At the free surface the force acting on the surface must vanish so taking **n** as a unit vector normal to the surface:

$$P_{\text{surface}} = -\sigma_{\text{ik}}\, n_{\text{k}} = 0 \tag{3-14}$$

where the stress tensor components for a viscous incompressible liquid in cartesian coordinates are:

$$\sigma_{\text{ik}} = -p\,\delta_{\text{ik}} + \eta\left(\frac{\partial u_{\text{i}}}{\partial x_{\text{k}}} + \frac{\partial u_{\text{k}}}{\partial x_{\text{i}}}\right) \tag{3-15}$$

In cylindrical polar coordinates:

$$\sigma_{\text{rr}} = -p + 2\eta\,\frac{\partial u_{\text{r}}}{\partial r} \tag{3-16}$$

$$\sigma_{\theta\theta} = -p + 2\eta\left(\frac{1}{r}\frac{\partial u_{\theta}}{\partial \theta} + \frac{u_{\text{r}}}{r}\right) \tag{3-17}$$

$$\sigma_{\text{zz}} = -p + 2\eta\,\frac{\partial u_{\text{z}}}{\partial z} \tag{3-18}$$

$$\sigma_{\text{r}\theta} = \eta\left(\frac{1}{r}\frac{\partial u_{\text{r}}}{\partial \theta} + \frac{\partial u_{\theta}}{\partial r} - \frac{u_{\theta}}{r}\right) \tag{3-19}$$

$$\sigma_{\theta z} = \eta \left(\frac{\partial u_\theta}{\partial z} + \frac{1}{r} \frac{\partial u_z}{\partial \theta} \right) \tag{3-20}$$

$$\sigma_{zr} = \eta \left(\frac{\partial u_z}{\partial r} + \frac{\partial u_r}{\partial z} \right) \tag{3-21}$$

For a saturated liquid the liquid surface is isothermal at the saturation temperature.

$$T_{\text{surface}} = T_{\text{sat}} \tag{3-22}$$

At the liquid/liquid interface the velocities of the liquids must be equal and the forces exerted are equal and opposite. Taking normal vectors to the interface as n_1 and n_2 such that $n_1 = -n_2$

$$n_i \, \sigma_{1,ik} = n_i \, \sigma_{2,ik} \tag{3-23}$$

where the suffices 1 and 2 refer to the two liquids.

Near the boundary of a liquid, in the boundary layer, the velocity gradients will be large and the terms in the equations of motion containing velocity gradients cannot be neglected even if the viscosity is small. The boundary layer is considered thin and the flow in the boundary layer is mainly parallel to the surface. In the laminar boundary layer the characteristic length in the x direction is δ, the thickness of the boundary layer while in turbulent boundary layers the characteristic length is the scale of the turbulence. In both cases the characteristic length in the z direction is h.

For free convection at the wall the transition from a laminar boundary layer to a turbulent one is governed by the Grashof number. Experimentally the transition occurs at approximately 10^9 which corresponds to a value for h of ~ 10m. Thus a real tank will have a turbulent boundary layer. In laboratory experiments with h ~ 10cm the Grashof number is of the order of 10^6 indicating laminar flow.

At the free surface turbulent eddies from the bulk must be strongly damped. Observation of the free surface under the experimental conditions of this study revealed no surface disturbances showing that the vertical component of velocity disappears. It was observed that 'balls' of LIN were often formed on the surface of the LIN during the preparation of stratified layers, presumably isolated from the surface material by vapour generation. These balls moved erratically and rapidly about the surface indicating that inhomogeneities were present in the surface perhaps either as variations in boiloff or as considerable variations in velocity components of the surface material. Experiments with talc on the surface of ambient fluids does reveal that eddies, or equivalently plumes, do reach the surface and the velocity component parallel to the surface are not strongly suppressed.

If an eddy is incident upon the surface there must be a force balance between the eddy and the deformation. In the case of the free surface an eddy with a vertical velocity u_z will exert an effective pressure, p', given to a first approximation by:

$$p' = \rho u_z^{\,2} \tag{3-24}$$

then the force balance at the surface due to the deformation at the surface is a combination of surface tension and gravitational forces. If the eddy has a characteristic length l_e and the deformation in the surface is ζ with a maximum height ζ_{max} Davies[54] has found that the form of the deformation is an error function:

$$\zeta = \zeta_{max} \exp\left(-4r^2/l_e^{\,2}\right) \tag{3-25}$$

so that the radius of curvature of the deformation at its peak is given by:

$$r_{curv} = l_e^{\,2}/8\,\zeta_{max} \tag{3-26}$$

then balancing the pressures, with σ the surface tension, this leads to:

$$\rho u_z^{\,2} = \zeta_{max}\,\rho g + \frac{2\sigma}{r_{curv}} \tag{3-27}$$

and substituting for r_{curv} from (3-26) then:

$$\rho u_z^{\,2} = \frac{2\sigma}{r_{curv}} + \frac{l_e^{\,2}\rho g}{8 r_{curv}} \tag{3-28}$$

Thus the surface tension will be the dominant restoring force for small eddies while for larger eddies surface deformation will become dominant. The point of equal contribution comes at $l_e^{\,2} = 16\sigma/\rho g$ which corresponds to ~4mm in LIN. Therefore surface tension effects will be important for eddies in the experimental vessel but large eddies in a full scale tank, possibly as a result of mixing processes at the liquid-liquid interface, will not be significantly suppressed by surface tension effects and eddy size becomes important in consideration of the stability of the liquid-vapour interface. In effect the eddy size does not scale with the experimental investigation of liquid-vapour interfacial stability.

By eddy length here we mean the order of magnitude of length over which the velocity changes appreciably. The largest eddy size that can be considered is of the order of the dimension of the containing vessel and in a similar way the velocity fluctuations for large eddies will be of the order of the characteristic velocity of the flow in the vessel. The Reynolds number, R, for the largest eddies and for the whole tank will be of similar

magnitude and since for large R a liquid behaves as it were inviscid, we see that viscous dissipation effects on large eddies will be negligible and that viscous dissipation is only important for small eddies with R of the order of 1. By a dimensional analysis we can relate the kinematic velocity to the characteristics of this flow. The only quantities that characterise the flow that can be combined to give a quantity with the dimensions of kinematic viscosity are l_e and u so:

$$\nu \approx l_e u \tag{3-29}$$

This can be rearranged to give a characteristic time relating to the size of the eddy, t, in terms of its lengthscale.:

$$t \approx \frac{l_e^{\,2}}{\nu} \tag{3-30}$$

Thus large eddies have a large characteristic time and as the scale of the vessel increases such eddies will be correspondingly long-lived. Energy dissipation occurs through the interaction of large eddies producing smaller eddies. Eventually the smallest eddies will be subject to viscous effects where the energy is dissipated as heat.

MACROSCOPIC BEHAVIOUR OF THE FLUID IN A TANK

Assume a cylindrical tank filled to some level with a cryogenic liquid. By cryogenic here we mean any liquid that has its boiling point below ambient. There is heat inleak into the fluid through the base and walls of the vessel. The fluid may be stably stratified into a number of layers, or cells, of differing density. The unstratified tank can be considered as a single layer system. The heat inleak into the lowest layer is greater than the total heat flow from the lowest layer to the layer above so that the lower layer is warming. We are concerned with a stratified tank where the effect of the warming would be such that if two adjacent layers were not to mix for any other reason they would become unstable with respect to each other before nucleate boiling could take place.

From earlier experiments[48] we know that inside an unstratified vessel there is a boundary layer driven flow which rises up the wall until it reaches the surface. The flow is then directed radially inwards at the surface until it reaches near the centre of the vessel where it turns downwards to form a downward central jet. The jet impinges on the base of the cell and flows radially outwards to the walls of the vessel. There is no boiling in the vessel. If there is a strong convective flow in the cell the body of the cell is well mixed.

At the surface there is an evaporative mass flux by surface evaporation. The bulk of the topmost cell is superheated with respect to the equilibrium saturation temperature[56]. We can define the thermal overfill, TO, of a component as its excess enthalpy over saturation enthalpy (H - Ho). If TO > 0 the component is termed superheated and for

TO < 0 subcooled. For the tank the thermal overfill is the sum of the component thermal overfills

$$TO_{\text{tank}} = \sum_{i=1}^{n} \left(H_{\text{i}} - Ho_{\text{i}}\right) \tag{3-31}$$

In the case of a poorly mixed fluid in the tank there can be both positive and negative contributions to the overfill and it is useful to define TO_+ as the sum of all positive contributions and TO_- as the sum of all negative TO.

$$TO_{\text{tank}} = TO_+ + TO_- \tag{3-32}$$

In terms of the capacity of the system for excess vapour generation TO_+ may be the relevant measure if the superheated components are at or near the liquid surface and can contribute to the vapour generation without mixing with subcooled elements.

The rate of change of TO_{tank} is then the net result of heat inleak and surface vapourisation

$$\frac{\partial\left(TO_{\text{tank}}\right)}{\partial t} = \dot{Q} - \dot{m}L \tag{3-33}$$

Separating two fluid cells there is a liquid/liquid interface across which there is a compositional difference which is stabilising, a temperature difference which is destabilising and a velocity shear as the lower cell has a radially inward flow and the upper an opposite sense.

4. THE LIQUID-VAPOUR INTERFACE

UNSTRATIFIED LNG BEHAVIOUR

The behaviour of the liquid-vapour interface in stable LNG tanks has been widely observed through normal operation. Evaporation of the LNG occurs at the quiescent surface with no bubble formation, though operators have reported some boiling in underground tanks. Experiments with a variety of non-boiling liquids have shown that irrespective of the homogeneity of the bulk it is never in thermodynamic equilibrium with the vapour. Only the surface itself is at saturation temperature and the bulk liquid is superheated. The normal boiloff from an LNG tank is well modelled by the Hashemi-Wesson formula, which has become the accepted view of tank behaviour.

Hashemi & Wesson

In this paper[5] a model of the behaviour of an LNG tank is presented which considers the whole tank as a fluid layer heated from below such that the characteristic length is the depth of the liquid in the tank. The well known correlation for the heat transfer in a horizontal fluid layer is used:

$$N = C\,Ra^{1/3} \tag{4-1}$$

where the constant takes the value 0.13 for a liquid cooled by surface evaporation. This correlation having been obtained with liquids at ambient temperature which are not saturated. Substitution of the definitions of N and Ra into this formula leads to an expression for the heat flux which is independent of the depth of the fluid:

$$Q = C\,K_T \left(\frac{\beta_T g}{\alpha \nu}\right)^{1/3} \Delta T^{4/3} \tag{4-2}$$

hence this gives a rate of vapourisation as a function of the temperature difference across the fluid layer.

$$\dot{m} = C \left(\frac{K_T}{L}\right) \left(\frac{\beta_T g}{\alpha \nu}\right)^{1/3} \Delta T^{4/3} \tag{4-3}$$

A comparison of this rate of vapourisation with an experimental and theoretical study of water by Von Vilhelm Pruger[15] leads the authors to the important conclusion that rate of surface vapourisation is controlled by the heat transfer in the liquid rather than the mass transfer through the gas layer above the liquid surface.

It is postulated that the heat transfer to the surface is by a mechanism of convection from the bulk liquid. The vertical temperature distribution is presumed symmetric between the surface and the base of the tank and the bulk temperature, Tb, is taken to be half the temperature difference between the base and the surface, T_{sat}. This temperature gradient is a necessary condition to achieve any surface evaporation. The authors do refer to experiments with water and other liquids which demonstrate the existence of a surface layer some 2mm thick below which the temperature is higher than the surface temperature.

Implicit in the derivation of the relationship between boiloff and bulk temperature is the assumption that the heat inleak from the base and walls of the tank is manifest as the sensible heat of the bulk liquid. The authors do consider boundary layer flow at the walls delivering heat to the surface directly but this is not included in the derivation of the relationship between the bulk superheat and the rate of vapourisation.

The model is further developed to relate the supersaturation pressure of the liquid to the boiloff. The motivation of the model was to account for the behaviour of storage tanks and their boiloff compressors. Particular emphasis is given to oversized tank pressure control systems. It can readily be seen that the result of rapidly lowering the vapour pressure in the tank will be to reduce the surface temperature, increasing the temperature difference between bulk and surface. If the model is used in this way the assumptions are seen to be valid. The adjustment of the bulk temperature to the new conditions in the tank will be of longer time scale since this will require convective heat transfer.

It is found that the pressure rise after the compressors have been turned off is higher than that predicted by the Hashemi-Wesson formula. The authors account for this in terms of the heat inleak from the unwetted walls and tank ceiling, and some accumulation of warmer LNG near the surface when the boiloff ceases.

The Hashemi-Wesson formula takes no account of boundary layer flows or circulation in the LNG tank. It is a phenomenological model that cannot offer any useful description of rollover mechanisms

THERMAL CONVECTION IN CELLS

The premise adopted by Hashemi & Wesson is based upon experimental results from studies of the onset and development of convection in fluid layers heated from below. The study of thermal effects in a layer of fluid constrained between horizontal boundaries with

gravity as the only body force and an applied vertical temperature gradient (warmer below) has a long theoretical and experimental history.

The Linear Stability Theory and The Onset of Convection

A liquid layer heated from below is statically unstable if it is inviscid. In a real fluid the viscosity and diffusion act to suppress small perturbations that would otherwise result in convective flows in an inviscid fluid. Benard originally considered thin layers of fluid and was able to show that the fluid became unstable when the temperature difference exceeds a minimum value which is a strong function of depth and gave his name to the cellular pattern seen in such layers. Rayleigh[55] formulated this problem and solved the linearised Boussinesq equations by assuming a sinusoidal convection pattern in the horizontal plane and free conducting boundaries. Applying a perturbation analysis it was shown that below a Rayleigh number ($Ra = g\beta_T \Delta T h^3/\alpha\nu$, where ΔT is the temperature difference between the upper and lower surfaces and h is the distance between the surfaces) $Ra_c \cong 657$ the convection pattern would be stable to small disturbances. The Rayleigh number expresses the ratio of the buoyancy forces driving the motion to the viscous and thermal diffusive dissipation which tend to suppress the motion. Rayleigh's analysis of the system was later extended to the condition of solutal as well as thermal gradients in the layer and this is discussed later (see chapter 5).

In the Boussinesq approximation and with a horizontally infinite layer and no applied shear it is readily shown that the only dimensionless parameters that characterise the flow are the Rayleigh and Prandtl numbers ($\sigma = \nu/\kappa$). The Nusselt number is an important part of the general problem (the heat flux divided by the conductive heat flux). In particular it has been generally found that there is a relation of $N = kR^{1/3}$ observed experimentally where k is a constant of the order of 0.1.

Other workers have expanded the theoretical treatment to include non-infinite non-rectangular systems. Pellew & Southwell [24] considered combinations of free and fixed upper and lower boundaries and perfectly insulating side walls of indefinite horizontal cross-section using the linearised Boussinesq approximation. They found Ra_c values of 657 for the two free surfaces and 1100 for one free surface and one rigid boundary.

In an experimental study Koschmeider[60] has shown that the convective pattern and the shape of the convective calls formed at the onset of convection depends on the geometry of the vessel. In a cylindrical vessel the convective cells have been observed to take on the shape of axisymmetric circular rolls.

From the earliest observations of the onset of convection it is apparent that the behaviour of the sample is a strong function of the depth of the fluid so long as the sample is thin. It is also evident from normal experience that the behaviour of a sample more than a few centimetres in depth is independent of the depth. It is clear therefore that the length scale operating in Rayleigh number is not that of the depth of the cell unless the cell is thin.

Since there is no other length scale in the vessel that is applicable it is assumed that there is an internal 'mixing-length'.

Linear stability theory cannot predict the behaviour of the fluid after the onset of instability, it is limited to describing the growth of small perturbations. Certainly the approximation of linearity excludes any description of turbulence and it is the nonlinear terms that account for the progression to non-periodicity. The Benard problem has been a major area of research in nonlinear hydrodynamics[21].

The Development of the Layer at High Rayleigh Number

As the temperature difference between the lower and upper surfaces of the Benard cell is increased the fluid passes from a conductive state to a condition whereby the heat transfer is through convective processes. It is the nature of these convective processes and their relationship to evaporating cryogens that is considered here.

Ahlers[59] measures the heat transport as a function of the Rayleigh number in thin cylindrical cells containing helium at temperatures near 4 K. This allowed measurements of high accuracy. The Nusselt value, N, as a function of Rayleigh, Ra, is redrawn here as fig.2 with $r = Ra/Ra_c$. The function is everywhere smooth in spite of the finding of a transition to a turbulent state near $r = 2$. This transition was manifest in a non-periodic time dependence of N with amplitudes $\sim 5x10^{-3}N$.

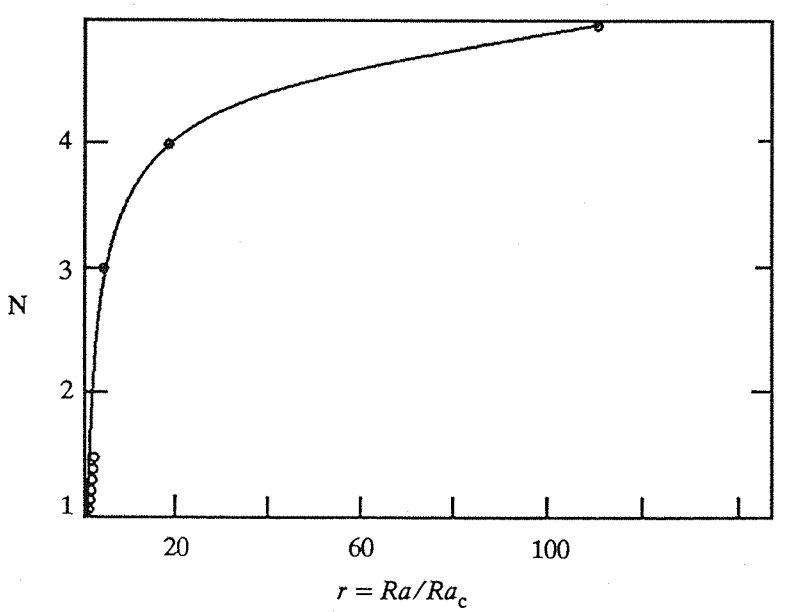

Fig. 2 Nusselt number as a function of Rayleigh number

Intermittent Convection

Howard[57] discusses the role of 'thermals' in the development of turbulent convection. Consider a Benard cell initially at uniform temperature heated from below. As the vertical temperature gradient starts to develop the only form of heat transmission will be by conduction. As Ra_c is passed the gradient becomes unstable to small perturbations cause thermals to develop. At this point Howard introduces as a fact of observation that the thermals will break away from the heated surface. Defining a plume as a maintained thermal it can be said that facts of observation do include plumes. The time scale of the convective instability is considered smaller than the characteristic time scale of conduction l^2/K_T. The total heat transport averaged over a period of time is considered to be both conductive and convective with the convective phase of small time intervals. An observation of the vertical temperature gradient would then reveal values linked to the conductive mode. Such a heat transport may also fulfil the role of a non-periodic time-dependent heat transport. Howard emphasises the importance of the short lifetime of the thermals such that the conductive temperature gradient is maintained. In fact if the temperature is averaged over the horizontal extent of the cell plumes would be allowable provided they occupy a small volume compared to the liquid in the conductive phase. Foster[58] expands upon this model, terming it intermittent convection.

Surface Tension Effects

Experimental data on free surfaces does reveal discrepancy with the predictions of the above analysis. Generally the critical Rayleigh number is lower than that predicted by the analysis, see Berg *et al*[16]. Pearson[17] examined the mode of instability of the surface in terms of a surface tension driven mechanism. If the surface layer has a tension higher than that of the underlying liquid the system is potentially unstable as the potential energy of the surface is not at a minimum; surface tension being the free energy/unit area. Pearson was able to show that for thin layers the surface tension driven instability would occur before a buoyancy driven instability. Later Nield[18] theoretically investigated the situation where both buoyancy and surface tension mechanisms are included in the model of evaporative convection and concluded that the two modes of instability may reinforce eachother.

In Pearson's work the surface tension is considered only as a function of temperature. If the system under consideration is multicomponent or there is an absorbed component at the surface the surface tension will also depend on the solute. Berg & Acrivos[20] describe 'surface elasticity' due to the local increase in surface tension as fresh liquid, with greater surface tension, displaces the existing surface material and forces develop to oppose the outward flow of fresh liquid. Surface elasticity was found to have a strongly stabilising effect on the onset of convection.

Cryogenic liquids will rarely be in a pure state. Contaminants which are gaseous at ambient temperatures will readily condense into the surface layers and may be present in significant quantities. Rebai *et al*[19] has demonstrated a hitherto unexpected solubility of

water in nitrogen, but these results await further confirmation; carbon dioxide has a relatively high solubility. In multicomponent liquids one component will have a higher vapour pressure and weathering will give rise to concentration gradients at the surface. Chatterjee & Geist[8] have discussed the effects of nitrogen in LNG as an agent to cause stratification.

Surface Morphology

Berg[21] has used schlieren techniques to examine the convective patterns in the free surface of pure liquids and the effect of layer depth and surface contamination. Four modes of convection are identified in his results: cells, streamers, ribs and vermiculated rolls. Cells are dominant in layers 2mm thick or less and the streamers appear when the liquid depth exceeds 7 or 8mm, being cold sheets of liquid plunging into the body of the liquid. In contrast to the cells these streamers move sluggishly about the surface. Ribs appeared in pure liquids without surface contamination and coexisted with the streamers. Vermiculated rolls were seen when the surface region contained a nonvolatile material of large molecular size.

When the base of the liquid is subject to velocity shear it has been observed that the convective pattern is aligned with the direction of flow and this was seen originally in Benard's experiments and by many others.

Berg, Acrivos & Boudart[16] carried out extensive investigations of the structure of the convective flows in ambient fluids as a function of the properties of the fluid, the depth of the pool and surface contaminants.

Three convective patterns were identified in pure liquids:

- Cellular flow in the form of hexagons where hot liquid rises in the centre of each cell, then cools and descends along the cell boundary. These cells appear with 2mm of the liquid surface.

- Streamers, along the length of which cold liquid descends to the bulk and hot liquid rises. These can be thought of a long circulating loops into the bulk of the liquid.

- Ribs, consisting of intersecting streamers where the cold fluid plunges from the surface to the bulk and between which hot liquid rises to the surface.

Fluids with low viscosity and low surface tension produced larger cells. The form of the streamer is shown in fig.3. Water did not exhibit rib or cell production, only streamers. This was attributed to surface contaminants.

Surface contamination, at levels as low as 10^{-9} moles/cm^2 was reported to exert a strong influence on the horizontal wavenumber and form of convective modes. When a

non-volatile component was present the convection exhibited vermiculated roll convection as shown in fig.4.

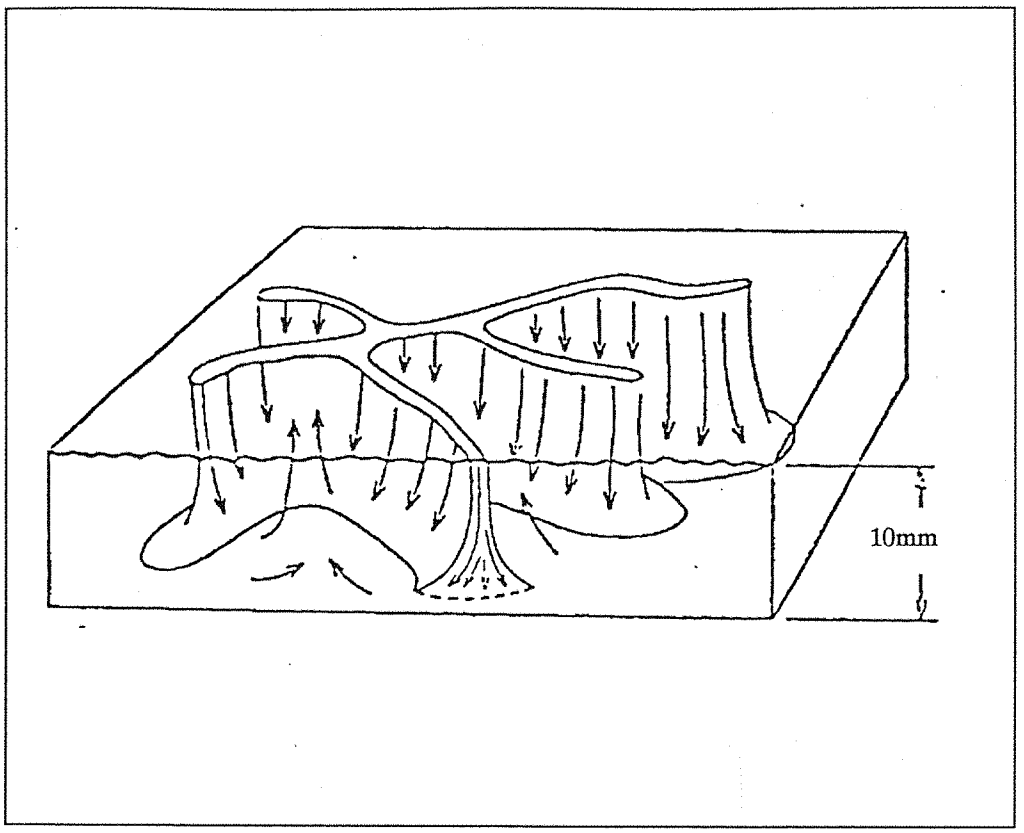

Fig. 3 Convective Streamers

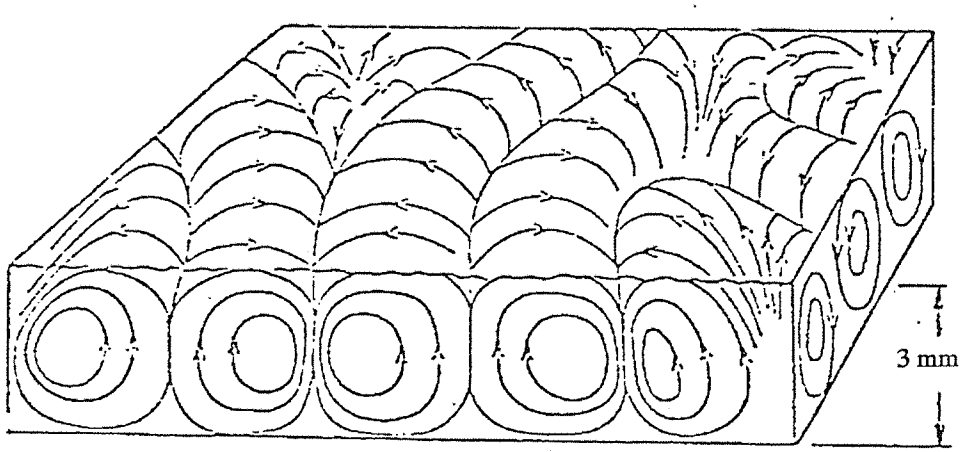

Fig. 4 Vermiculated Rolls

5. THE LIQUID-LIQUID INTERFACE

In stratified LNG tanks we are concerned with the interface between miscible liquids. At the interface there is both a temperature gradient and a compositional gradient. Since the major heat inleak into the tank is through the base, where support structures are sufficiently large to bear the weight of the tank, the lower layer will increase in temperature more rapidly as long as the heat flux through the interfacial layer is less than the total heat inleak through the base and lower walls of the tank. The initial stratification will be due to a stable configuration and thus the lower layer will also be more dense. The compositional gradient is thus stabilising and the temperature gradient destabilising. This situation has been variously termed double-diffusive convection, thermosolutal convection or thermohaline convection. The first term indicates a diffusive mechanism of mixing but the sense has been broadened, wrongly, by common usage to include mixing processes on a longer length scale; the situation may be considered double-diffusive since diffusion of the components act in an opposite sense on stability but the mixing processes are not confined to diffusive transport. The term 'thermohaline' reflects the origins of the study in oceanography and also the large number of results based upon saline/water systems. It is the differing molecular diffusivities of the heat and solute which gives rise to some interesting effects and attracts considerable interest from a wide range of investigators. Turner[11] gives a good account of the nature of double-diffusive convection and Narusawa[14] has discussed some aspects of double-diffusive convection in LNG tanks.

In an LNG tank that contains stratified liquid we have to consider instability of the liquid-liquid layer in the presence of turbulent convection from below arising from the heat inleak at the base and the lower walls. Rollover models have assumed a convective loop in the lower layer as in fig. 5. If this is so the interfacial stability must also be considered in terms of:

- Entrainment of the interface by the turbulent flow,
- Double-diffusive instability
- The hot boundary layer rising up at the walls and penetrating the interface.

Each of these three mechanisms can be considered in turn. For a given configuration the dominant mode which gives rise to large scale mixing will determine the criterion for rollover and the behaviour of the interface. In particular it will be seen in chapter 7 that:

- The interface moves upwards, away from turbulence in entrainment.
- The position of the boundary layer moves down as a consequence of boundary layer penetration.
- The interface may be expected to remain in its origin position if the mixing is purely diffusive.

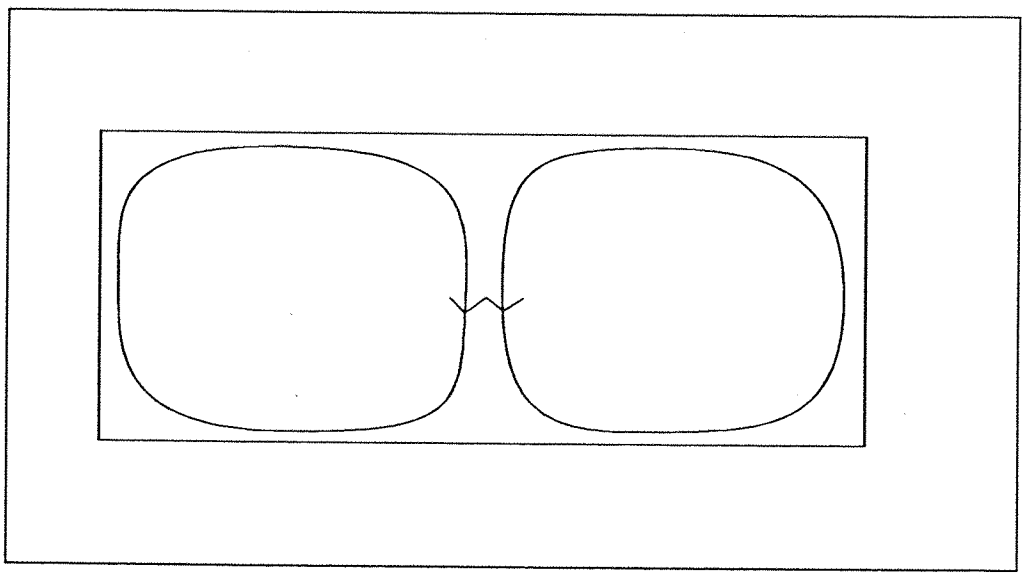

Fig.5 Conceptual Model of Convective Flow in Layer

INSTABILITIES IN THE LAYER

In considering an infinitesimal amplitude instability the limit is obtained by considering the marginal point, that is where the real part of the growth rate of the instability is zero. In fact there is considerable simplification in the analysis if the imaginary part is also set to zero, referred to as the principle of exchange of stabilities. This was shown to be correct by Rayleigh for the boundary conditions considered in his original paper and Pellew & Southwell[24] considered the possibility of oscillatory convective motion for a further set of boundary conditions and were able to show that the principle held for their systems.

In 1960 Stern[23] considered the double-diffusive system in a footnote to his paper discussing a salt fountain. He adjudged that the mode of instability would be oscillatory, i.e. the imaginary part would be non-zero. Free horizontal boundaries above and below are at fixed temperatures and solute concentrations with the gradients opposing such that solute is stabilising and temperature destabilising. The stability of the layer to infinitesimal disturbances is considered.

The density distribution to a linear approximation is:

$$\rho = \rho_m \left(1 - \beta_T \Delta T + \beta_S \Delta S\right) \tag{5-1}$$

where ρ_m is the mean density at a height z and is assumed to vary linearly from $z = 0$ to $z =$ h. The linearised Boussinesq equations (3-13) in two dimensions are expressed in terms of the stream function such that $u_x = \partial\psi/\partial z$ and $u_z = -\partial\psi/\partial x$ in a dimensionless form by scaling $z' = z/h$ and defining T and S relative to the mean linear gradients.

$$\left(\frac{1}{Pr}\frac{\partial}{\partial t} - \nabla^2\right)\nabla^2\psi = -Ra\frac{\partial T}{\partial x} + Rs\frac{\partial S}{\partial x} \tag{5-2}$$

Where Ra is the normal thermal Rayleigh number $g\beta_T \Delta T h^3/\alpha\nu$ and Rs is its solutal counterpart $g\beta_S \Delta S h^3/\alpha\nu$

The diffusion equations are:

$$\left(\frac{\partial}{\partial t} - \nabla^2\right)T = -\frac{\partial\psi}{\partial x} \tag{5-3}$$
$$\left(\frac{\partial}{\partial t} - \tau\nabla^2\right)S = -\frac{\partial\psi}{\partial x}$$

With the ratio of diffusivities represented by τ, the ratio of the solutal to the thermal diffusivity. The diffusivity of a solute in a liquid like LNG is typically ~ 10^{-9} while the thermal diffusivity ~ 10^{-6} hence τ ~ 10^{-3}. The boundary conditions are

$$\left\{\begin{array}{r} \psi = 0 \\ \dfrac{\partial^2\psi}{\partial z^2} = 0 \\ T = S = 0 \end{array}\right\}_{z\,=\,0,1} \tag{5-4}$$

Then a solution is sought that satisfies (5-4) in the form:

$$\psi \approx e^{\omega t}\sin\pi c x \sin\pi k z \tag{5-5}$$
$$T,S \approx e^{\omega t}\cos\pi c x \sin\pi k z$$

Here ω is the time constant of the solutions and hence can be used to identify the development of the perturbation.

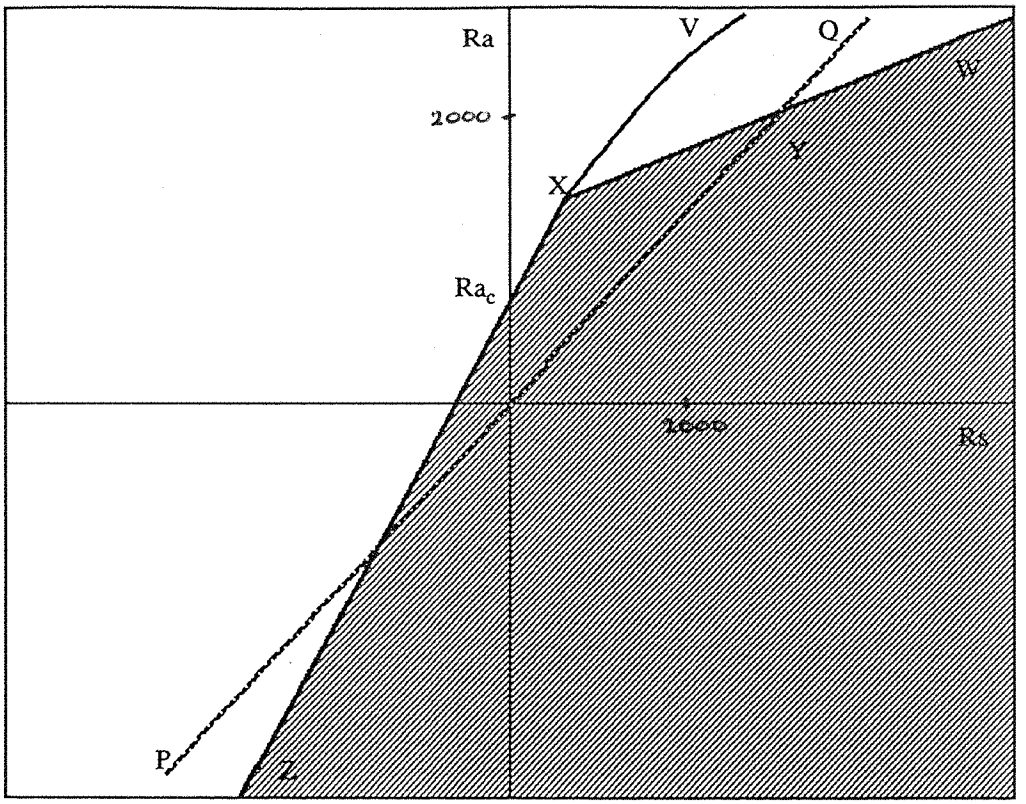

Fig. 6 The Plane Ra,Rs for Double Diffusive Convection

These are substituted in (5-2) and (5-3) to give an expression for ω:

$$\left\{\begin{array}{l}\omega^3 + \\ +\left(Pr+\tau+1\right)k^2\omega^2 + \\ +\left(\left(Pr+\tau Pr+\tau\right)k^4-\left(Ra-Rs\right)Pr\,\pi^2\frac{c^2}{k^2}\right)\omega + \\ +\tau Prk^6+\left(Rs-\tau Ra\right)Pr\,\pi^2c^2\end{array}\right\}=0 \qquad (5\text{-}6)$$

Minimising this solution for Ra with *real* $\omega = 0$, indicating the limit of the solution for stability, gives two solutions for Ra:

$$Ra=\frac{Rs}{\tau}+\frac{27\pi^4}{4} \qquad (5\text{-}7)$$

$$Ra=\frac{Pr+\tau}{Pr+1}Rs+\left(1+\tau\right)\left(1+\frac{\tau}{Pr}\right)\frac{27\pi^4}{4}$$

These are plotted in fig 6 and correspond to the lines XZ and XW respectively. The stable modes are shaded.

The vertical axis Rs = 0 corresponds to the single component system with onset of convection at Ra_c exactly the configuration considered by Rayleigh in his original paper.

From Ra = 0 to Ra_c viscous effects stabilise the liquid by damping the perturbations that would otherwise lead to convection. The upper right quadrant is the so called 'diffusive' regime where solute gradient is stabilising and temperature destabilising as in the case of the stratified LNG tank. The line PQ is the unit slope where Ra = Rs and density gradient due to solvent is balanced by thermal expansion leading to a constant density. For the case of $\tau << 1$ as would be expected for thermosolutal diffusivity the second line of (5-7) reduces to:

$$Ra = \frac{Pr}{Pr + 1} Rs + Ra_c \tag{5-8}$$

In this expression the constant term $27\pi^4/4$, which is the value for the critical Rayleigh number in the non-solutal case, has been replaced by Ra_c

In the area VXW the instability is characterised by $imag\ \omega > 0$ and is interpreted as the oscillatory mode of double-diffusive convection.

The following is a widely quoted qualitative description of the instability due to double-diffusive convection. [23]

The rate of diffusion of a solute is, in general, much less than that of heat. Consider a hot, concentrated solution underlying a cooler, less dense layer. There is a region where there is a strong compositional gradient and an opposing temperature gradient. A small element from the lower part of this region is perturbed into the upper part. The heat diffuses more rapidly out of the element than the solute, leaving the element cold and dense. The fluid element will then sink towards the lower layer and overshoot the starting position. As it absorbs heat again the cycle will be repeated giving rise to an oscillatory, or overstable motion. The effect of this motion is to transport heat by motion of the liquid. If there is a lag in temperature between the fluid element and its surroundings there is a net buoyancy force for most of the cycle and the oscillations will grow.

Along the line Ra_c-X the stability limit increases with Rs. Crossing this line results in a direct convective instability without the oscillatory mode of the VXW region.

It should be noted that the layer is stable in the shaded region between X and the line PQ despite the fact that density is increasing vertically through the layer. The stable region extends above the line Ra = Rs and thus density equalisation is not a sufficient condition for diffusive mixing of layers in this region. In this respect some of the LNG models discussed in chapter 2 are inconsistent. The Hashemi-Wesson model explicitly states that the surface layer of the cryogen is cooler, and hence more dense, than the bulk of the liquid. The single component system is hydrostatically unstable with a density increasing upwards and those rollover models which have adopted a diffusive mechanism of mixing have used density equalisation as the limit of stability.

For higher values of Rs the line XW crosses the line of equal density, PQ, at Y and thus at high solutal stability the interface is predicted to undergo an oscillatory instability, before it is statically unstable, with an enhanced diffusive transfer of heat corresponding to the description given earlier on page 38.

Fig.7 illustrates the development of the layer as the temperature difference across the interface is increased. In the limit of infinitesimal disturbances leading to rollover the state of the system starts in the shaded region of fig. 6 with Rs > 0 corresponding to fig.7. As the temperature of the lower layer increases due to base and lower wall heat inleak the system moves vertically until it reaches the line corresponding to Ra_c-W. In the region Ra_c-X the instability is to direct convection as in the solute free case. For X-W the instability is oscillatory leading to a transfer of heat but little solute if $\tau << 1$. If the convective heat transfer at the interface is less than the total lower layer heat inleak the

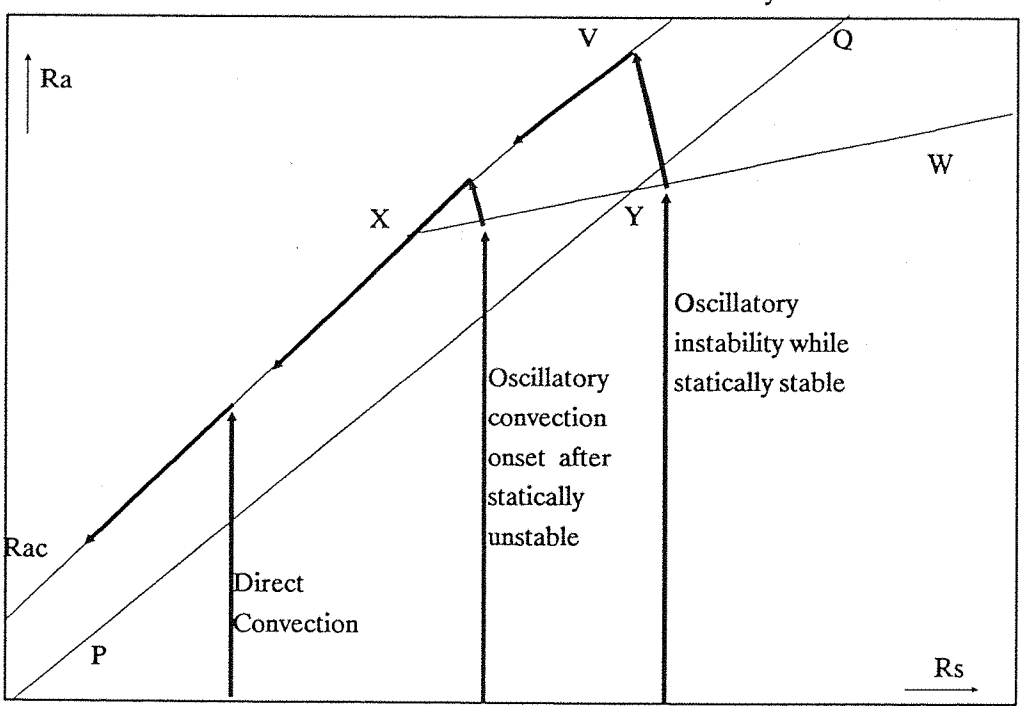

Fig.7 Paths of Instability for the Diffusive Quadrant

path will continue almost vertically to the line XV where direct instability will transfer heat and solute corresponding to a mixing of the layers. The paths corresponding to these developments are shown in Fig7as heavy lines, the lighter lines correspond to the lines in Fig.6.

The locus of points VXZ in fig.6, corresponding to $VXRa_c$ in the upper right quadrant shown in Fig.7, represents the limit of stability of the layers for infinitesimal perturbations.

Veronis[22] presented an analysis of the finite amplitude instability in a two-dimensional Boussinesq fluid which confirmed the ideas of Stern but predicted an oscillatory instability in the solutal case below the critical Rayleigh number for solute-free convection. Veronis described the velocity potential, temperature and salinity by a minimal form which could

take into account the finite amplitude motion and the distortion of the temperature and salinity field. Subsequently Veronis[27] found that the representation that had been used was insufficient to account for the variation in the temperature, salinity and velocity fields. In particular the oscillatory instability which had been predicted to occur for a lower critical Rayleigh number than the solute-free case was found to be absent.

This led to a system of five equations which are asymptotically exact to the Boussinesq equations to $O(a^3)$. If the salinity gradient is set to zero the equations reduce to the Lorenz[25] system for convective motion. Moore et al[26] have investigated the dynamical behaviour of this system.

HEAT AND SALT FLUXES THROUGH AN INTERFACE.

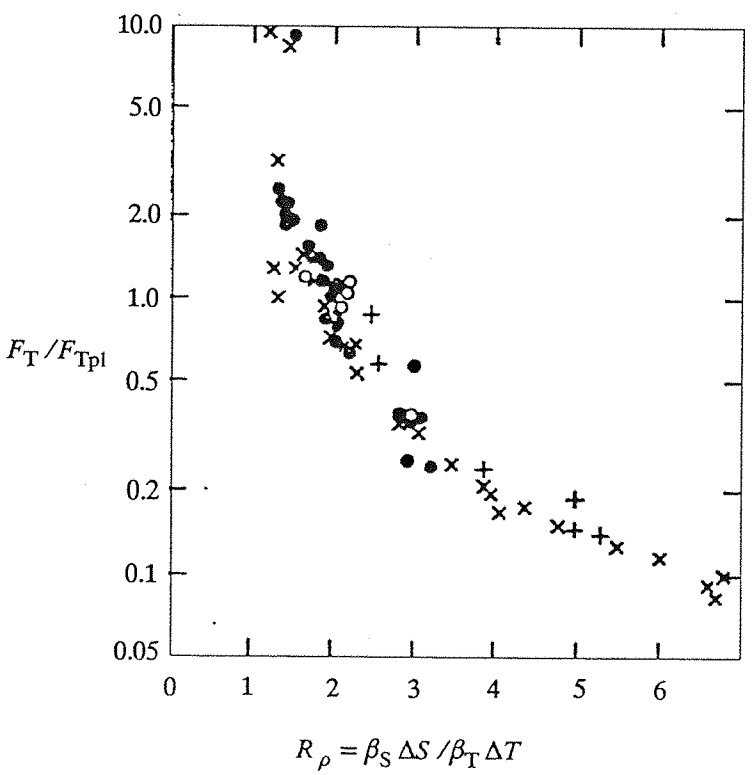

Fig. 8 Heat flux versus density ratio (Turner)

Here F_T / F_{Tpl} is the measured heat transfer compared with F_{Tpl}, the calculated value for a solid plane.

Turner's[33] experiments measured the heat flux and solute flux across a double-diffusive interface for a system where cold fresh water overlays hot brine and these results have been used in several of the models of LNG rollover. These are reproduced in figures 8 and 9.

The heat transfer coefficient is defined as:

$$h_T = \frac{Q_T}{A\,\Delta T} \tag{5-9}$$

where Q_T is the heat transfer rate and the heat transfer velocity is defined as :

$$U_T = \frac{h_T}{\rho C_p} = \frac{Q_T}{\rho C_p A\,\Delta T} \tag{5-10}$$

Then the quantity F_T (the ratio of heat flux to fluid specific heat) is defined as $F_T = U_T \Delta T$ with similar definitions for the solute case.

In a later publication Turner[11] warns that the heat fluxes reported for low stability values may be unreliable.

Starting from the relation of the Nusselt number to the Rayleigh number for convection (4-1) and considering the flux through the interface as a function of the thermal and solutal Rayleigh numbers, Turner suggests an equivalent relation for diffusive thermohaline fluxes.

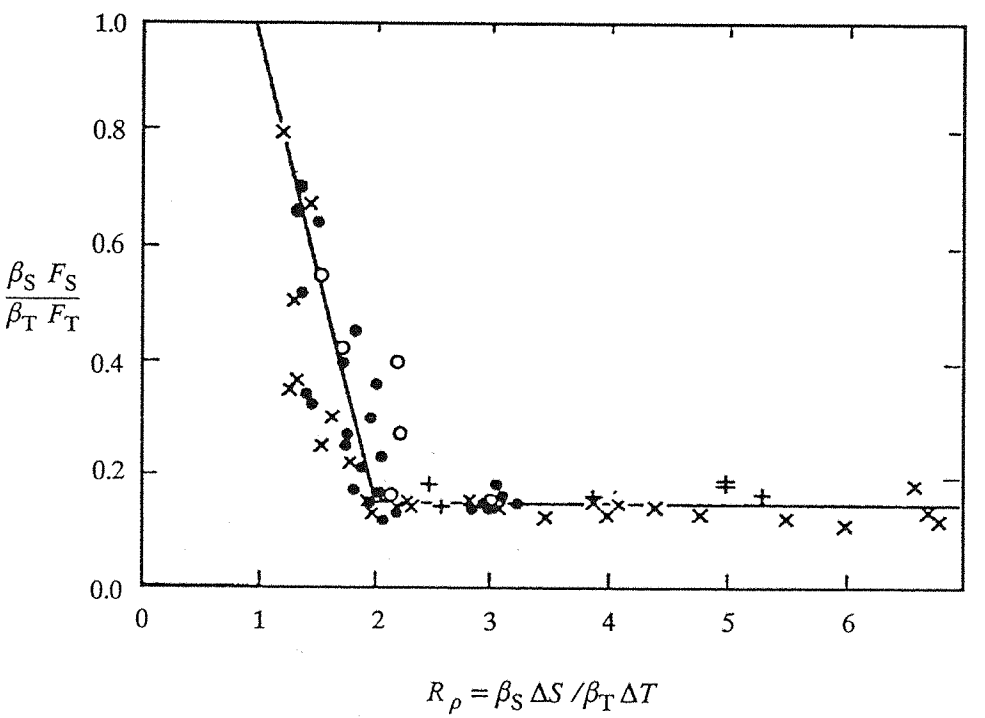

Fig. 9 Potential energy change vs density ratio (Turner)

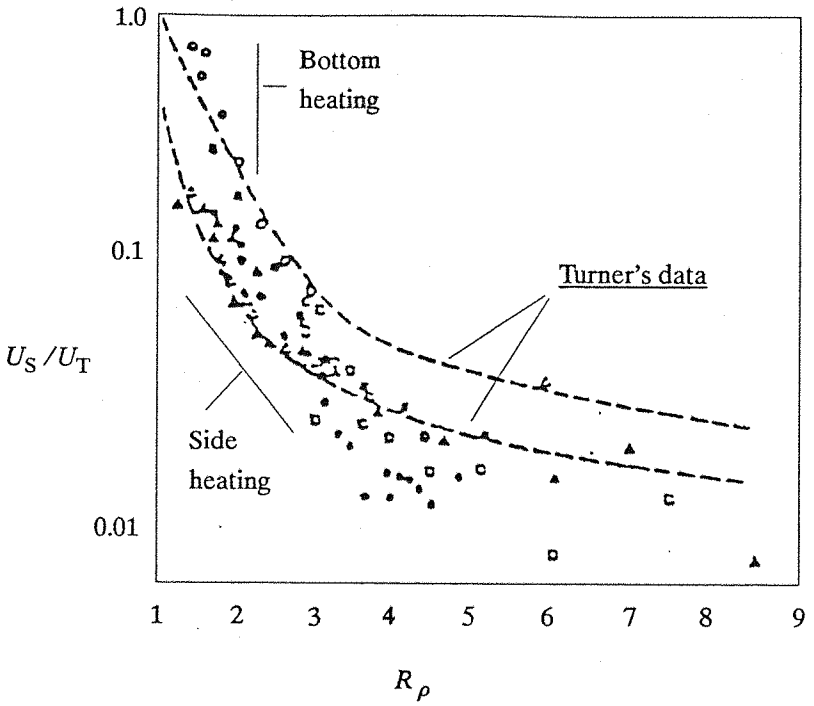

Fig.10 Ratio of solute flux to heat flux through interface

$$N = f_1\left(\frac{\beta_s \Delta S}{\beta_T \Delta T}\right) Ra^{1/3} \tag{5-11}$$

Where $\beta_s \Delta S/\beta_T \Delta T = Rs/Ra = R_\rho$ is the density, or stability, ratio. Then using the definitions of Ra in a similar way to Hashemi-Wesson, page 26, the heat flux is expressed in terms of the temperature difference across the layer and the stability ratio.

$$\beta_T F_T = C_1 \left(\beta_T \Delta T\right)^{4/3} \tag{5-12}$$

Here C_1 is a constant with the dimensions of velocity. Expressing the ratio C_1/C where C is the constant for an equivalent system with a thin conducting foil through the centre of the interface gives a measure of the effect of ΔS on the heat flux. It is important to note in fig.8 that below $R_\rho = 2$ the heat flux ratio is greater than 1 and it is suggested that this is due to the behaviour of the interface as a free surface with mixing effects. This indicates that in Turner's system the limit $R_\rho = 2$ represents the upper bound of internal mixing effects. From some point $R_\rho < 1$ which is the theoretical lower bound for stability of a viscid layer to infinitesimal perturbations shown in figure 6 to the upper limit $R_\rho = 2$ the heat and solute are transported by turbulent motions. As $R_\rho \rightarrow 1$ in fig.9 it is evident that $\beta_S F_S / \beta_T F_T \rightarrow 1$ indicating that heat and solute are being transported by the same mechanism

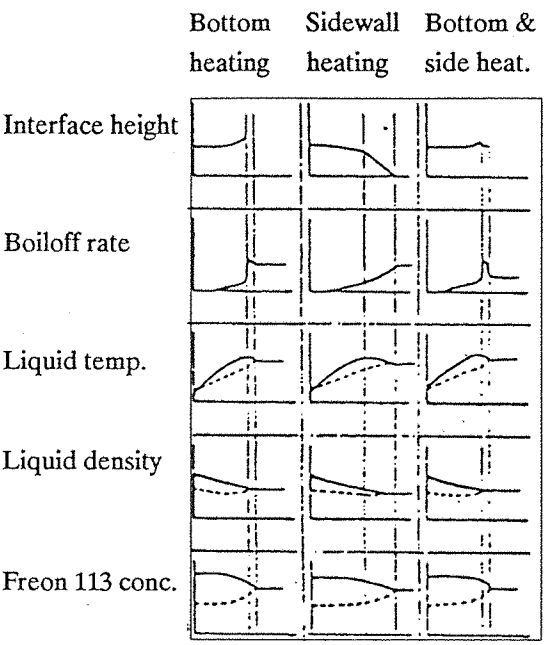

Fig.11 Effect of bottom vs sidewall heating (Nakano)

Huppert[29] fits the experimental data in fig.8 to a form

$$\frac{C_1}{C} = 3.8\left(\frac{\beta_S \Delta S}{\beta_T \Delta T}\right)^{-2} \tag{5-13}$$

which was used in the Germeles[2] model, though Chatterjee & Geist[1] had already used Turner's data directly in their modelling of LNG rollover.

Heat Flux Between Hot Brine Below and Cold Fresh Above

Baines & Gill[28] point out that Goroff's[30] experiments on convection restrained by rotation did show an increase in Nusselt number at the point where linear theory predicts the onset of direct, convective instability and suggest that this is evidence for the overstable mode of instability being less efficient in transporting heat than the convective mode.

Nakano & Sugawara[36] have reported on the mixing of stratified freons in a rectangular tank with combinations of base heating and wall heating. It was noted that the time to mixing of the layers was shortened as the heat inleak into the lower cell was increased. With bottom heating, and evidently some wall heat inleak to produce boundary layer flow,

the mixing process proceeded by intrusion of the side wall boundary layers into the upper cell and liquid from the upper cell descended through the centre of the interface; the mixing process, from the onset of mixing, was completed rapidly. The published results indicate that 'bottom heating induced mixing' started when the densities were nearly equal, in contrast to sidewall heating.

When side wall heating was used the boundary layer again penetrated into the upper cell but the mixing process was developed more slowly with no intrusion of the upper cell into the lower; the interface descended slowly in the tank and the total time for mixing was greater than in the case of bottom heating only. In this case the boundary layer incident upon the interface was sufficient to carry lower layer material into the upper layer which

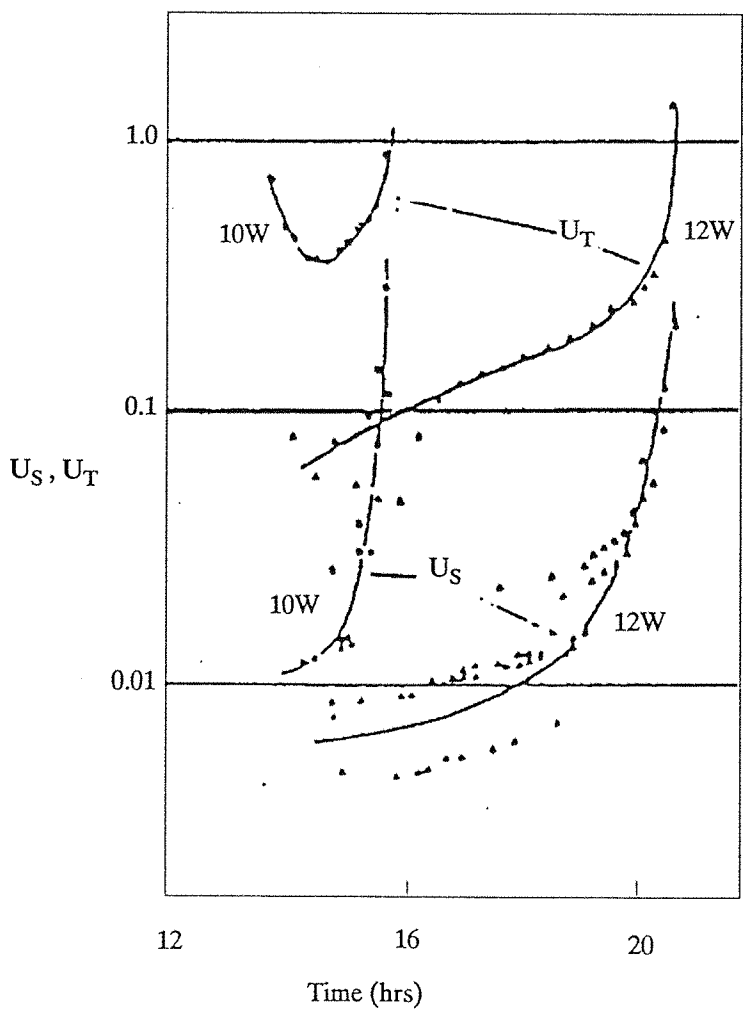

Fig. 12 Results from the Nakano study

Four sets of data and fitted lines are shown here, they are heat flux velocity and solute flux velocity for experiments at 10 W and 12W. Note that the heat and solute flux velocities for each experiment approach a common trend later in the runs, indicating a common mode of heat and solute transfer.

accounts for the longer period of mixing. The time to onset of mixing is reduced compared to the bottom heating results.

It is apparent from the above results that the onset of mixing at the interfacial layer depends upon the circulatory flows induced by the heat inleak into the lower layer. Once large scale mixing is initiated the rate at which rollover proceeds is a function of how heat enters the lower layer. The measurements of Nakano & Sugawara, analogous to the Turner data are reproduced as figures 10 and 11. Turner's data does not exhibit such a dependency on the rate of heating of the lower boundary.

Mixing at Low Stability Ratios

The large scale mixing effects which occur at low stability ratios dominate heat and mass transfer as can be seen in Turner's data, figure 9. In the rollover test reported by Sugawara *et al*[7] on an actual LNG tank it is reported that entrainment of liquid was the dominant mechanism, though movement of the interface was reported in both directions. In laboratory scale tests with freons Nakano *et al*[36] the interface was seen to move downwards with sidewall heating while with bottom heating the interface hardly moved at all; the boundary layer penetrating through the interface in both cases. It seems therefore that both penetrative convection and entrainment must be considered as candidate mechanisms for the rapid mixing at rollover.

Penetrative Convection

Chatterjee & Geist[8] first considered the penetration of the interfacial layer by hot fluid from the lower layer having sufficient buoyancy to reach the upper surface. The condition for the boundary layer flow to fail to reach the liquid/vapour interface being a sufficient one for the formation of stable stratification. In an appendix to the above paper the estimated velocity of boundary layer flow is used to determine the time to circulate the contents of the tank. The result obtained for a 15.2m liquid depth is 8 hr which is of the same order as the time scale of high vapour generation during actual rollover events. Chatterjee & Geist also point out that the liquid in the boundary layer penetrating the interfacial layer will also be entrained but do not explicitly consider penetration as the mechanism of mixing of the layers.

Nakano *et al*[36] have observed the mixing of stratified layers of freons. They observed that the convective flow in the boundary layer penetrated the interfacial layer and the interface descended. Two modes of penetration were observed and identified in the paper.

'Rapid mixing pattern' was seen with bottom heating. A slight upward motion of the interfacial region was observed at first and then the wave motion in the interfacial region became large. The liquid in the lower layer rose up the walls of the containing vessel and reached the liquid surface. The upper liquid descended through the central region of the tank and total mixing occurred.

'Boundary layer penetration pattern' was associated with side wall heating. The boundary layer was seen to penetrate the interfacial layer and mix with the upper layer. As a result the liquid/liquid interface descended slowly and eventually reached the base of the vessel.

This form of mixing was observed to take considerably longer than the 'rapid mixing pattern'. Nakano does not comment on the appearance of wave motions in the interfacial region in this mode.

A combination of side wall and base heating achieved intermediate results apparently depending upon the intensity of convection in the boundary layer. The mixing time scale was seen to be 2-5 minutes for 'rapid mixing' and of the order of 20 minutes for 'boundary layer penetration'.

The results of heat and mass transfer from the Nakano[36] study are reproduced in fig.12 for bottom heating at two heat fluxes. It can be seen that the mass and heat transfer rates approach as time progresses indicating a common mechanism of transfer and the lessening influence of diffusion.

The Effect of Side and Base Heating on Mixing

It seems that a form of penetration of the incident boundary layer through the interfacial layer accounts for the fall in level of the liquid/liquid interface seen previously by Sugawara[7] and the comments made by Nakano indicate that there may have been some entrainment in the runs where heat was applied to the test vessel through the base, since the interface was seen to rise at first, the interface accelerated, and wave motions were observed. The most rapid mode of mixing occurred when the boundary layer was able to penetrate the interface.

It is apparent from the data reported by Nakano, shown in fig.10 that side wall heating initiated mixing before the densities of the upper and lower layers were equal whereas bottom only heating caused the onset of mixing when the layers were very close to equal density. It can also be seen in fig.11 that sidewall heating alone produced almost no peak in boiloff gas rate.

These results suggest that, in the case of an actual LNG tank, the worst case would occur when the lower layer is superheated to a point where densities become nearly equal. Some entrainment may then occur at the interface and the buoyancy flux through the interface is large, perhaps occurring at a rate determined by the case of a near homogeneous fluid. The boundary layer may then penetrate the interfacial region and reach the surface causing rapid mixing of the tank contents. In this way the maximum superheat is achieved in the lower layer before mixing occurs. Conversely if predominantly side wall heating is used in experimental observations the mixing process will be initiated by boundary layer penetration into the upper layer before the densities become equal.

Buoyant Plumes in LNG Storage Tanks

It is apparent from the above discussion of mixing patterns seen in test tanks that the mixing process is on a larger length scale than diffusion and that fluid flows in the bulk liquid instigate the mixing process. Buoyant plumes will occur at the wall as a boundary layer and in the centre of a cell. If there is an established convective flow pattern in a cell of the tank Beresford[48] has demonstrated a central downflow in the centre of the bulk. If

there are convective flows in adjacent cells we can see that the interface between the cells, considered here to be a sharp interface, will suffer a vertical plume acting on the upper surface and liquid in the lower cell will flow down and away from the centre of the underside of the interface. As the plume impinges on a stable interface the flow spreads into a horizontal layer. Similarly the inwardly directed boundary layer flow in the lower cell flows radially towards the central region before being directed downwards forming the central jet. The maximal velocity shear across the interface must be, by continuity arguments, near the centreline of the tank.

The height, or depth, to which a fluid element will penetrate, neglecting frictional forces and entrainment with the surroundings, can be seen by energy considerations to be determined by the velocity of the element, its density and the density of the surrounding fluid. Where h is the depth of penetration, u is the velocity of the element, ρ_2 is the density of the element and ρ_1 is the density of the surrounding fluid:

$$\frac{u^2}{2g} = \frac{h(\rho_2 - \rho_1)}{\rho_2} \tag{5-14}$$

As part of a study into the development of stratification in LNG tanks Germeles[13] investigated the mixing of a tank when new liquid of differing density is injected into a partially full tank following the theoretical model of Morton[45]. The aim of this work was to elucidate the mechanisms of stratification subsequent to filling procedures and as such the mathematical theory primarily considered a buoyancy driven upward central jet entering horizontally from near the base of the tank. Other configurations are also considered including the wall effect for a plume close to the wall and inclined plumes. The mathematical predictions were then tested in laboratory scale tanks and a good agreement was found between predictions and experiment supporting the assumptions made.

Three main assumptions are made:

- The rate of entrainment at the edge of the plume is proportional to some characteristic velocity at that height.
- The profiles of the mean vertical velocity and mean buoyancy force in horizontal sections are of similar form at all heights.
- The local variations in density in the field of motion are small compared to the reference density taken to be the ambient density at the base of the plume.

The plume diameter grows as surrounding fluid is entrained into the body of the plume and thus the density of the developing plume front will approach that of the surrounding medium. The transfer of matter between the medium and the plume are caused by eddies

characterised by the relative velocity of the plume edge and the medium. For the downward jet seen in convecting cryogenic vessels the minimum diameter and highest velocity of the plume is just below the upper surface where, by the first assumption, the rate of entrainment will be greatest and this indicates why the bulk liquid is so well mixed and uniform in temperature as will be seen in chapter 7. Morton[45] gives the conservation equations of volume(5-16), momentum(5-17) and density deficiency (5-18) for a Gaussian velocity and buoyancy distribution in the plume:

$$u(r,z) = u(z)\, e^{-r^2/b^2} \tag{5-15}$$

$$g\frac{(\rho_o - \rho)}{\rho_1}(z,r) = g\frac{(\rho_o - \rho)}{\rho_1}(z)\, e^{-r^2/b^2} \tag{5-16}$$

where b is the plume diameter defined as the characteristic length for the Gaussian distribution such that values fall off as 1/e and the conservation equations, integrated over a horizontal section of the plume, are

$$\frac{d}{dz}(\pi b^2 u) = 2\pi b\, \alpha u \tag{5-17}$$

$$\frac{d}{dz}\left(\frac{\pi}{2} b^2 u^2 \rho\right) = \pi b^2 g(\rho_o - \rho) \tag{5-18}$$

$$\frac{d}{dz}\left(\frac{\pi}{2} b^2 u(\rho_o - \rho)\right) = \pi b^2 u \frac{d\rho_o}{dz} \tag{5-19}$$

where ρ and ρ_o are the densities inside and outside the plume respectively . The plume diameter b = b(z).

The above equations may then be rearranged and higher order terms in the density dropped to give:

$$\frac{d}{dz}(b^2 u) = 2\alpha b\, u \tag{5-20}$$

$$\frac{d}{dz}(b^2 u^2) = 2b^2 g\, \frac{\rho_o - \rho}{\rho_1} \tag{5-21}$$

$$\frac{d}{dz}\left(b^2 u g\, \frac{\rho_o - \rho}{\rho_1}\right) = 2b^2 u\, \frac{g\, d\rho_o}{\rho_1\, dz} \tag{5-22}$$

For the case of a plume in uniform density surroundings then $\rho_o = \rho_1$ and the r.h.s of (5-21) vanishes so that:

$$b^2 u g \frac{\rho_1 - \rho}{\rho_1} = constant \tag{5-23}$$

so that the vertical flux of buoyancy, that is the flux of density = $\Delta\rho\, g\, u/\rho_o$, is constant at all heights.

If we consider the boundary layer flow vertically incident on the interface in a stably stratified configuration so that the density increases with height then the body force acting on the plume will reduce the momentum of the plume and bring it to rest. Following the first assumption that the entrainment is proportional to the velocity we see that the entrainment at the slowing front will not be large and the plume will fall back as it spreads sideways.

ENTRAINMENT

In the previous sections entrainment has been shown to play an important part in the bulk of the liquid and in the mixing mechanisms whether by buoyant boundary layer plumes incident on the liquid-liquid interface or from the central jet incident downwards onto the interface or even potentially as the velocity shear across the interface increases with convection in the upper and lower bulk liquids.

Most experiments on entrainment and liquid-liquid layers involve an oscillating grid near the interface. It is observed that a well mixed layer is formed, bounded by a sharp interface, and the interface moves away from the source of the turbulence, Cromwell[37]. In the case of two sources of turbulent energy with an interface in the region between the sources it is observed that the interface will move away from the strongest source such that the movement halts once there is a balance of entrainment on each side of the interface.

The circulatory flow in a layer is driven by the vertical temperature gradient in the layer. In the case of a cryogenic storage tank the driving force for stirring in the bottom layer would be the heat inleak, which is predominantly from the base of the tank, driving a circulatory flow as the lower layer warms. This flow may switch off if the temperature gradient is insufficient to maintain convection i.e. the Rayleigh number is too small. Turbulent energy will only be incident on the upper side of the interfacial layer once sufficient heat transport is achieved through the liquid-liquid interface to drive a convective loop in the upper layer. It is therefore reasonable to expect that the interfacial movement would be upwards as liquid is entrained into the lower layer.

Four principal mechanisms have been proposed for the entrainment process. These are illustrated in fig.13 and will become important in interpreting the schlieren observations in chapter 7.

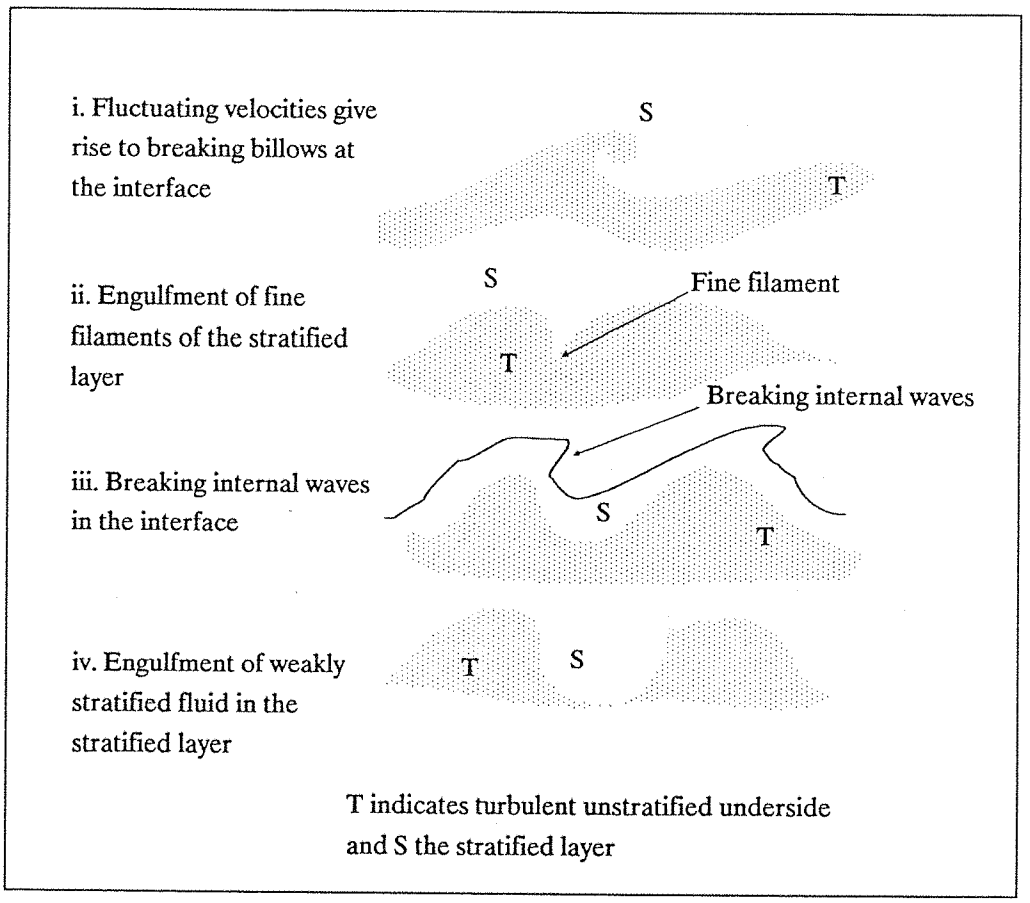

Fig 13 Modes of entrainment

In fig. 13.i. turbulent eddies are incident upon the interfacial region and the local gradient Richardson number, Ri, given by

$$Ri = -g\frac{\partial \rho/\partial z}{\rho\left(\partial u/\partial z\right)^2} \tag{5-24}$$

is sufficiently small for Kelvin-Helmholz billows to grow and break. As Long[40] has pointed out this mode of mixing would be expected when the interface is strongly stable and the vertical turbulent scale is damped at the interface. In the case of the shear flow at the interface due to bulk convective flows in the upper and lower layers the velocity gradient will be maximum near the centreline of the vessel.

Fig. 13.ii shows the turbulence is sufficiently energetic for the eddies impinging on the interface to distort the stratified layer and entrap fine filaments of the stratified material into the bulk where short lengthscale viscous effects then complete the mixing process. For the incident eddies not to engulf the stratified layer the density gradient must be strongly stable.

In fig. 13.iii the eddies incident upon the interface set up internal waves in the interface and these waves then break causing mixing in the interface, collapsing the density gradient inside the stratified layer.

Fig .13.iv shows an extension of the mechanism proposed in fig. 13.ii but the stratification in the interface is sufficiently weak for the incident eddies to engulf portions of the interface by inducing large motions in the interface.

Turner[38] describes the observed mechanism of entrainment in his saline/water experiments, the results of which are shown in fig.8 and fig.9. Large eddies of the stirred fluid are thrust into the unstirred liquid, trapping some of the latter, while the smaller eddies are rapidly damped. The eddies that dominate the entrainment process are larger than the thickness of the interface and remain largely outside the interfacial layer. The whole process looks like the breaking of steeply forced waves and the sweeping away of the mixed fluid which again sharpens the interface. Within the density gradient Grigg & Stewart[39] have demonstrated that the largest scale motions are suppressed first and the smaller scale turbulence is practically unchanged. This latter observation is important in explaining the effect of the sidewall boundary layer incident on the interfacial region as well as the lack of penetration of large scale eddies into the density gradient. When stirring is performed on both sides of an interface Turner[11] reports that the mixing rate is not substantially changed and hence the large scale turbulent eddies are strongly damped in the interface; this supports the observations of Grigg & Stewart.

It can be noted here that Turner refers to the system as double-diffusive though clearly the mixing mechanism is not diffusive. This is not in error, as explained at the start of this chapter, but workers who have modelled rollover processes have confused the terminology.

The interfacial region is typically seen to be typified by wave motion, Wolanski & Brush[42], with a frequency proportional to the Brunt-Vaisala, or buoyancy, frequency.

$$\omega_{BV} = \left(g \left(- \frac{\partial \bar{\rho} / \partial z}{\bar{\rho}} \right) \right)^{1/2} \qquad (5\text{-}25)$$

Experimental observations suggest that the interfacial region consists of intermittent turbulent patches caused by the sporadic breaking of the internal waves and that those patches which are at the boundary between the interfacial layer and the homogeneous layer are responsible for the transport of buoyancy.

The large scale motions will not be damped as the gradient of the density in the interfacial region approaches zero, i.e. the case where the densities of the upper and lower layers become equal. Thus entrainment mixing should be operative before the onset of convection within the mixing layer and the criterion for the onset of rollover for an entrainment mechanism of mixing is that the densities of the lower layer is close to, or equal to, the density of the upper layer provided that their are convection processes in the upper or lower layers to provide the energetic eddies.

Considering the mixing process as a balance between buoyancy forces and inertial forces only, Turner[11] shows that the ratio of the entrainment velocity to the r.m.s of the horizontal component of the turbulent velocity will be a function of an overall Richardson number which is consistent with his observations of the mechanism of breaking waves in the interface depicted in fig 13.i.

$$\frac{u_e}{u_1} = f\left(Ri_o\right) \tag{5-26}$$

In the case of no-shear entrainment experimenters have suggested a relationship:

$$\frac{u_e}{u_1} \propto Ri_o^{-3/2} \tag{5-27}$$

while experimental simulations of entrainment with shear suggest an exponent near -1.

Sugawara et al[7] considered this relationship in their observations of the rollover process in an LNG tank and concluded, from the fit to the data points, that entrainment was the dominant mechanism in the movement of the interfacial layer. They also found that their experimental results fit a -1 exponent well though do not comment on this agreement in the text of their paper. The interfacial layer moved downwards and accelerated as the system proceeded to rollover; this is in contrast to what would normally be expected for entrainment mixing where the interface should move away from the source of turbulent energy.

Long[40] has developed a theory for mixing in a stably stratified fluid and large Richardson numbers in the absence of shear. The nature of the entraining interface and the original theory have recently been examined in an experimental study by Fernando & Long[41] where the turbulence in one layer was produced by a horizontal grid oscillating vertically with small amplitude. The latter paper showed good agreement with Long's earlier theory at high stabilities, indicating a -7/4 power law dependency of the entrainment coefficient for Richard son numbers $5x10^{-2}$. At low Richardson numbers the entrainment coefficient is independent of the Richardson number indicating that large scale eddies are responsible for the entrainment, these larger eddies do not flatten when they impinge on the interface.

Variation of Entrainment with Richardson Number

In the work by Fernando & Long[41] some conclusions are also drawn on the nature of entrainment mixing at low stabilities. In particular it is concluded that entrainment, in the case of an homogeneous fluid, is via large-scale eddies rather than the viscous diffusion of vorticity. Either way the progression of a turbulent front follows a $t^{1/2}$ law, as originally observed by Dickinson & Long[43]. Following the above argument, based upon the role of the large scale eddies in entrainment, a condition is determined for the rate of progression of the interface and the transition from a $t^{2/11}$ dependency to the quasi-homogeneous case when the interface moves with a dependency of $t^{1/2}$. It is noted that after a certain lower,

homogeneous, layer depth is exceeded the results obtained by Fernando & Long[41] deviate from Long's theory and the conjecture is made that this may be due to a wall effect.

Thus in the case of an entrainment mechanism of mixing in an LNG tank, ignoring shear and any wall effect, we would expect to see an acceleration of the interfacial layer as the density jump across that layer becomes small and large scale eddies dominate the transfer of buoyancy.

Gravity Waves In The Interface

We are interested in the behaviour of the interface as it is perturbed from its equilibrium position and, in particular, the nature and form of the oscillations at the interface.

An incompressible, inviscid and irrotational approximation for the fluid is used. First the form of the solution and then the boundary conditions will be applied.

If the fluid is irrotational we can introduce the scalar velocity potential:

$$\mathbf{v} = \nabla\varphi \tag{5-28}$$

For an incompressible fluid $div\,\mathbf{v} = 0$ so that:

$$\Delta\varphi = 0 \tag{5-29}$$

A solution for φ is sought that satisfies the wave equation:

$$\frac{\partial^2\varphi}{\partial t^2} = \kappa^2\,\nabla^2\varphi \tag{5-30}$$

In the normal separation of variables way we set $\varphi = UT$ where U is the spatial dependence and T the time dependence, then:

$$\frac{T''}{T} = constant = -\,c_T{}^2 \tag{5-31}$$

for which the general solution is:

$$T = c_1\,e^{\,ic_T t} + c_2\,e^{\,-ic_T t} \tag{5-32}$$

For the spatial component then

$$\kappa^2\,\frac{\nabla^2 U}{U} = -c_T{}^2 \tag{5-33}$$

and set $k = c_T / \kappa$ so $\nabla^2 U + k^2 U = 0$. Cylindrical polar coordinates are appropriate for the LNG tank and we take $z = 0$ at the liquid/liquid interface. The free surface is at h' and the base of the tank is $z = -h$. The tank wall is $r = a$.

Then separating the spatial variables further as $U = \mathrm{F}(r)\ \mathrm{Z}(z)\ \Phi(\theta)$ in (5-33) so that

$$\ddot{\mathrm{Z}} = -c_z{}^2 \mathrm{Z} \tag{5-34}$$

$$\ddot{\Phi} = -c_\Phi{}^2 \Phi$$

$$r^2 \ddot{\mathrm{F}} + r\dot{\mathrm{F}} - \left(\left(c_z{}^2 - k^2\right) r^2 + c_\Phi{}^2\right) \mathrm{F} = 0$$

The last equation of (5-34) is Bessel's equation and requiring F(0) = 0 thesolutions are

$$\varphi = C\, e^{\pm i\left(c_z z \pm c_\Phi \theta \pm c_T t\right)} J_{c_\Phi}\left(\sqrt{k^2 - c_z{}^2}\, r\right) \tag{5-35}$$

Here c_Φ must be integral since $\varphi(\theta) = \varphi(\theta + 2\pi)$ and if circular symmetry is sought $c_\Phi = 0$. At the wall of the tank the velocity must vanish and therefore the argument of the Bessel function must be such that it is a root of the function at r = a. This is the form of the solution.

Boundary conditions:

At the interface the normal components of the velocity must be equal

$$\frac{\partial \varphi}{\partial z} = \frac{\partial \varphi'}{\partial z}\bigg|_{z=0} \tag{5-36}$$

At the base of the tank the normal component of the velocity vanishes.

$$\frac{\partial \varphi}{\partial z} = 0\bigg|_{z=-h} \tag{5-37}$$

At the free surface and the interface the pressure must be continuous. For irrotational flow Eulers equation (3-11) is :

$$\frac{\partial \varphi}{\partial t} + \frac{v^2}{2} + w = f(t) \tag{5-38}$$

As the potential is not uniquely defined f(t) can be set to zero and for incompressible flow w is replaced by p/ρ and a gravitational term gz.

$$\frac{\partial \varphi}{\partial t} + \frac{v^2}{2} + \frac{p}{\rho} + gz = 0 \tag{5-39}$$

Now assume that velocities are small and drop the terms in v^2.

$$p = -\rho g z - \rho \frac{\partial \varphi}{\partial t} \tag{5-40}$$

The pressure at the surface is constant so set p = 0. For $z = \zeta$ such that at equilibrium $\zeta = 0$ and ζ is of the form of a vertical displacement of the surface then

$$u_z = \frac{\partial \zeta}{\partial t} \tag{5-41}$$

and $u_z = \partial\varphi/\partial z$ then from (5-40) at $z = \zeta$ by differentiating with respect to t

$$\frac{\partial \varphi}{\partial z} + \frac{1}{g}\frac{\partial^2 \varphi}{\partial t^2} = 0 \Big|_{z=\zeta} \tag{5-42}$$

If the oscillations are small at the surface the derivatives can be taken at $z = h'$.

For the interface from (5-40) in a similar manner:

$$\rho g \zeta + \rho \frac{\partial \varphi}{\partial t} = \rho' g \zeta + \rho' \frac{\partial \varphi'}{\partial t} \tag{5-43}$$

for $u_z = \partial\varphi/\partial z = \partial\zeta/\partial t$ and $\partial\varphi/\partial z = \partial\varphi'/\partial z$ at z = 0 so that:

$$g(\rho - \rho')\frac{\partial \varphi}{\partial z} = \rho' \frac{\partial^2 \varphi'}{\partial t^2} - \rho \frac{\partial^2 \varphi}{\partial t^2} \tag{5-44}$$

The Specific Form

Now we can write down a form of the solution for φ and φ' for the lower and upper layers of liquid noting that the above boundary conditions specify the system in terms of z. For clarity the radial components of (5-35) are set to χ and k, the wave number, has been substituted as notation for c_z with circularly symmetry considered.

$$\varphi = \left(A e^{kz} + B e^{-kz}\right) e^{i c_T t} \chi \tag{5-45}$$

$$\varphi' = \left(C e^{kz} + D e^{-kz}\right) e^{i c_T t} \chi$$

These can be substituted into the expressions for the boundary conditions giving three equations in three unknowns that can be solved generally to give a rather large expression for the constants and a dispersion relation obtained for c_T and k. If the lower layer is deep this approximates to two solutions :

$$c_T{}^2 = kg \frac{(\rho - \rho')\left(1 - e^{-2kh'}\right)}{\rho + \rho' + (\rho - \rho') e^{-2kh'}} \quad \text{and} \quad c_T{}^2 = kg \tag{5-46}$$

where the second solution is that of waves independently propagated on the free surface for the condition that the upper layer is very deep. In this case the first solution approximates to:

$$c_T{}^2 = kg \frac{\rho - \rho'}{\rho + \rho'} \tag{5-47}$$

so for a given wavenumber k the time constant, or frequency, of the gravity wave will become small as the densities approach.

6. EXPERIMENTAL METHODS

A CHRONOLOGY

As can be seen from a theoretical analysis and an examination of the published literature the central system in a rollover situation is the liquid/liquid interface between two cells. An understanding of the statics and dynamics in this region should reveal the mechanism of stratification and rollover. The cell itself, we believe, is probably homogeneous and the boundary layer flow at the wall has every indication of being the same as a boundary layer flow in an unstratified vessel except in so far as the height to which the flow rises is limited by the top of the cell. At the top of the cell the buoyancy induced flow impinges on the density gradient and a radially inwards flow results. The interaction of the boundary layer and the cell top is of prime interest and yet there is little known about how a boundary flow meets the free surface.

The structure of the non-boiling cryogenic free surface is not well understood and models have relied upon ambient data. In reality this surface is very different from a surface with no evaporative mass flux and the fact that the topmost cell has a surface in equilibrium with the vapour space affects that top cell and consequently the rest of the stratified system.

It was recognised at the outset that a laboratory model with a liquid/liquid interface would be needed. Using nitrogen and nitrogen/argon mixtures rather than LNG solved a problem of safety without recourse to less available cryogens. Early attempts used a technique of freezing a mixture of nitrogen and argon into a solid plug that could be covered with liquid nitrogen and allowed to melt forming a denser lower layer. This procedure was difficult in the manufacture and handling of the solid plug. It was possible to produce a plug of high argon content but the super-stable layers that were so formed would not become unstable until a point was reached that the layer would experience nucleate boiling before a rollover instability. Moreover it was observed that the initial melt mixed readily with the upper-layer material causing an ill-defined interface and an unknown composition of the upper cell. With a system of a rotary pumped bath of nitrogen cooling a thin copper pot it was found impossible to prepare a frozen plug with less than 50% argon. From the stability of the interface it was apparent that the concentration of argon in the lower layer would have to be far lower.

Some experience had been gained in the preparation of 25μm copper/constantan thermocouples that promised to have both a spatial resolution of the order of an anticipated fine structure and a time constant of the order of 2ms allowing sampling rates of up to 500 measurements/s and, in the Nyquist limit, reconstruction of waveforms of up

to 250Hz. These thermocouples were employed as differentials. Initially it was found that these thermocouples were very difficult to prepare in a uniform way without any appreciable solder joint and survive thermal cycling to LIN temperatures.

With the reference junction attached to a thermal mass deep in the bulk of the liquid measurements were taken by allowing surface evaporation to lower the surface past the sensing junction providing a vertical temperature profile. At first these measurements were collected onto a pen recorder and later a computer-controlled data logger.

This data indicated a hitherto unsuspected richness in the surface layer which was difficult to interpret in terms of structures. A schlieren technique was developed to visualise these structures and attempt to correlate the thermal measurements with flow patterns.

Earlier workers had started to use laser doppler anemometry (LDA) to measure velocities in the liquid. The data was limited to the flow in the central downflowing core of the vessel and values near the surface were obstructed by refraction of the beams at the liquid surface. These experiments were not easy technically. The apparatus was difficult to align and misting of the optics from the evaporating LIN was a continual problem. Furthermore the equipment was only suitable for the measurement of the average velocity in a flow though the technique itself measured actual velocity components of microscopic particles. New apparatus was designed and built that enabled the LDA to record every particle that passed through the reference volume. At the end of the research period a further piece of electronics was designed that permitted each event to be time stamped and enabled reconstruction of the velocity waveform.

At this time an understanding of the relationship between the vapour phase and the deep bulk was reached and this posed questions as to the nature of the structure in the liquid/liquid interface and if it was related to the mechanisms seen in the surface layer.

With no satisfactory laboratory model yet developed, some observations were carried out on saline/water systems that had been the backbone of other worker's rollover models. An array of ten differential copper/constantan thermocouples connected to a computer-controlled data logger was used to map the vertical temperature profile during a rollover and shadowgraph illumination gave a visual record. From the stability of this interface it became apparent that any argon/nitrogen rollover model would require concentrations of argon of 5% or less. This prompted an alternative approach to layer formation.

A transfer dewar was developed and this allowed a controlled, slow flow of nitrogen to be introduced into an experimental vessel. Stratification was achieved by subcooling the mixture of argon and nitrogen in the test dewar and then slowly adding the nitrogen to the surface from the transfer dewar. In this way both the composition and temperature were stabilising and stratification could be achieved with argon concentrations less than 1%. The existence of the layer could be ascertained by moving a differential thermocouple through the fluid.

Over a period of time significant improvements were made in the preparation of 25μm thermocouples. An array of ten equally spaced differentials was fabricated and this was used to measure vertical temperature profiles in the stratified system. The schlieren experiments, designed for visualisation of the surface structures, were then modified and repeated on the liquid/liquid interface.

At this time it became apparent that much could be learned about the nature of the flows and rollover if flow visualisation could be achieved in the cryogenic model. Beresford[48] had used a spray of oil and hollow glass spheres which were frozen on contact with the cryogen. A number of these particles would have a neutral density which would follow the flow and long exposure photography revealed flow patterns. This proved impossible when a density gradient existed in the fluid. Very fine particles of aluminium, which were effective in water, were too dense in LIN or accumulated in the liquid/liquid interface. Particulate matter tended to provide nucleation sites leading to boiling and mixing. Fine particles of urethane foam were also tried as well as many other materials, but it became apparent that the addition of a neutral density particle to a stratified system would inevitably lead to particles failing to penetrate into the lower cell. A range of particle densities was selected by removing the floating particles from a LIN bath and then the sinking ones from a LIN/argon bath. Many of these particles would then be electrostatically attracted to the glass dewar walls and not enough would follow the flow.

The laser doppler equipment used the strong forward scattering of a HeNe laser light from very fine particulate targets. A plane of white light was used in a similar way and unexpectedly it was observed that the cryogens were rich with microscopic particles, probably ice. In this way it was possible to directly observe the circulation in the cell and the mechanisms of mixing at rollover.

LIQUID-VAPOUR INTERFACE EXPERIMENTS

Temperature Profiles

Microthermometer studies were carried out on non-boiling LIN, LOX, LAr Freon-R12 and LNG in cylindrical geometries with a controlled heat inleak through the walls and base of the vessel. The containing vessel was a double walled glass dewar with the inner either 50mm or 80mm in diameter. In the vacuum space of the experimental vessel a heater element was wound to provide a controllable uniform heat flux through the inner wall. Initially the inner wall was round-bottomed with primarily wall heating, but later versions had a flat base with bottom and/or wall heaters to enable investigation of the effect of boundary layer flow on the bulk superheat versus boiloff.

The experimental vessel was surrounded by a second bath of the liquid nitrogen serving to eliminate a baseline heat inleak. The boiloff rate was controlled by the current into the heaters.

The thermometer was either absolute or differential, 25μm copper/constantan thermocouples with carefully soldered joints of the order of 10μm long. With the fine wires and careful joint preparation the time constant of the thermocouple sensing junction is of the order of 2ms. The sensing junction was mounted horizontally and rigidly fixed with respect to the dewar and scanned through the liquid surface by allowing the liquid level to fall by evaporation. The support structure for the microthermocouple was designed to allow positioning of the sensing junction across the diameter of the pool. A single calibration point for the thermocouples was made against a calibrated platinum resistance immersed in rapidly boiling LIN.

For absolute measurements the reference junction was immersed in boiling liquid nitrogen or melting ice point depending on the nature of the liquid under test. In differential measurements the reference junction was 10cm vertically below the sensing junction in such a way as to provide a reference against the bulk temperature. The reference junction was soldered into a thermal mass of copper to increase the time constant of the reference.

At the beginning of the experiment the depth of the pool was typically 15-20cm prepared by careful filtration of the test fluid through a sintered glass microfilter with a pore size of 5-15μm to minimise the solid particles in the fluid and hence the possibility of boiling during the experiment. Great care was taken to ensure that no dust or other foreign matter was able to enter the experimental vessel once the pool had been prepared. The fluid in the bulk was then allowed to equilibrate to a superheated state prior to measurements as the process of filtering under reduced pressure subcools the fluid.

Initial experiments were carried out with an analogue amplifier and pen recorder. Later the data was preamplified, logged and recorded directly into a computer to allow further processing. The preamplifier, with a fixed gain of 100, was battery powered and located close to the experimental dewar to minimise stray pickup. To further reduce noise some development was done to include the preamplifier in the vessel itself, operating at 77K. The results for AC signals were good but a persistent offset in the DC component precluded their use in this experiment. The results were published and the publication is included in the appendices.

A single run consisted of 32000 data points logged with a Spectra multichannel data logger with an integration time of 10ms and a resolution of 0.6μV. The data was recorded into a minicomputer. Each run lasted 250s or 128 readings/s. The evaporation rate was recorded with a Hastings gas flow meter by direct readings or, more precisely, using a digital voltmeter attached to the Hastings analogue output. The Hastings was then calibrated against a Chell 258/259 flow meter with a guaranteed accuracy of $\pm$0.5% full scale for each of the fluids under examination.

Considerable care was taken to ensure that the data recording of 32000 points in a period of 250s was not distorted by the operation of the minicomputer or the data logger. The data logging apparatus was calibrated against a frequency generator at 2, 10, 20, 50 and 100 Hz which were then Fourier transformed to examined for evidence of other time constants in the system and this data is shown in fig.14. Data buffers at the logger, the input/output module and in the microcomputer ensured that no data readings were delayed by virtue of full buffer conditions. All the minicomputer software was optimised to enable faster recording of data. It was found that the limiting factor in fast data recording at these sensitivities resided with the operation of the reed relays in the data logger which required 5ms or so to settle. If the data so obtained had indicated smaller time constants in the fluid these reed relays could have been readily excluded since they pertain to the multichannel operation of the data logger used in later, multi-thermocouple measurements.

The LNG used in these experiments was liquefied from the commercial gas supply and has a nominal composition by volume[1]:

CH_4	91.8%
N_2	1.8%
C_2H_6	5.8%
C_3H_8	0.5%
$(i+n)C_4H_{10}$	0.1%

1 Information from Southern Gas

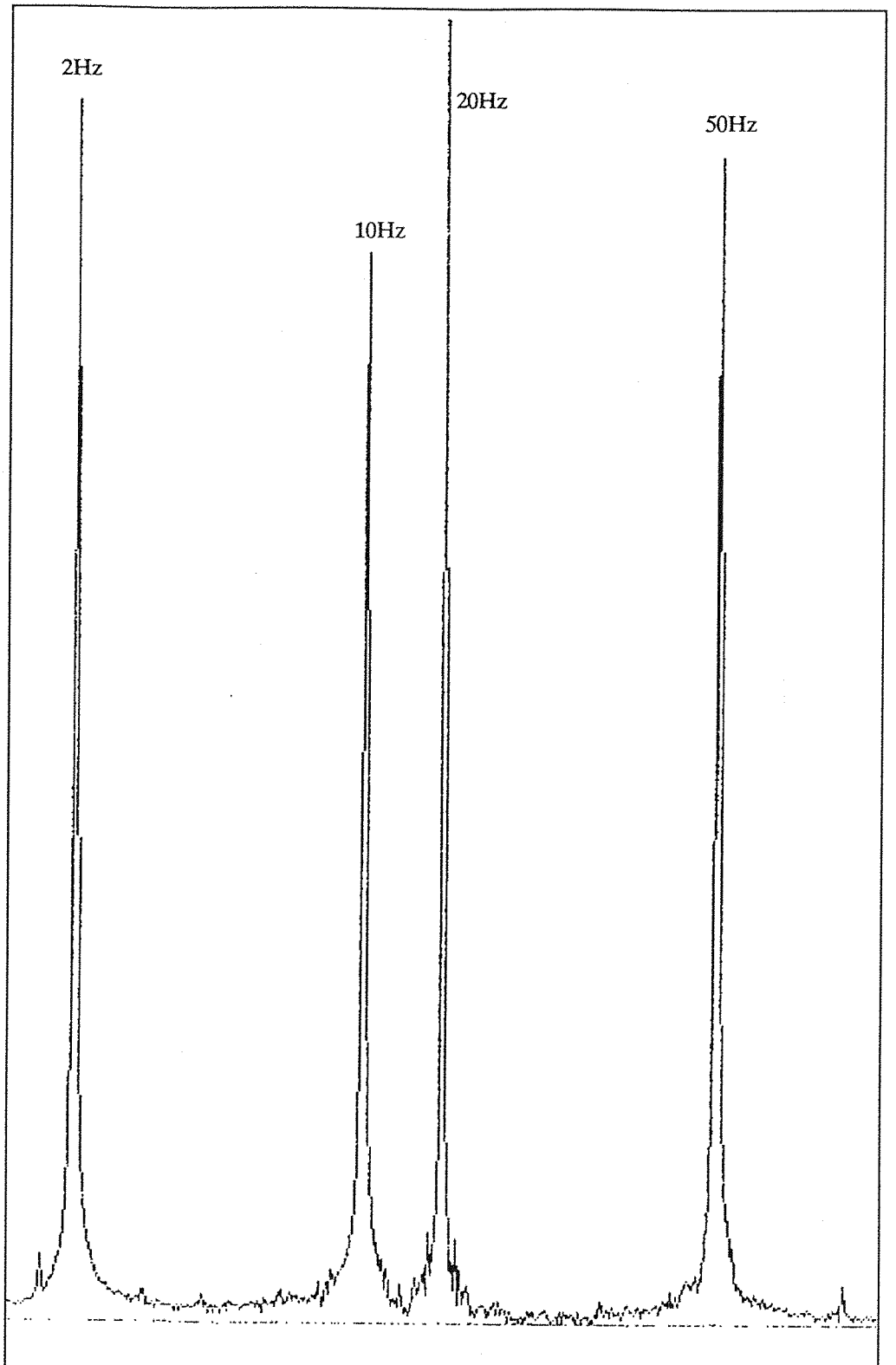

Fig. 14 Power Spectrum of Sine Wave Data

These are the computed power spectra of calibration frequencies through the measurement apparatus individually recorded at 2,10,20 and 50Hz and added digitally prior to Fourier transform and computation of the power spectrum. No significant 50Hz noise was evident in the non-50Hz measurements indicating good noise control and the instrumentation is clearly sensitive to frequencies up to 50Hz..

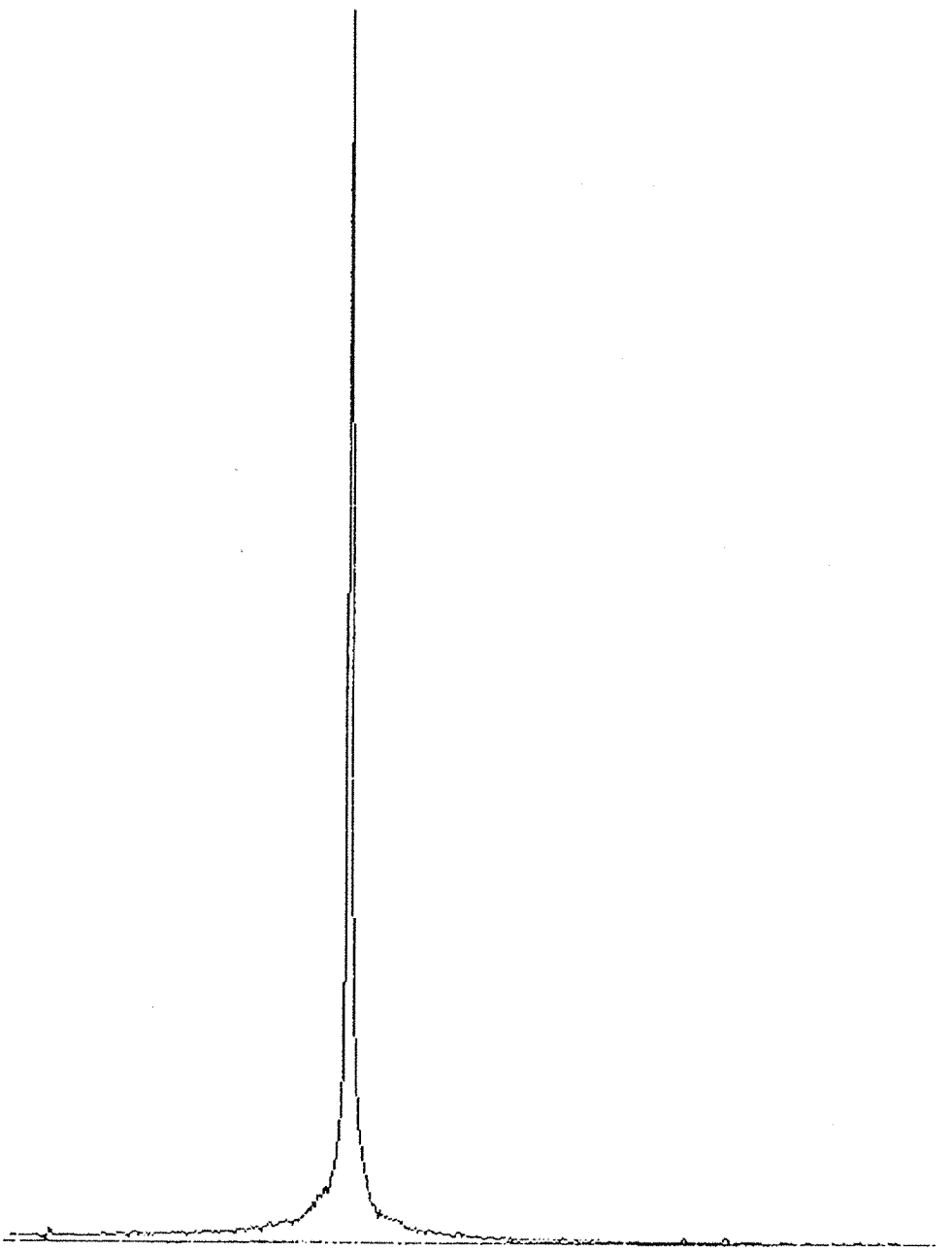

Fig. 15 Power Spectrum of 10Hz Signal

This plot of a 10 Hz test signal shows clearly that external noise had been largely eliminated from the measurement system. Note the absence of a 50Hz peak which would be seen in a position corresponding to the calibration data in the previous figure.

Schlieren Visualisation of the Surface Layer

The schlieren[1] visualisations of the liquid-vapour interface were designed to give a qualitative interpretation of the structures seen in the temperature scans described above. There were many parameters that could be adjusted in the experiments. The test fluids were either LAr or LIN as LOX and LNG were considered hazardous in the necessary environment. The surface effect of contaminants was a parameter of particular interest since this may have modified the behaviour of the sublayer whose existence had been identified in the temperature scans. Ultra-high purity LIN was prepared to test this hypothesis and compare the observations with bench grade LIN.

Fig.17 shows the experimental setup for this technique. A carefully polished rectangular stainless steel mirror (12mm x 35mm) was solder mounted on a stainless steel support. During the experiment this was lowered into a 50mm diameter pool of filtered non-boiling LIN such that the surface of the mirror was at an adjustable depth, typically 10-80mm below the surface of the liquid.

A parallel beam of white light, obtained from a near point source at the focal point of a converging lens, was directed vertically down the containing dewar illuminating the mirror. The beam was then reflected back along its course to a half-silvered mirror which directed the beam into an optical focussing arrangement with a knife edge at the focal point. The image was recorded directly into a film or video camera or viewed on a screen. The mirror and the beam must be carefully aligned. A HeNe laser was used to obtain a precise setting for the mirror parallel to the top flange.

The experimental dewar was sealed by the clear glass top flange and the boiloff gases directed through a flowmeter. Every precaution must be taken to ensure that the dewar is clean and free from nucleation sites that would initiate boiling before high bulk superheat convection patterns could be observed. The apparatus was isolated from vibrations and to prevent disturbances from the outer bath of LIN it was first sub-cooled to a non-boiling state by bubbling helium gas through the outer bath prior to observations.

The light source was a 250 watt mercury light passed through an adjustable pinhole aperture. The adjustment consisted simply of varying sized pinholes on a circular disk such that one pinhole would act as the aperture at any time.

With no perturbation to the beam the focussing arrangement is capable of reproducing the image of the pinhole source. The parallel rays of the beam are displaced however by variations in the refractive index of the liquid in front of the mirror. The amount of angular

1 From the German 'schliere' indicating an inhomogeneity in an otherwise transparent medium and not, as many believe, from a Dr Schlieren.

deflection of the ray is proportional to the gradient of the refractive index at the point in the liquid. As the rays pass back through the liquid in the reverse direction the very small angular deflection on the first pass does not materially affect the route of the ray. There is a second additive deflection as a result of this, equal in magnitude to the deflection of the downward path. The rays so deflected are then blocked by the knife edge with the result that the deflected rays do not reach the screen or camera and the screen at that point appears dark. With the knife edge oriented parallel to the long axis of the mirror the horizontal gradient of the refractive index perpendicular to the mirror could be visualised.

The pool of liquid is contained in a dewar similar to the one used in the thermometry experiments with wall and base heaters. The heat inleak and thus the evaporative mass flux through the surface is adjusted with the heater current. Evaporation rates could be varied from 200 cc/min to 3000 cc/min and were recorded with either a Hastings gas flow meter or a Chell flowmeter

The depth of the mirror could be adjusted to view the effect of a greater height of fluid and the effect of the mirror on the convective flows within the experimental dewar. As reported later this did not affect the image. A later dewar design incorporated the mirror as the circular base of the dewar.

The knife edge is adjusted in the setup of the experiment to maximise the contrast in the image. Since the refractive index is a function of temperature for the cryogen the illumination on the screen is proportional to the horizontal temperature gradient in the liquid. Fig.16 shows the conceptual design of the schlieren method.

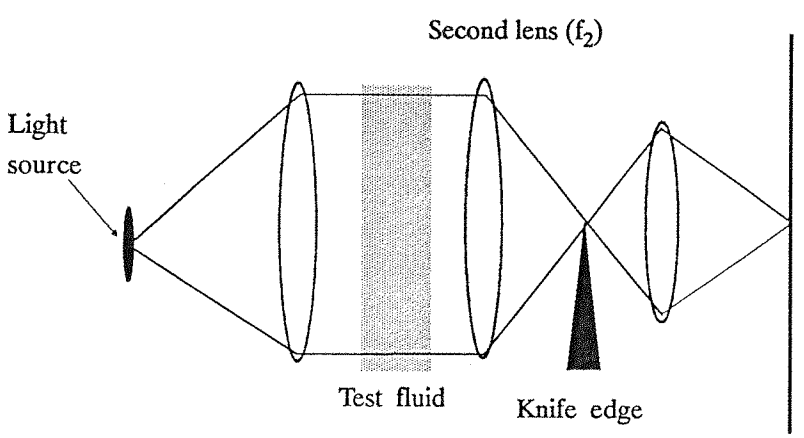

Fig. 16 The Schlieren Method with Parallel Light

An image of the light source is formed at the knife edge which is placed in the focal plane of the second lens. If the knife edge cuts off part of the image of the source the light intensity at the screen will be reduced. If the dimensions of the light source image at the

knife edge are a and b then the illumination at a point (x,y) on the screen is I given by:

$$I(x,y) = vI_o\left(\frac{ab}{f_c^{\,2}}\right) = constant \tag{6-1}$$

here v is the an absorption coefficient describing the loss of intensity from the source to the screen and f_c is the focal length of the camera lens. If the light image is deflected by a disturbance in the refractive index of the medium by an amount Δa,Δb and with parallel light passing through the medium the Δa is independent of the distance from the medium to the second lens. Now if the light rays are deflected an angle ε due to this disturbance then taking ε_y as the component such that

$$\Delta a = f_2 \tan \varepsilon_y \approx f_2\, \varepsilon_y \tag{6-2}$$

The light intensity at the point (x,y) is then changed by an amount

$$\Delta I = vI_o\left(\frac{\Delta a\, b}{f_c^{\,2}}\right) \tag{6-3}$$

Then the relative change in intensity at a point is $\Delta I/I$ and

$$\Delta I/I = \Delta a/a = \varepsilon\left(\frac{f_2}{a}\right) \tag{6-4}$$

From Fermat's principle Weyl[62] has shown that the deflection of the ray in an inhomogenous refractive medium satisfies the equation:

$$\frac{d^{\,2}x}{dz^{\,2}} = \left\{1 + \left(\frac{dx}{dz}\right)^2 + \left(\frac{dy}{dz}\right)^2\right\}\left\{\frac{1}{n}\frac{\partial n}{\partial x} - \frac{dx}{dz}\frac{1}{n}\frac{\partial n}{\partial z}\right\} \tag{6-5}$$

and similarly for the y coordinate. The ray follows a path through the medium x = x(z) and y = y(z) which is a solution of (6-4). The terms in dx/dz and dy/dz are small compared to one so (6-4) reduces to

$$\frac{d^{\,2}x}{dz^{\,2}} = \frac{1}{n}\frac{\partial n}{\partial x} \tag{6-6}$$

Thus the ray leaves the medium at the same (x,y) coordinates as it enters but at a changed angle. The ray reflected from the mirror in the liquid can be assumed to travel the same route down and up the fluid sample in the dewar. Then the angle in deflection due to a

change in the refractive index in the medium over the thickness,ζ, of the medium is:

$$\tan \varepsilon_y = \int_0^{\zeta} \frac{1}{n} \frac{\partial n}{\partial y} dz \tag{6-7}$$

So, according to (6-3), depending on the orientation of the knife edge we can visualise either the x or y component of the refractive index. As the light travels down through the liquid and back the angle of deflection is effectively doubled by virtue of the integration in (6-6) extending from -h to h where h is the depth of the mirror in the fluid. It can be seen from the analysis above that the maximum contrast is achieved for small a and a long second lens focal length. For very small a diffraction effects become important and with HeNe laser light, used originally in the early phase of the experiments, the fringes interfere with clear observation.

The problem then relates to the change in refractive index as a function of temperature. From the Clausius-Mosotti equation the refractive index is related to the density as:

$$\frac{n^2 - 1}{n^2 + 1} = \rho K_{GD} \tag{6-8}$$

where K_{GD} is the Gladstone-Dale constant. Taking ρ as linear in T and variations in n small and n only occurs as terms like n + 1 then:

$$\frac{\Delta I}{I} = \frac{C}{a} f_2 \int_{-h}^{h} \frac{\partial T}{\partial y} dz \tag{6-9}$$

where constants have been collected in C showing the relationship of the illumination to the temperature gradient perpendicular to the knife edge.

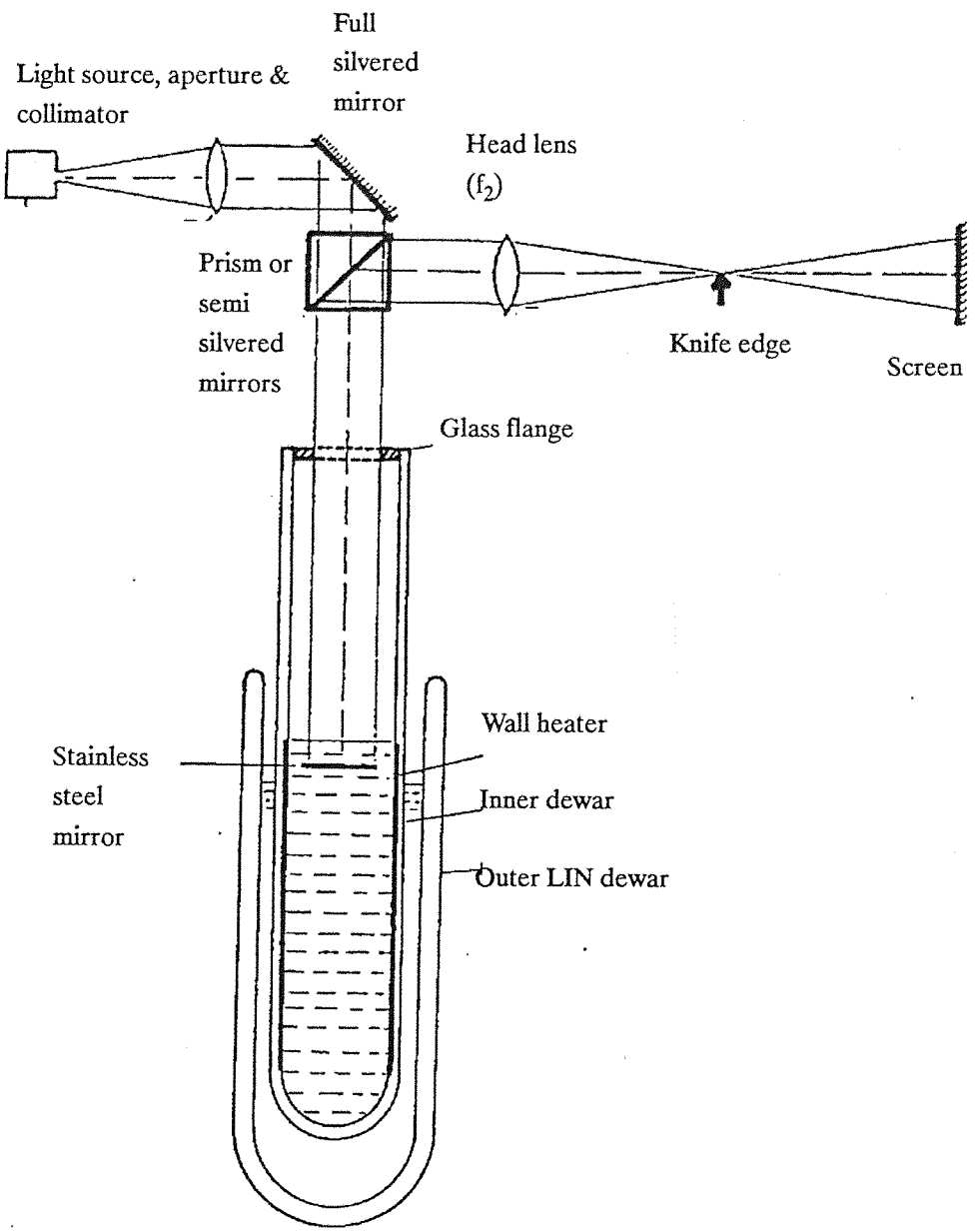

Fig. 17 The Experimental Setup for Schlieren Observation

SALINE/WATER STRATIFICATION EXPERIMENTS

A short set of experiments were carried out with saline/water systems in experimental vessels similar to those used in the cryogenic measurements. These observations were used to test the validity of the designs being used in the laboratory scale rollover models. The experiments observed the effect of varying saline concentrations on the mechanism of rollover in cylindrical vessels and imposing realistic cryogenic boundary conditions on the system.

The experimental vessel was a flat bottomed glass container which could be suspended in a heated oil bath. The vessel was partially filled with water and then a saline solution was introduced into the bottom by means of a flexible tube. The saline was typically 20g of NaCl in 1 litre of water and coloured to facilitate viewing the rollover process. In initial experiments the dissolved air in the saline appeared as bubbles when the lower layer was heated; to avoid this in later observations the saline was boiled and cooled prior to the experiment. An array of absolute copper/constantan thermocouples was arranged in a vertical formation and referenced against an ice point. The data was collected by a multi-channel data logger and the results recorded with a minicomputer as in the argon/nitrogen rollover experiments.

During the experiment the data was continually logged and the vessel was illuminated with white light to produce shadowgraphs which could be photographed. In contrast with the schlieren technique used to visualise convective flows in the surface layers of cryogens the shadow technique produces an image where the illumination is proportional to the divergence of the refractive index gradient. Since the convective flows are both hot and salty there is a combined contribution to the change in refractive index from both the compositional and temperature differences.

It has earlier been noted that the free surface of the cryogenic liquid under storage is in equilibrium with the vapour and rapidly attains such an equilibrium leading to the conclusion that the free surface has a low thermal impedance. The earlier experiments on cryogens had revealed a uniform bulk temperature in a cryogenic cell showing that the convective loop is efficient at connecting the bulk material with the surface evaporation process. To model such a process a second set of saline/water experiments were done with a copper heat exchanger was placed in contact with the free surface of the superposed water layer. A continuous flow of water through the exchanger cooled the upper surface. In this way it was hoped that a convective instability in the upper layer may more closely simulate a cryogenic system.

ARGON NITROGEN STRATIFICATION EXPERIMENTS

The Preparation of Stratified Cryogens

The experimental model for laboratory scale stratification experiments consisted of a bottom layer of a mixture of LAr and LIN with a superposed layer of LIN. The lower layer was first prepared by mixing a volume of LAr with LIN. It was found that nucleate boiling would be experienced in the lower layer before mixing could ensue between the layers if the concentration of LAr in LIN exceeded 3% v/v.

The mixture was filtered through a micropore filter into the clean experimental dewar and then pumped with a rotary pump to subcool and ensure that no boiling developed during the layer preparation.

A quantity of LIN was filtered into the transfer dewar shown in fig.18 mounted on the experimental dewar. The assemble was then lowered so that the point stainless steel transfer tube, enclosed in a cotton wool and filter paper cover, was a few mm above the surface of the lower layer. Once the experimental vessel had returned to atmospheric pressure the needle valve in the transfer dewar was adjusted for a slow steady flow.

Concentrations of ~0.5% of LAr in LIN were found to readily form layers under LIN in this way and it is our experience that suggests that stratification could readily be achieved with much smaller concentration gradients using this technique. A range of 0.5% to 3% LAr in LIN was sufficient to simulate mixing effects at the liquid-liquid interface in this set of experiments.

As a corollary to the experimental technique developed in this study it is seen that the liquid-liquid interface forms quite readily when a marginally less dense liquid is poured slowly onto the surface of another. A slow jet of fluid incident on another is insufficient to cause mixing even in the case of almost identical densities of heel and load.

Flow Visualisation

Despite micropore filtering it was observed that the lower layer contained very fine particles, probably ice or carbon dioxide, and it is presumed that these were present in the argon cylinder from which the LAr was prepared. These appeared as a mist rather than particulate matter. These particles could readily be introduced by blowing on the surface of the liquid whereupon material would condense.

A plane beam of white light from a 1kW water-cooled halogen lamp through an adjustable vertical slit was used to illuminate the dewar. A wall heaters was mounted on the outside of the inner wall of a flat-bottomed dewar and the lower section of the dewar was cooled in the vapour space of a rapidly boiling outer bath of LIN. The flat base of the dewar more closely follows the design of an LNG tank and avoids the uncertain boundary layer flow that would result from an attempt to base heat a classical round bottomed vessel. The

flows were observed by forward scattering of the light from the particles , that is dark field observation. A video camera recorded the visualisation and a Chell flowmeter was used to monitor the rate of vapour evolution. The output from the flowmeter was measured with a DVM and the readings from the DVM were included in the video frame to enable a precise alignment of boiloff to rollover event. Dark field illumination is difficult to record with still photographs and the use of a video camera avoided these problems.

This technique is considerably simpler than the methods of Beresford[48] and can be applied where there are moderate density gradients. It should therefore find wide application in the observation of cryogenic flows.

Single Thermocouple Measurements

A single vertically mounted differential microthermocouple similar to that developed for surface investigations was positioned near the interfacial region. The stability of the interface during formation of the layers, determined from thermocouple array measurements, was sufficient for the thermocouple to be located prior to the formation of the stratification, though it could be moved. The data was taken in an identical manner to the liquid-vapour measurements to facilitate comparisons.

Temperature Profiles

A vertical array of ten 25μm copper-constantan microthermocouples were prepared with 1.5cm spacing between junctions. The vertical constantan wire acted as a support and a common connection. The reference was held in boiling LIN. The junctions were connected directly to a Spectra multichannel data logger controlled by a microcomputer. Care was taken to ensure low noise on the signals. In contrast to the single thermocouple measurements there was no preamplification of the signal near to the dewar. At LIN temperatures the copper-constantan thermocouple has a sensitivity of 16 μV/K and the A/D converter with preamplifier in the data logger has a resolution of 0.6 μV, with no missing codes, giving a digital scale of 26 counts/degree. At this accuracy many precautions had to be taken to ensure that external noise sources did not interfere with the measurements. All cabling into the vessel and from the vessel to the data logger were screened with heavy copper braid and secured to the laboratory earth. In addition the measurements were made in the evening to avoid signal pickup from other equipment in the vicinity used during the daytime.

Schlieren Observations of the LIN/LIN-LAr Interface

The techniques of schlieren observation of the liquid-vapour interface were extended to observation of the liquid-liquid interface.

A stainless steel dewar was prepared with a highly polished stainless steel mirror clamped with an indium seal as the base of the dewar. A circular heater was mounted on the reverse of the mirror and wall heaters wound around the lower section of the dewar.

Provided the heat inleak into the upper layer is small it had been observed that the changes in illumination contributed by convective flows in the liquid-vapour interface are

negligible. The illumination pattern of a stratified system is then the contribution from changes in the refractive index due to horizontal temperature and compositional gradients at the liquid-liquid interface. To ensure that the image was a representation of the temperature gradients deep in the liquid a solid perspex rod with optically polished ends was used to bypass the surface thermal gradients.

The rod, some 10cm in length, extended from the vapour space vertically down into the liquid and could be moved so that the lower end of the rod was above the interface. This addition to the optical system made the optical alignments considerably more difficult and the quality of the image obtained was poor but it did serve to confirm the observations made with the rod present.

Laser Doppler Anemometry

Beresford[48] had used laser doppler anemometry to measure mean velocity values in an unstratified system. The alignment of this apparatus is difficult and typically takes several hours with repeated adjustments to compensate for changes in the optical path through the dewars: the light path traverses four glass walls; two as part of the experimental vessel itself and two from the enclosing LIN bath.

It was found that the timescale of the changes in the experimental vessel was shorter than the time that a practised experimenter needed to realign the optics. Application of LDA to stratified systems requires development of automation to overcome these problems.

However some enhancements were made to the usefulness of the LDA by adapting the electronic data analysis section to provide an intermediate output which is a DC voltage proportional to the velocity of the last validated particle through the LDA test volume. Some instrumentation was then prepared to convert the analogue signal to an 8-bit digital value that could easily be read by a computer with a parallel input port. In this way the distribution of the velocity component of the flow can be measured as well as the mean.

The regions of the fluid which are of most interest to the investigator are near the boundaries. LDA in circular non-optical glass dewars is confined to regions away from the walls of the vessel.

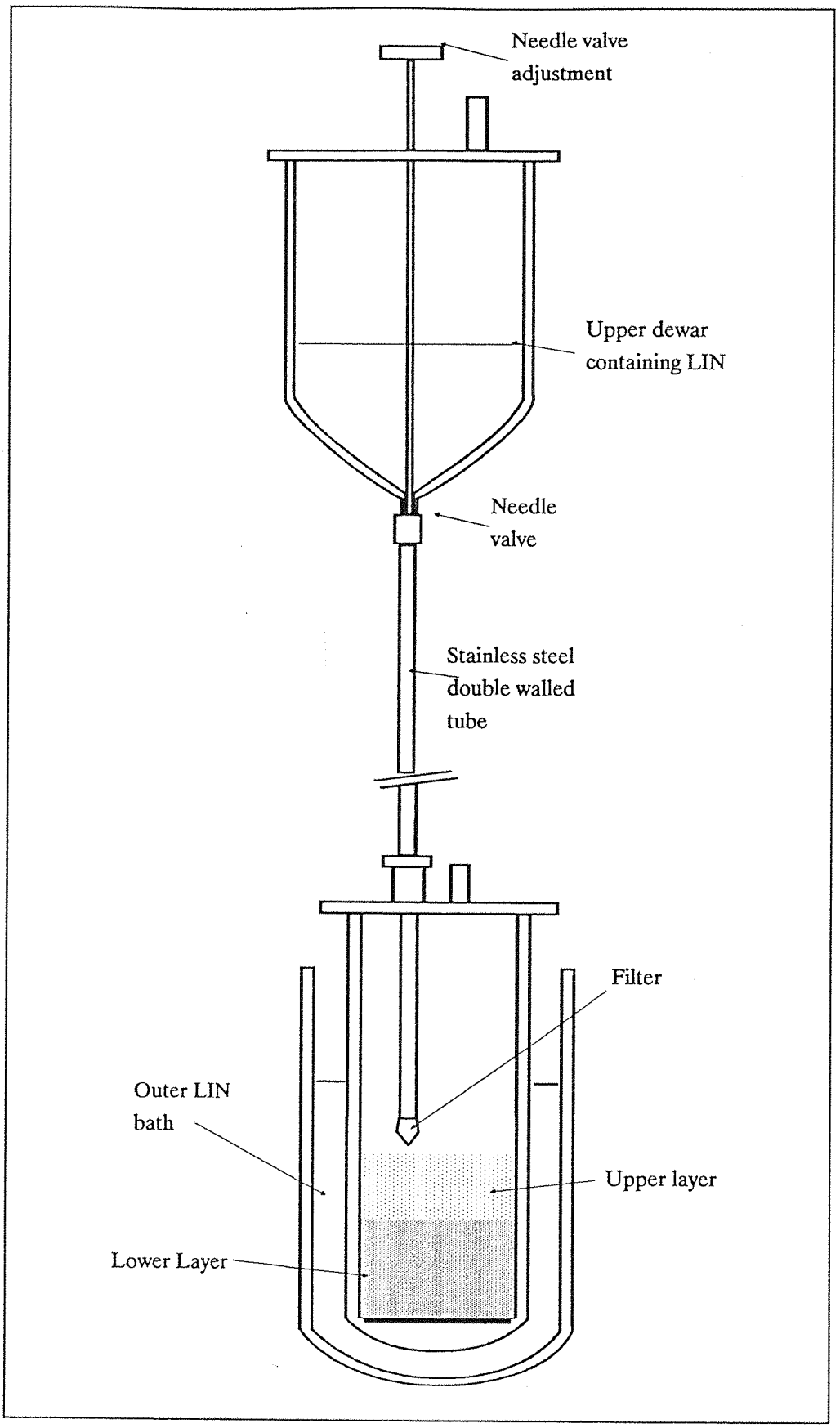

Fig. 18 Stratification Setup with Transfer Dewar

7. RESULTS

THE LIQUID-VAPOUR INTERFACE

Temperature Measurements

An example plot of temperature scans from the bulk through the liquid-vapour interface are shown in fig. 19. The data recorded by digital means was then smoothed using a moving average algorithm, the plot of the smoothed plot is shown in fig.21. The RMS fluctuations in the temperature were similarly computed and shown in fig.22

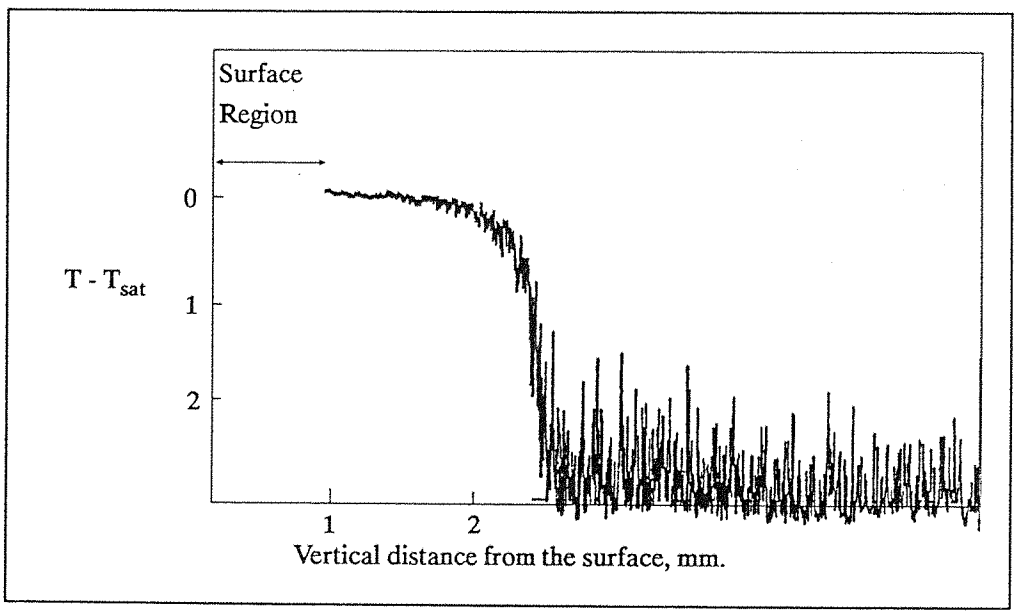

Fig. 19 Temperature Scan Through Surface (LIN #7)

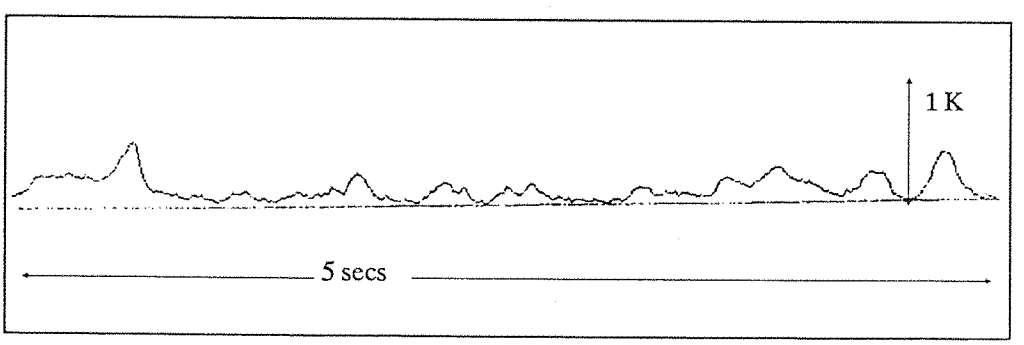

Fig. 20 Expanded Plot of Temperature ~ 5mm Below Surface

The plots are displayed with the surface to the left as the origin and vertical distance as the horizontal axis increasing into the bulk liquid. The actual zero corresponding to the surface is not clear since surface tension effects on the thermocouple tend to distort the

horizontal plane of the surface and liquid is pulled up with the thermocouple as the fluid layer falls.

The following features are evident:

- The temperature oscillations very near the surface are small and there is a small temperature gradient in this range. Surface tension effects make a precise measurement of the depth of this region difficult but it is estimated to be of the order of 0.1mm.

- A layer 0.1-0.5mm in thickness which exhibits a large temperature gradient and temperature oscillations. The smoothed plot fig.21 shows clearly that this layer has a near constant temperature gradient. Importantly it is found that the thickness of this layer depends on the mass flux through the liquid-vapour interface. It is also evident that temperature fluctuations are not strongly damped in this region as fig 22 illustrates. Therefore it is presumed that both convective and conductive processes are present.

- A region 10-15mm in depth extending into the bulk of the liquid where there is little thermal gradient and convective processes are dominant.

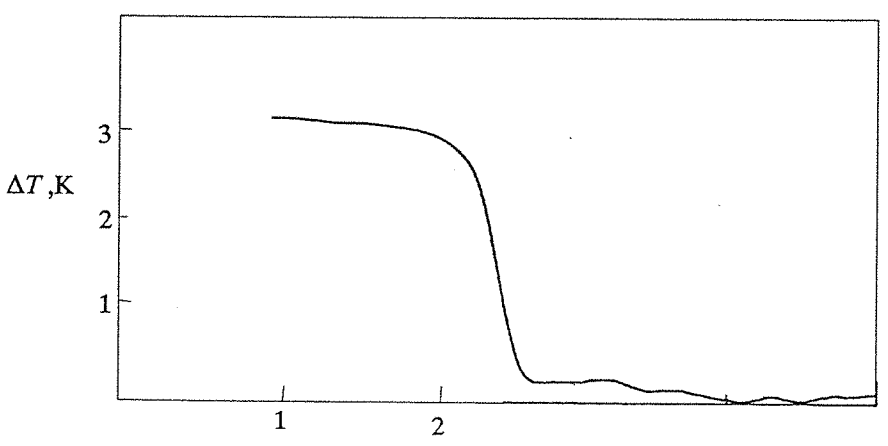

Fig. 21 Smoothed temperature plot T-Tbulk (LIN #7)

This plot was smoothed with a 1024 point moving average

The temperature scans were repeated in 50mm and 80mm pools with the microthermocouple positioned at the centre of the pool, within 1mm of the wall and near half the radius point. Within the accuracy of the experiment it was found that: the size of the pool did not affect the measurements; the surface temperature was constant across the surface; the bulk temperature was uniform after the pool was allowed to reach an

equilibrium and this typically took of the order of one hour.

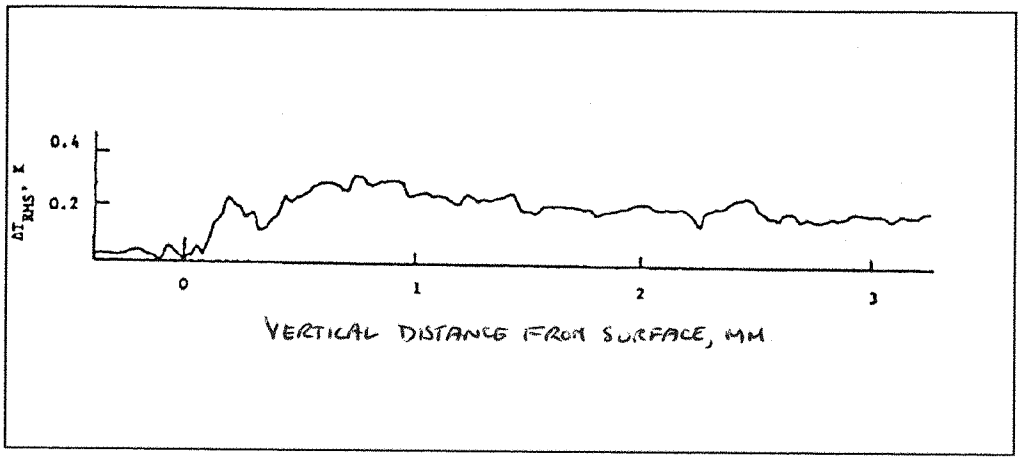

Fig. 22 RMS of Temperature Fluctuations T-Tbulk (LIN#7)

The complete record of one plot, with the exception of the exception of continuing surface data at a uniform temperature, is shown in fig.25 together with the power spectra of sequential 2048 points in the record in fig.26. The data is in the form of a time series with the first point 5mm below the surface and the temperature scale decreases in a vertical direction. The thermocouple scans upwards and through the surface. The DC component of the data was removed prior to a 2048 point transform and the data selected from the record with a 'top-hat' function.

The raw data shows clearly that the perturbations are cooler than the baseline since it is evident that the temperature fluctuations are negative peaks in temperature. In this set of data the surface temperature, at the end of the data, is 3K cooler than the mean bulk temperature.The surface data is very close to a uniform temperature and demonstrates the low noise in the observations. The width of the peaks remains near constant throughout the scan, at around 0.01mm, and if we associate the temperature fluctuations with eddies sweeping past the thermocouple this is indicative of a near uniform and unchanging scale length throughout the region though of course there is an implicit assumption here that velocities too remain constant.

The power spectra show no dominant frequency at any stage during the scan, only the random fluctuations of turbulent motion. A buoyancy frequency is not apparent.

Temperature Measurements Discussion

These results and extensive observations with schlieren imaging of the interface suggest that the convective process is by sustained 'plumes' with a long lifetime as opposed to intermittent thermals. The temperature scans through the interface reveal three characteristic regions as we descend from the free surface towards the bulk of the liquid:

- A thin layer of the order of 0.1mm in thickness with small fluctuations in temperature which may be an experimental artifact as the result of surface tension pulling on the microthermocouple.

- A sublayer that varies in thickness between 0.1mm and 0.5mm depending on the heat flux with a large temperature gradient where heat conduction is dominant and some eddy fluctuations in temperature are seen.

- A region 10-15mm in thickness where penetrative convection appears to the dominant process.

At the surface itself the temperature is observed to be constant at the saturation temperature and thermals appear to be prevented from penetrating to this upper layer.

The high temperature gradient and variation of thickness with heat flux of the intermediate layer suggests an analysis based upon a conductive heat flow. We can associate a critical Rayleigh number, R_b, to sustain the temperature gradient in this layer such that the dominant heat flow process is conductive and that the total of conductive and convective mechanisms when averaged over time give rise to a heat transport equal to the conduction across a flat plate of thickness δ with the same mean temperature gradient. This layer is then constantly in a state very near the onset of convection.

The critical Rayleigh number is then defined by:

$$R_b = \frac{g\beta_T \Delta T \delta^3}{\kappa\nu} \tag{7-1}$$

Using the elementary relation for heat flow across a plate of thickness δ

$$\dot{Q} = -\alpha\rho C_p \frac{\Delta T}{\delta} \tag{7-2}$$

The heat flux can be expressed in terms of R_b

$$\dot{Q} = \left(\frac{1}{R_b}\right)^{1/3} \left(\frac{\alpha^2 g \beta_T \rho^3 C_p{}^3}{\nu}\right)^{1/3} \Delta T^{4/3} \tag{7-3}$$

The mass flux at the surface of the saturated liquid is simply:

$$\dot{m} = \dot{Q}L \tag{7-4}$$

Then we can define a modified mass flux:

$$\dot{m}^* = \dot{m}L\left(\frac{\nu}{\alpha^2 g \beta_T \rho^3 C_p{}^3}\right)^{1/3} \tag{7-5}$$

There is then a correlation between $\dot{m}^*$ and ΔT that becomes independent of the fluid properties.

$$\dot{m}^* = \left(\frac{1}{R_b}\right)^{1/3} \Delta T^{4/3} \tag{7-6}$$

We note that the temperature dependence concords with the Hashemi-Wesson correlation. The results for a range of cryogens are plotted in Figs.23 and 24. Originally, in work published by Rebai[63], it was thought that all the cryogens tested fitted the above theory. Subsequent recalculation has revealed divergences for LNG and LCH_4. The constants for LIN, LOX and LAr are similar and account for this grouping. The theory does provide a useful correlation in this form and is based upon sound experimental observations. Refinement of the model will come with a better understanding of the sublayer. The deviation in linearity for small ΔT (less than 1K) may be related to a change in the convective pattern or poor mixing in the bulk with resulting temperature gradients. For larger ΔT good correlation is obtained with $R_b \sim 30$ for LIN,LOX and LAr. The averaged values for slope and R_b are shown in table 5 which includes exponent values for ΔT compared to the theoretical value of 1.33. These values were obtained with a least squares fit across a number of experiments. LCH4 and LNG deviate consistently from these values and also have a lower exponent value. Foster[58] developed a time dependent theory for intermittent convection in a surface layer with constant heat flux that gives $R_b = 8.5$. The intermittent convection model due to Howard[57] gives a thickness for the conducting layer an order of magnitude larger than these results.

	ΔT EXPONENT	R_b
LIN	1.085	33
LAr	1.114	16
LOX	1.190	25
LCH_4	0.794	5
LNG	0.868	4

Table 5 Exponent and R_b Values for Tested Cryogens

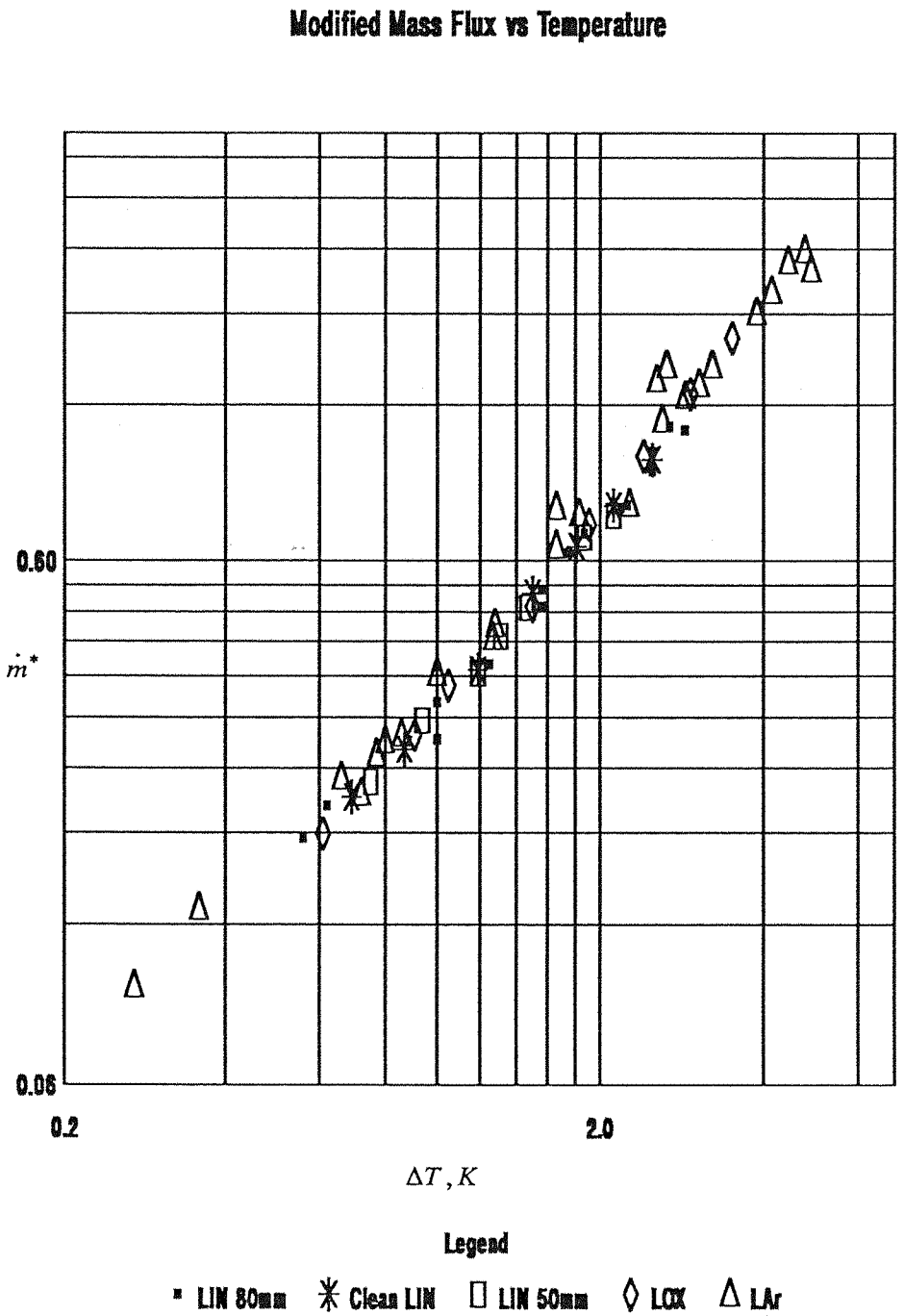

Fig. 23 Modified Mass Flux as a Function of Bulk Superheat

Plotted here are the results for LIN, LOX and LAr, the next figure shows the results for LNG and LCH_4.

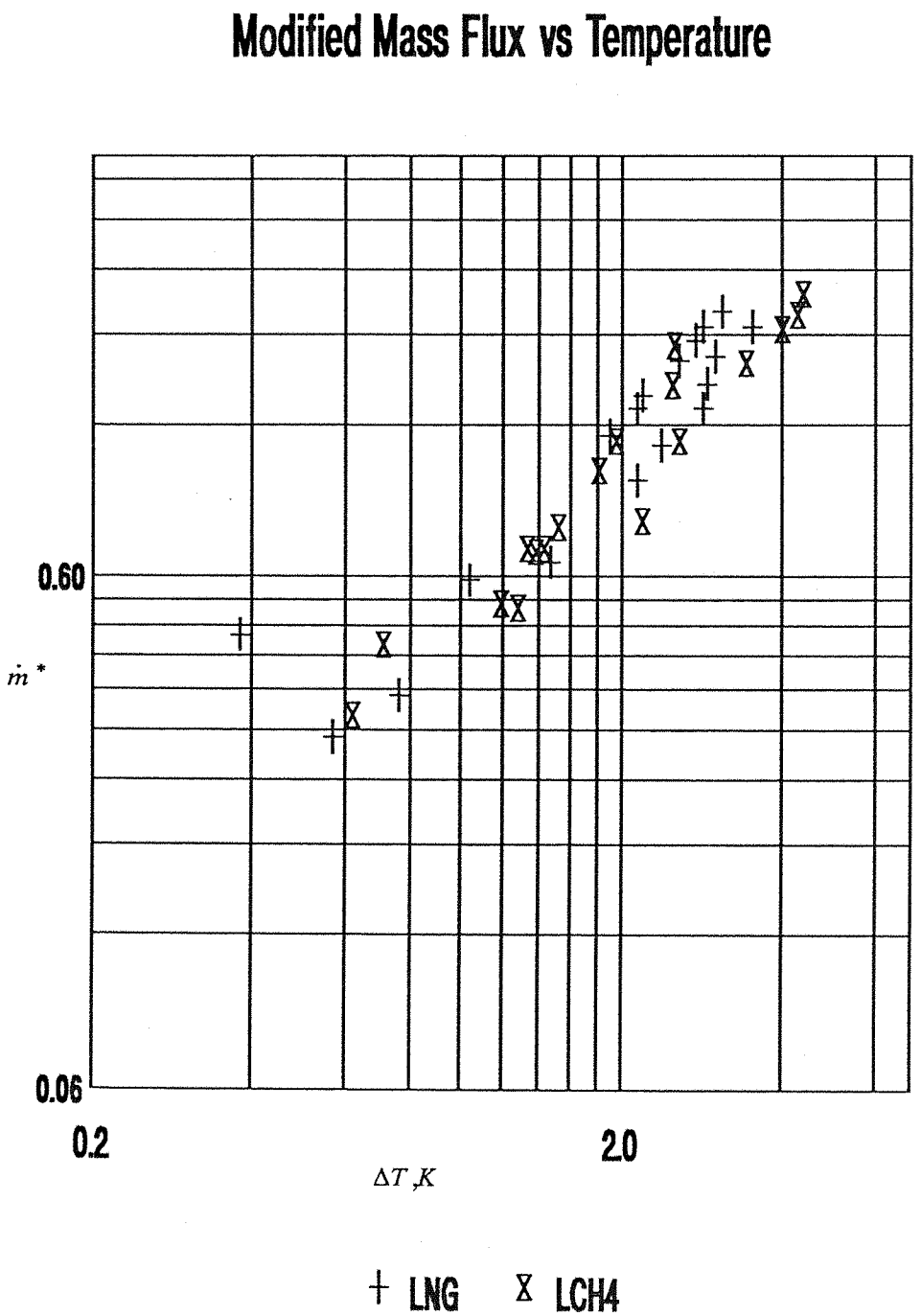

Fig. 24 Modified Mass Flux vs Temperature LNG and LCH_4

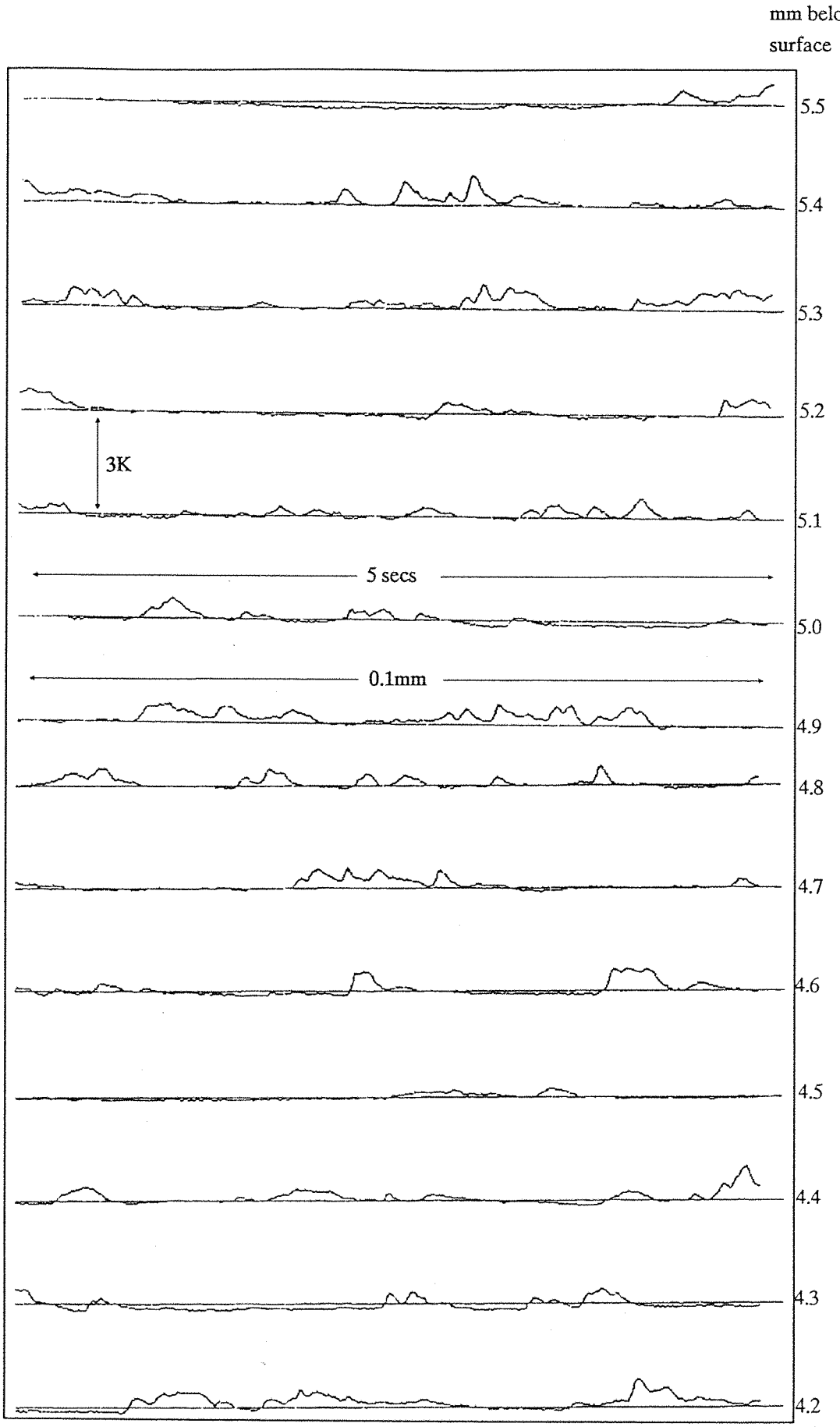

Fig. 25 Raw Data from Temperature Scan (LIN#7)

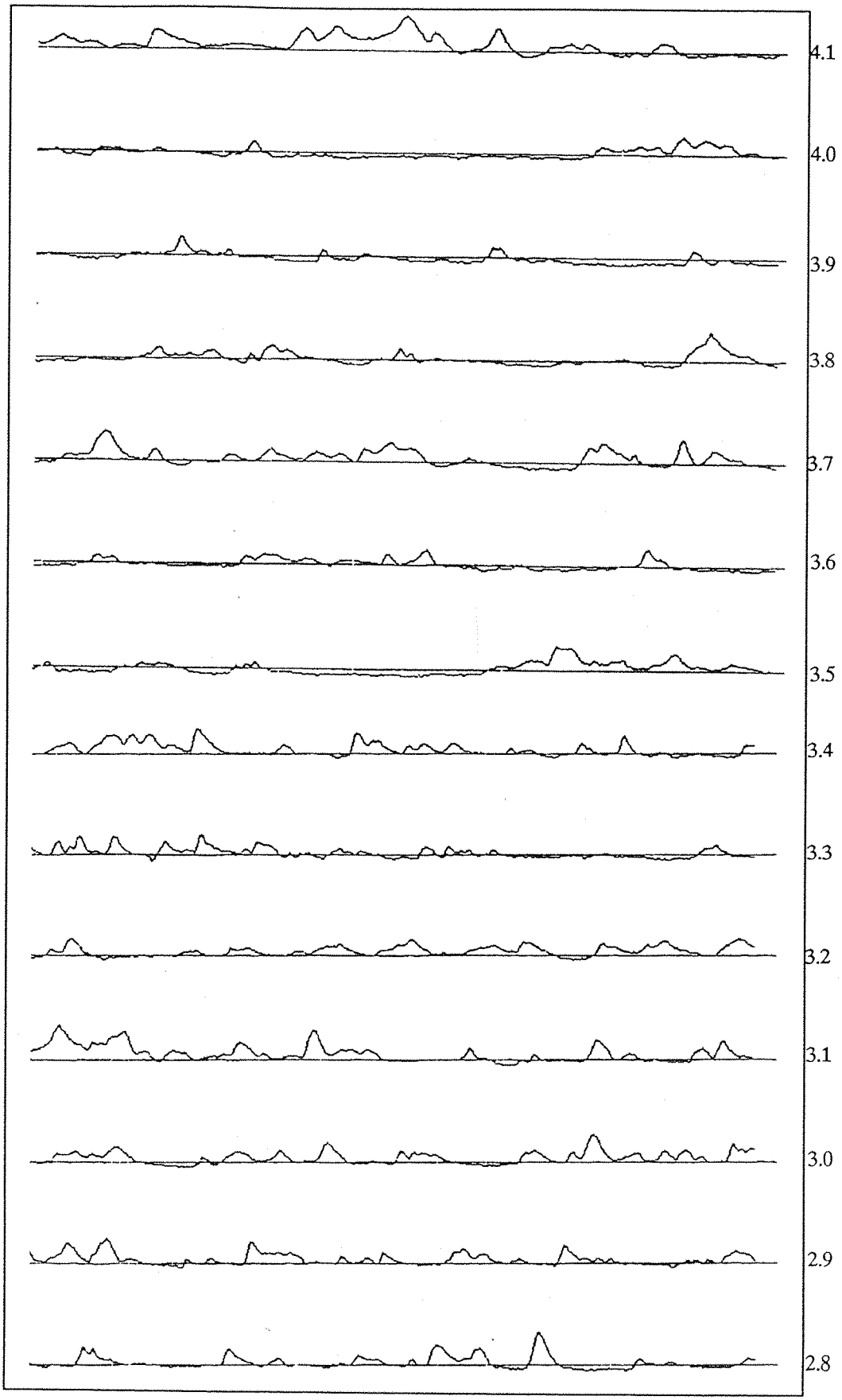

Temperature Data Continued from Previous Figure

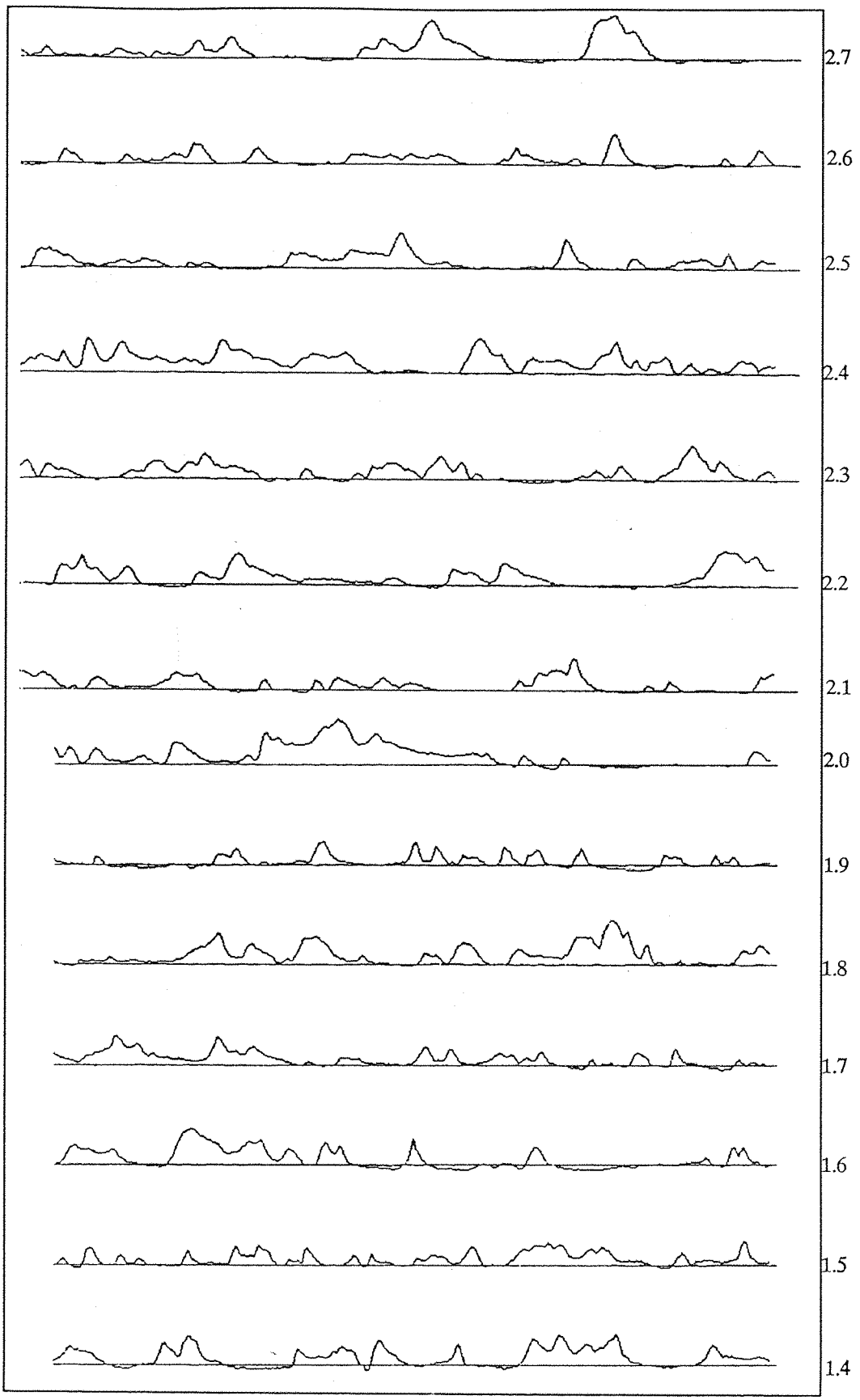

Temperature Data Continued from Previous Figure

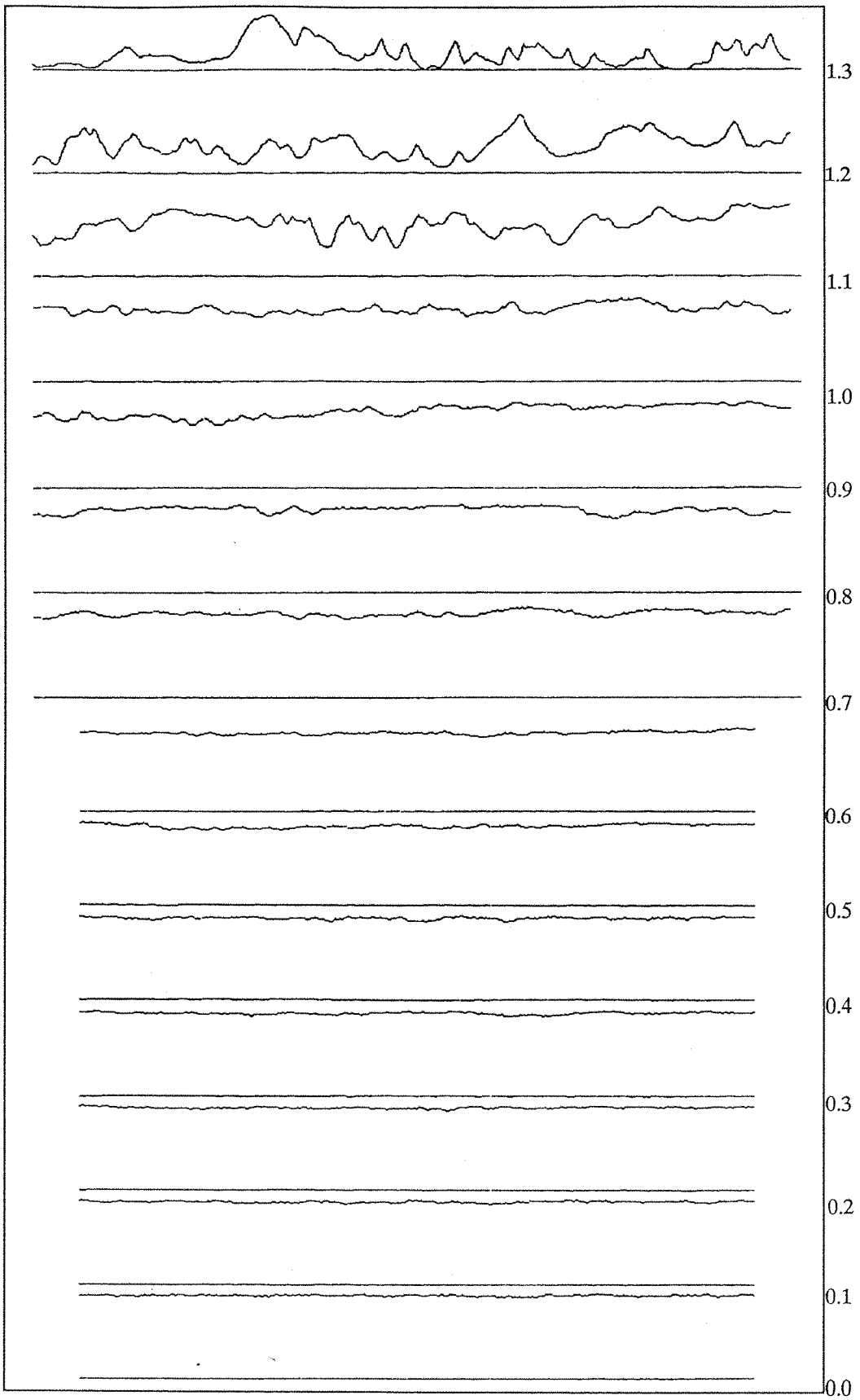

Temperature Data Continued from Previous Figure

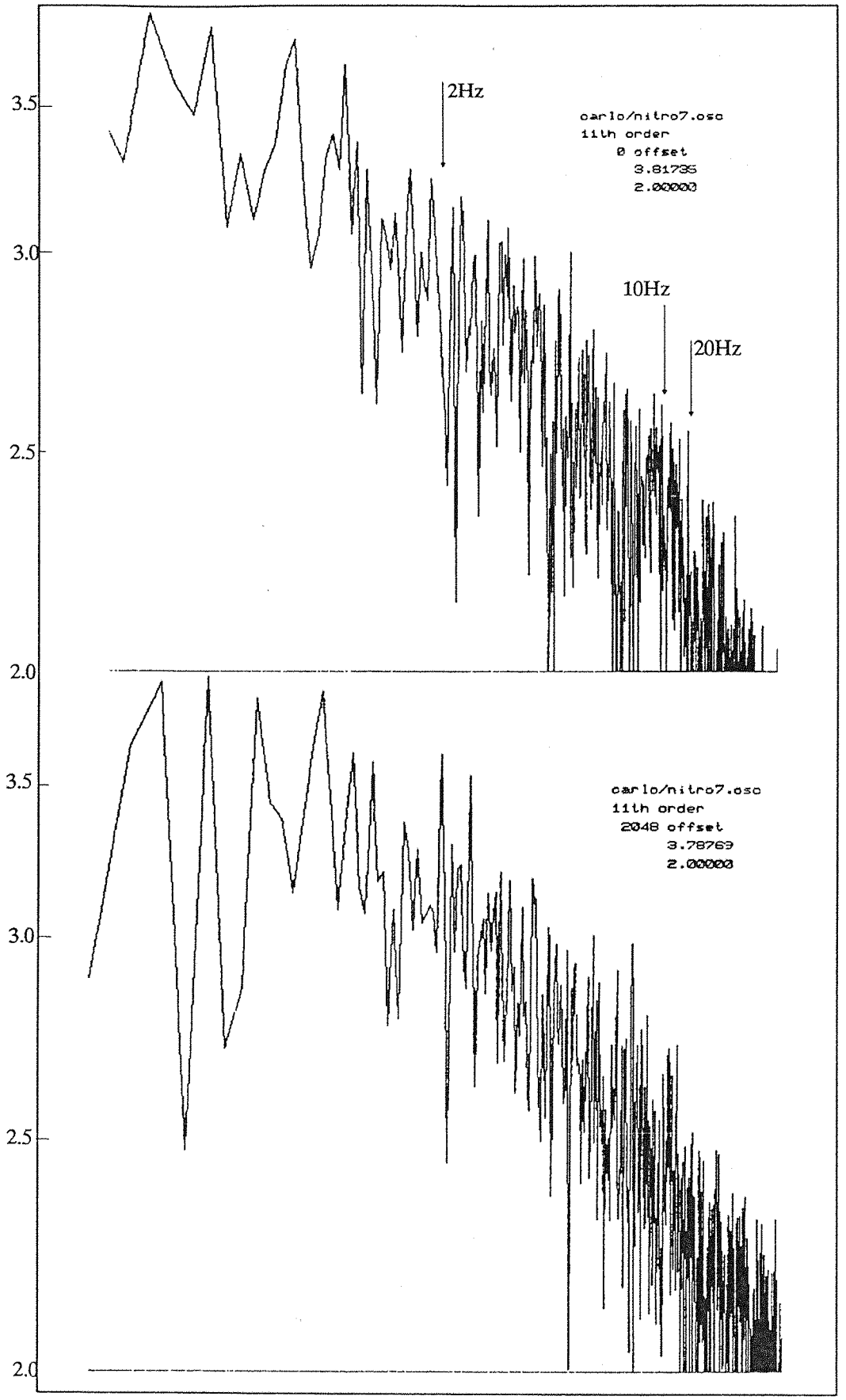

Fig. 26 Log-Log Power Spectra of Temperature Scan (LIN#7)

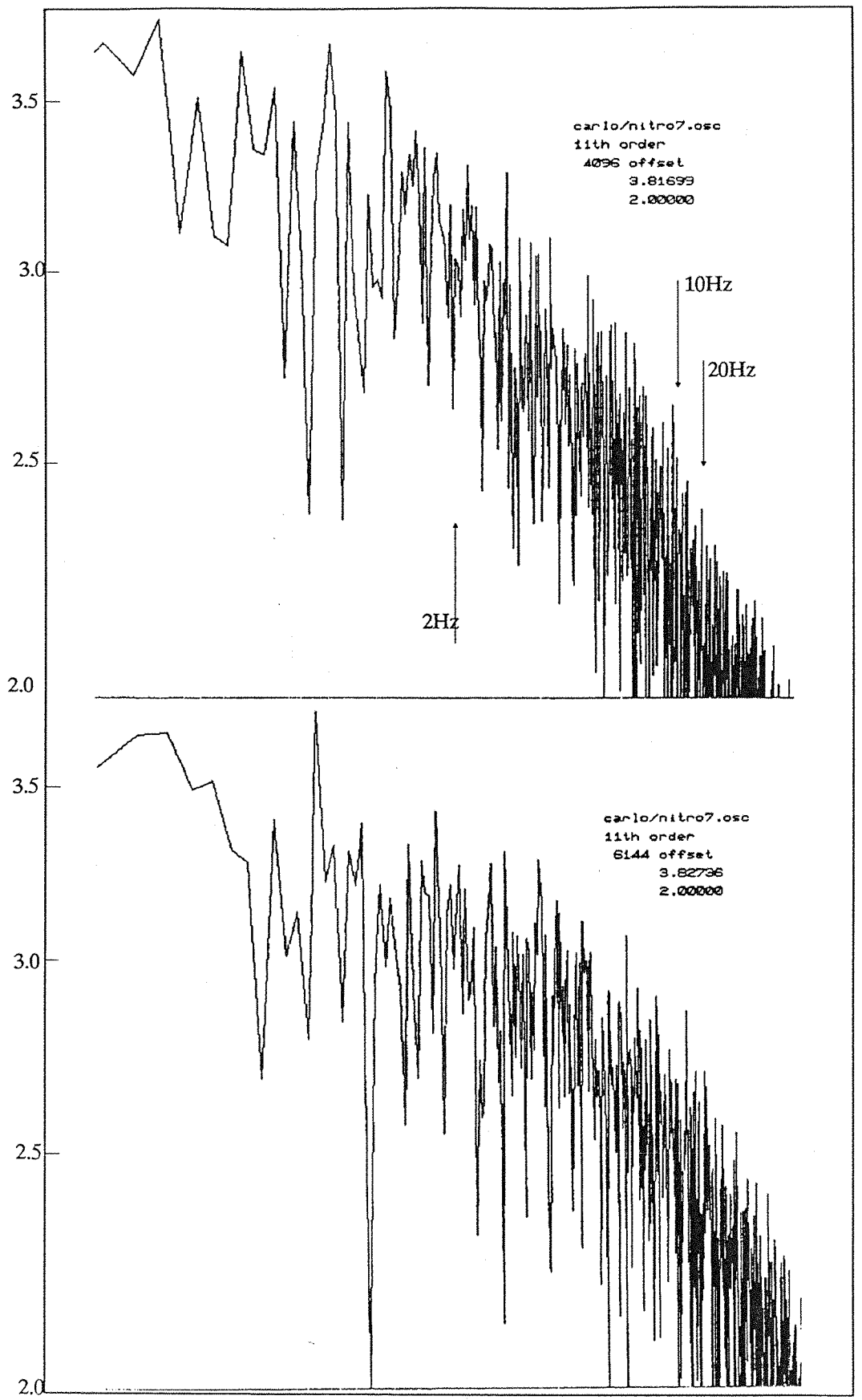

Power Spectra of Temperature Data from Previous Figure

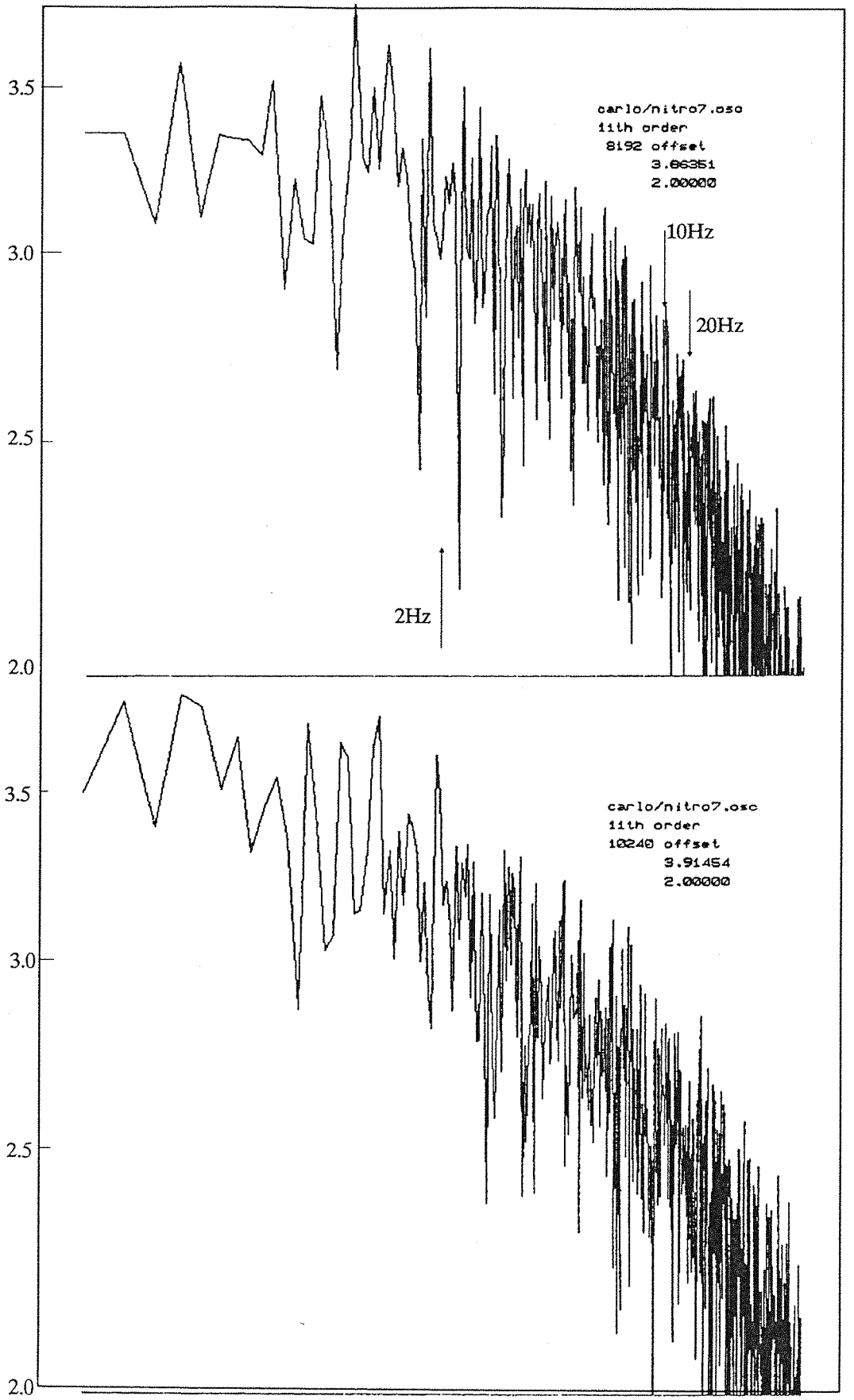

Power Spectra of Temperature Data Continued

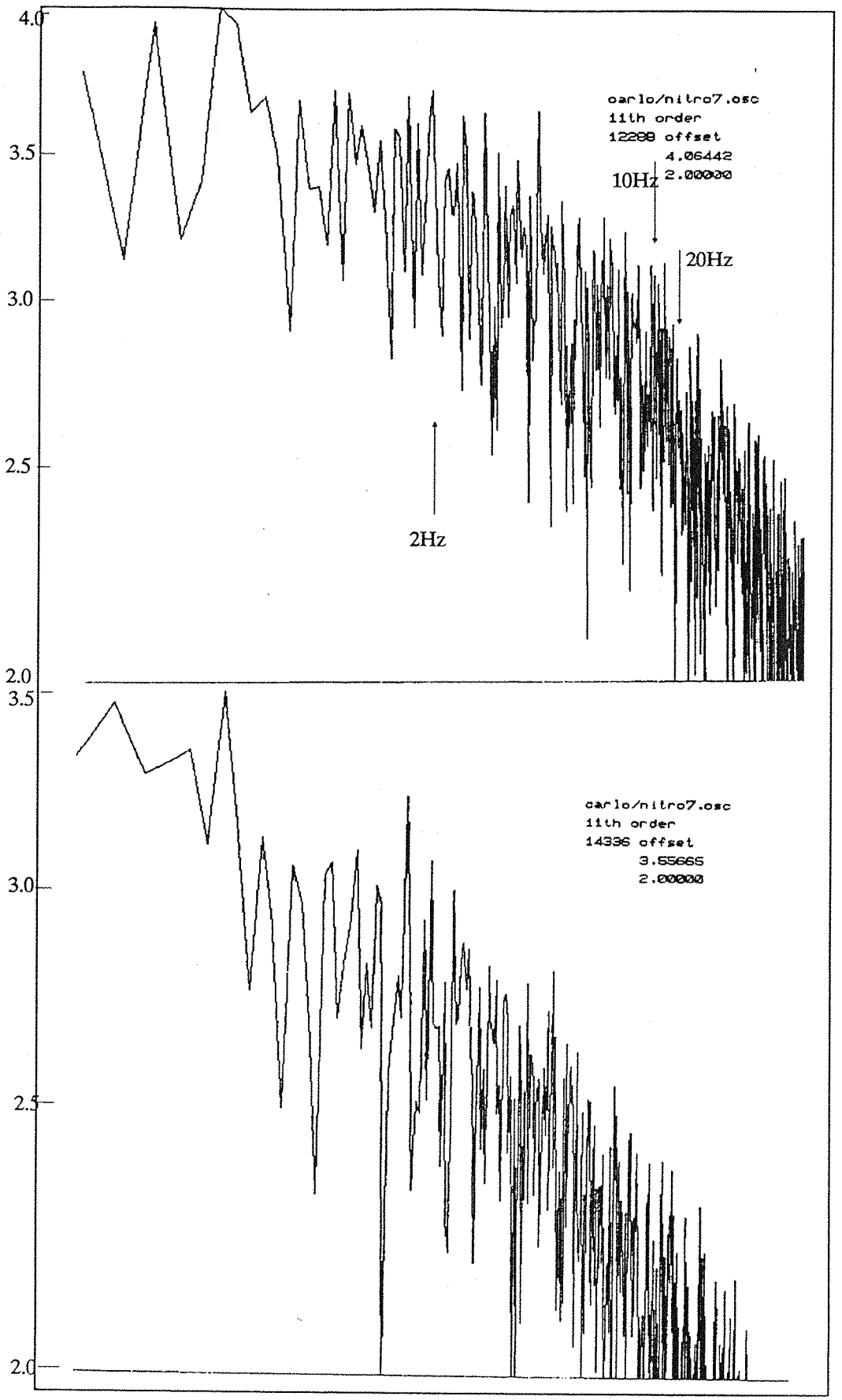

Power Spectra of Temperature Data Continued

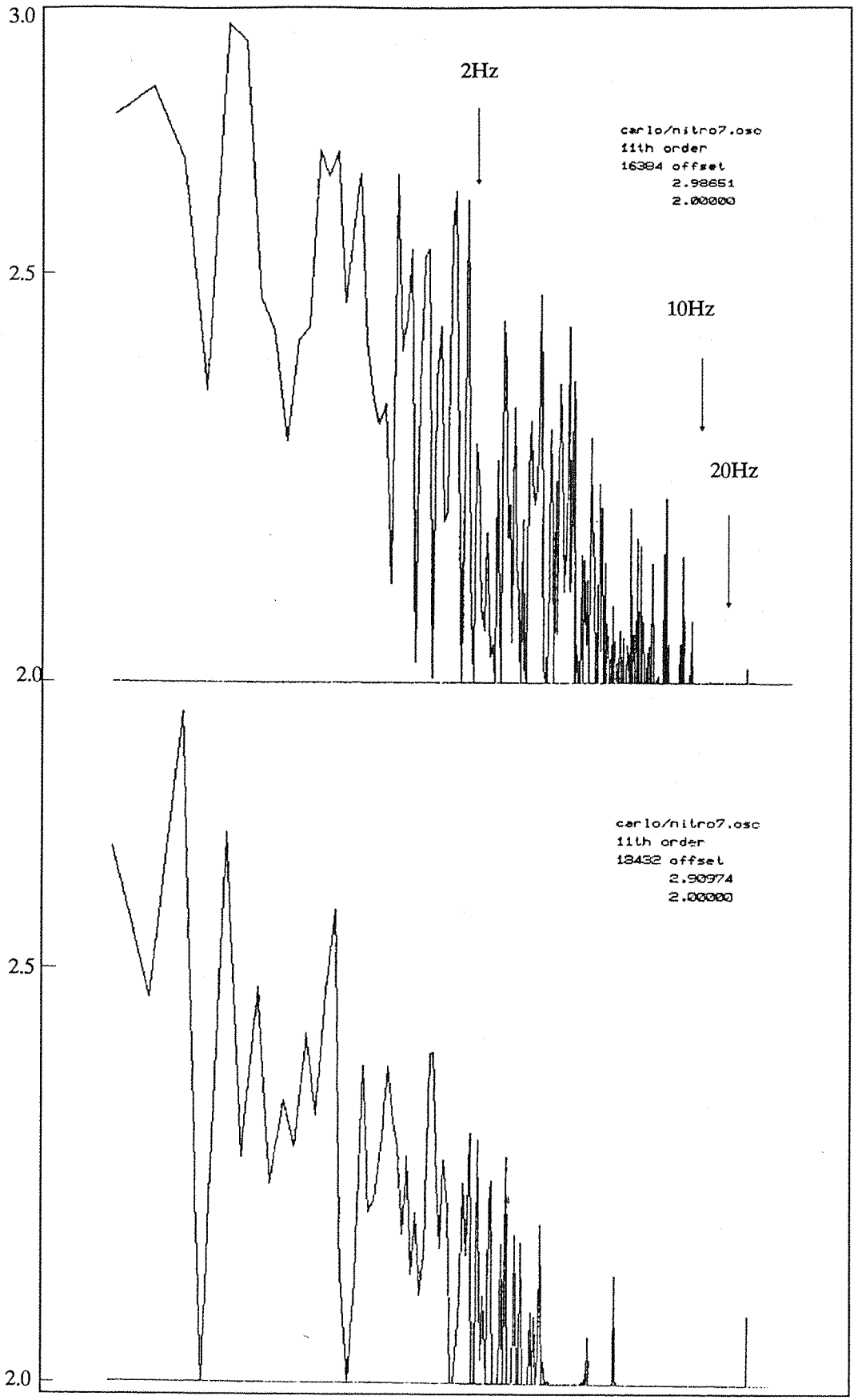

Power Spectra of Temperature Continued

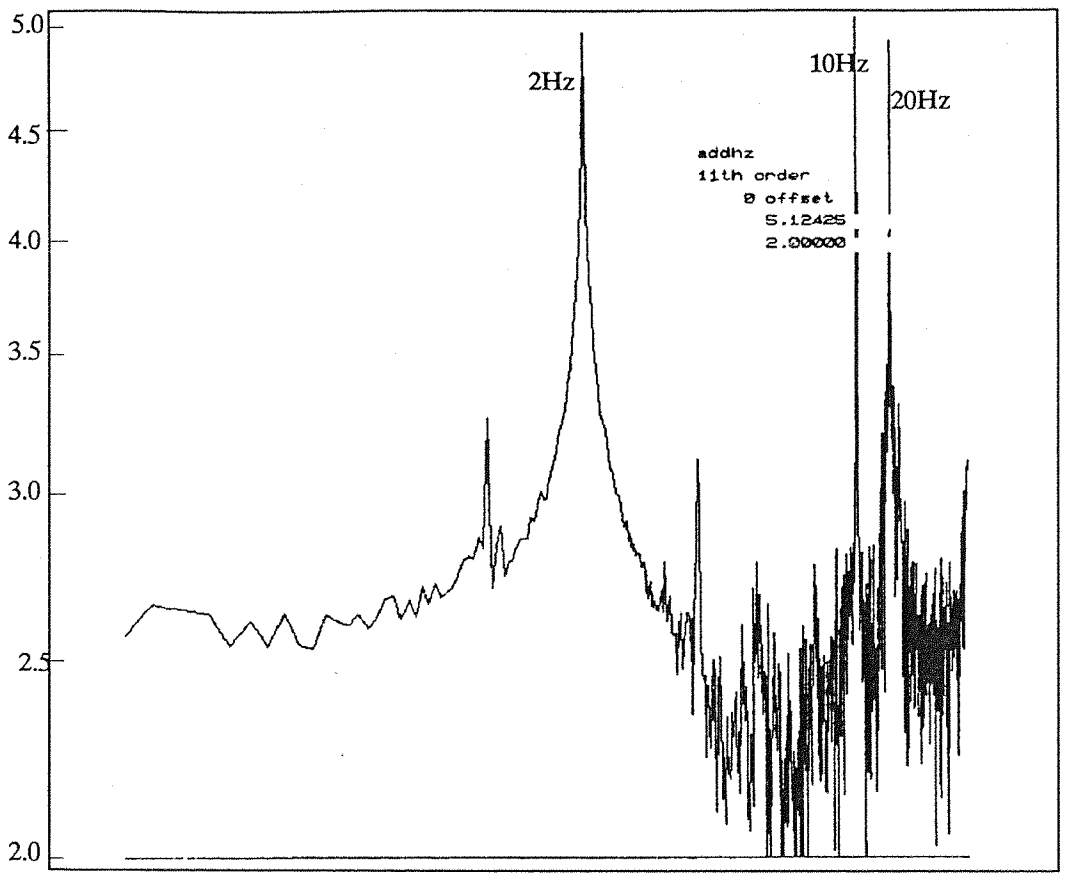

Fig. 27 Log-Log Power Spectra of Calibration Frequencies

Schlieren Imaging

As has been shown in the previous chapter the illumination of the screen is proportional to the horizontal temperature gradient in the fluid.

The schlieren images revealed structures in the fluid whose vertical position could be ascertained by moving the mirror nearer the surface. All of the structures that were seen were identified in this way to be located within the upper 5mm of the fluid. As the mirror was moved closer than 5mm to the surface the mirror itself changed the fluid flow patterns in the liquid but the thermal structures were apparent until the mirror was some 0.5mm from the free surface. Thus the orientation and the movement of the structures changed but not the form of the structures.

At all boiloffs the single most pervasive thermal structure in the fluid appeared to be a streamer in the sense of the discussion in chapter 4. It was generally aligned with the flow, which was radial for sufficient heat inleak into the pool and did not have one end at the wall. Careful examination of the prints included with this chapter will show that the streamer image is well defined upon a medium grey field as an object with one side dark and the other bright.

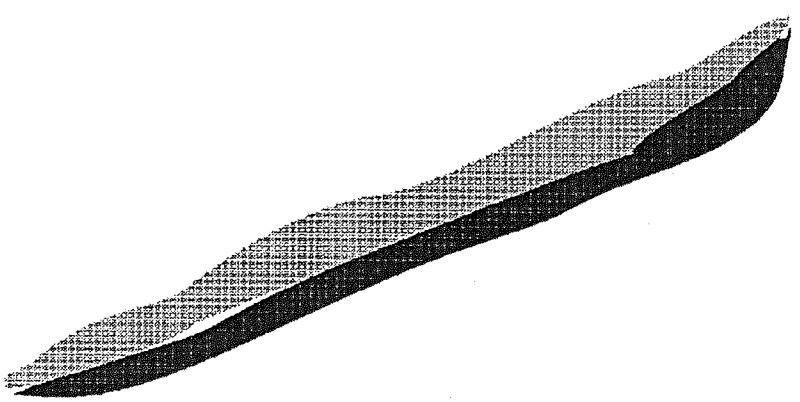

Fig.28 The Form of a Streamer

The bright side of the streamer is shown in a lighter pattern

The image can be integrated by hand to give a qualitative form for the temperature profile of a streamer as shown in Fig.30. For clarity the cross-section illumination is shown in fig.29

The integration across the streamer indicates a simple hotter, or colder region in the surface layers. The temperature scans reported earlier show that the structures appear to be colder as evidenced by the fluctuations in fig.20 where cold flows and eddies pass across the thermocouple and are evident are relatively isolated peaks in the temperature scan. In contrast there were no hot lines or peaks in the temperature scan. The streamers

are regions of cold liquid descending into the bulk and this is in agreement with the picture of streamers as lines of cold fluid found by Berg[16] and reproduced as fig.3

For mass flux through the surface less than ~ 100 litres s^{-1} m^{-2} (gas N_2 at S.T.P the radial flow in the liquid was insufficient to orientate the streamers towards the centre of the pool. The streamers were few in number and extended approximately the diameter of the pool. The change in illumination across the streamer is weak indicating relatively small thermal gradients. As streamer cross they may join but branching of streamers is not a feature. Some vorticity is evident and streamers appeared involved in vortex formation. Frequently vortices will terminate streamers at one end but commonly vortices appear at kinks in the streamer.

As the mass flux through the surface is increased to a region 100 to 200 litres s^{-1} m^{-2} the streamers become strongly aligned with the radial flow towards the centre of the pool. The thermal gradients in the streamers become larger but the width of the streamer remains quite similar to the low mass flux case. Instead the number density of streamers in the pool increases. Towards the centre of the pool the streamers terminate and vortices develop but apparently not linked to a particular streamer.

The central region of the pool develops a turbulent characteristic at higher mass fluxes. The streamers, which at this point are very numerous and almost cover the surface of the pool, develop an oscillatory instability in the θ plane. This oscillation may be damped as r decreases but usually the oscillation grows quite slowly in a similar way to the instability seen in rising cigarette smoke. The central core of the pool, whose diameter depends on the mass flux, is highly turbulent but the individual streamers remain easily identifiable. The length scale represented by the width of the streamer has not changed as the mass flux is increased nor as the streamer reaches the turbulent core. Diffusive mixing is not evident, rather the mixing processes appear to be associated with vortex motion and billows in the core.

In some experiments there appeared a 'crocodile skin' cell structure superimposed upon the streamer structure. This can be seen in the published prints and some others have been published, Atkinson *et at*[6] and by a colleague Rebai[63]. This pattern was only evident on reviewing the prints after the experiment and did not reappear so clearly in any later observations though there are faint patches with a similar structure. In this sense the observation was not repeatable in a controlled fashion. This pattern may be a result of some condensation in the optical path despite stringent efforts to ensure that no misting occurred. In so far as precautions could be taken these patterned results are believed to be real structures in the surface layer and no examination or hypothesis has revealed any other mechanism which could account for their appearance. Many photographs, films and video recordings of the experiments have now been done and the pattern remains elusive and must therefore be viewed with some scepticism.

To ascertain the effect of surface contamination on the form of the structures one experiment was undertaken in which a good quality image was viewed while carbon dioxide gas was introduced into the experimental vessel and thus condensed onto the surface of the fluid. No changes were seen in the image.

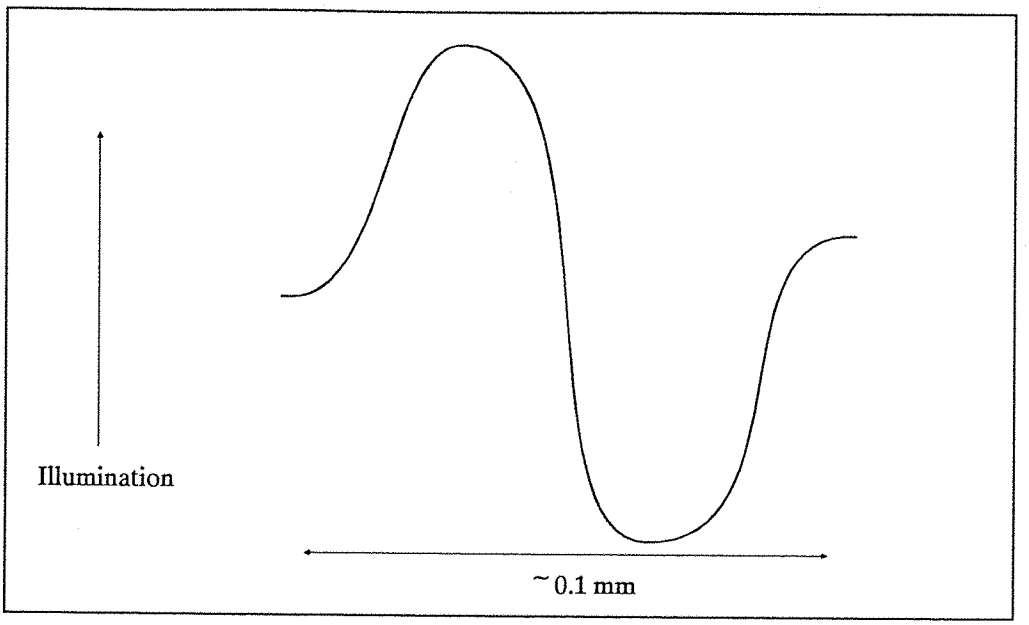

Fig. 29 Illumination Across a Streamer

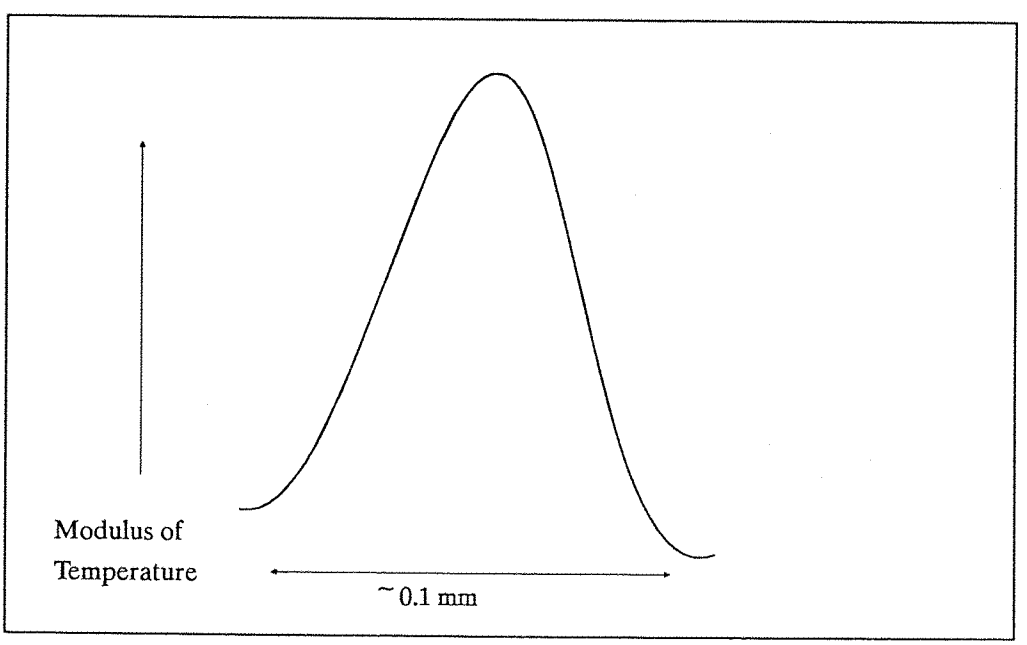

Fig. 30 Streamer Cross-Section Integrated by Hand

Fig. 31 Schlieren Image of LIN in a 50mm Diameter Vessel with an Evaporation Rate of 200 cc/min. gas N_2 at S.T.P

The image in the photograph corresponds to the 12mm wide mirror used in this experiment

Fig. 32 Schlieren Image of LIN in a 50mm Diameter Vessel with an Evaporation Rate of 400 cc/min. gas N_2 at S.T.P

Compared to the last figure the streamers are well defined showing larger temperature gradients in the fluid.

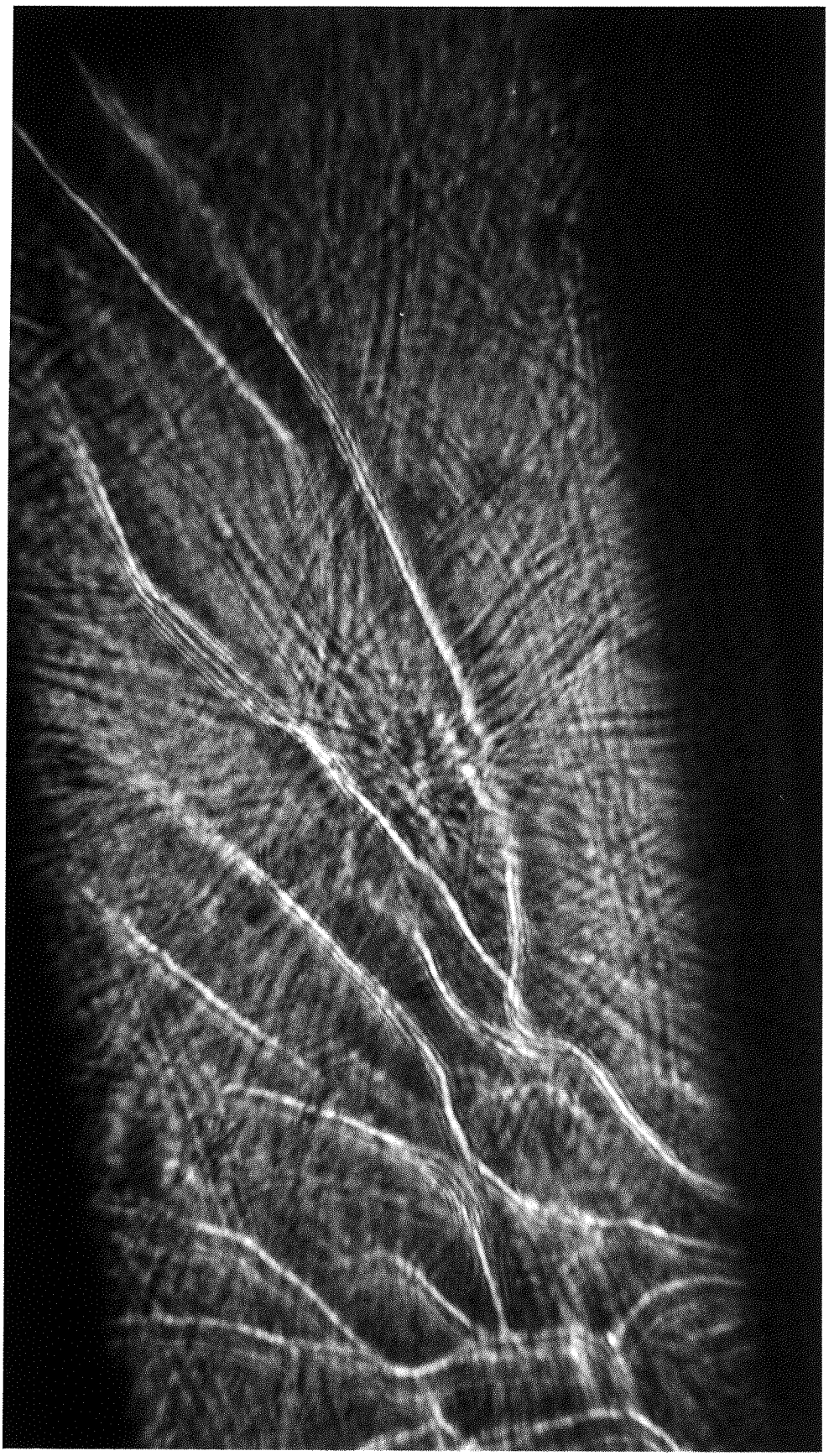

Fig. 33 Schlieren Image of LIN in a 50mm Diameter Vessel with an Evaporation Rate of 500 cc/min. gas N_2 at S.T.P

As the evaporation rate has increased the number of streamers increases, compare this to the earlier images.

Fig. 34 Schlieren Image of LIN in a 50mm Diameter Vessel with an Evaporation Rate of 900 cc/min. gas N_2 at S.T.P

This photograph demonstrates well the development of the turbulent centre of the surface. The centre of the pool to the right of the centre of the mirror.

Fig. 35 Schlieren Image of LIN in a 50mm Diameter Vessel with an Evaporation Rate of 1500 cc/min. gas N_2 at S.T.P

The central region of the surface is very turbulent at this level of mass flux, there are many streamers and the motion of these streamers indicates a high fluid velocity.

THE STRATIFIED SYSTEM

Saline-Water Observations

The set of experiments on saline and water layers reconciled the ambient results used by other workers with the experimental approach used in this study. It was important to compare and contrast the observations of the saline system with real cryogenic rollover and in particular to observe the mechanisms of mixing and the effect of the convective flow patterns on rollover behaviour.

Several runs were made with the base and some 10cm of the lower wall surface warmed by the oil bath. A typical time to rollover was 2-3hrs and this could easily be extended by reducing the oil bath temperature. However as the parameters of heat flux and wall/base heating ratio were varied the qualitative development of interfacial instability was similar.

In some observations it was noted that dissolved gases in the lower layer would form bubbles which would then detach from the wall and rise through the interfacial region. It was apparent from the shadowgraph that the turbulent wake of the bubble entrained fluid from the lower layer into the upper layer and the interface moved downwards.

As the temperature difference between upper and lower layers increased large motions were induced in the interfacial region. The motions were of greatest amplitude near the wall where the boundary layer flow had a high velocity normal to the interface. Little convective flow was seen in the upper layer. The oscillatory motions in the interface grew in amplitude and eventually broke, entraining fluid into the lower layer and the interface moved upwards. No saline was entrained into the upper layer at this point.The movement was not smooth but occurred in a stepwise fashion and this is clearly seen in fig.36.

Over some time the oscillations grew less distinct and took on the appearance of eddies and convective flows. The eddies were of a similar length scale to the wavelength of the oscillations. The penetration of the eddies took on some characteristics of percolation into the upper layer for the eddies were of a well defined scale and did not appear to mix well with the material in the upper layer. The movement of the interface now became smoothly upwards. The transport of heat into the upper layer was now sufficient for convective motions. It can be seen in fig.36 that the temperature of the upper layer now increased. The interface accelerated and final mixing occurred near the top surface, effectively the whole of the upper layer had been entrained into the lower layer.

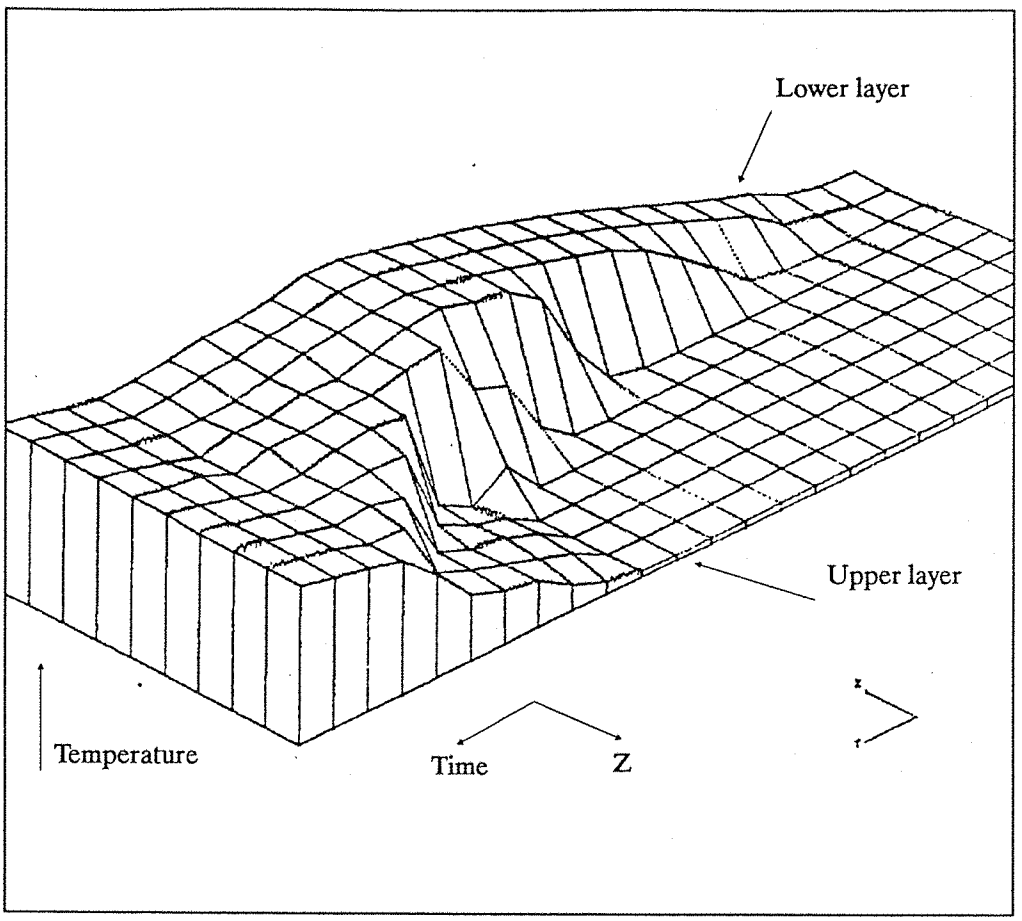

Fig. 36 Saline/Water Rollover Temperature Profile

Flow Visualisation of the LIN/LIN-LAr System

Much important information was gained from these observations but the image did not appear clearly in photographs, instead a video record of the experiments has been kept. In these experiments the heat inleak was provided by a base only heater covering the base of the flat-bottomed dewar 50mm in diameter, the absence of sidewall heaters enabled a clear view of the rollover process. A heating of 0.3W was delivered through the heater corresponding to a heat inleak of $150W/m^2$, a value that had been used in previous observations of rollover phenomena in the laboratory.

At the start of the experiment the heat inleak into the vessel was very small and it was evident that there were no convective motions in either the upper or lower layers. As heat was applied through the base heater a convective circulation developed in the lower layer and only a small distortion was seen in the interface. Even in the absence of wall heating the flow was seen to rise near the walls and descend near the centre of the layer. The central core forming a downflow stayed, in general, near the centre of the vessel and although it was never central it did not move appreciably. The form of the core flow was evident and similar to the flow seen in slow liquid jets. There was little evidence of turbulence at the boundary of the core flow.

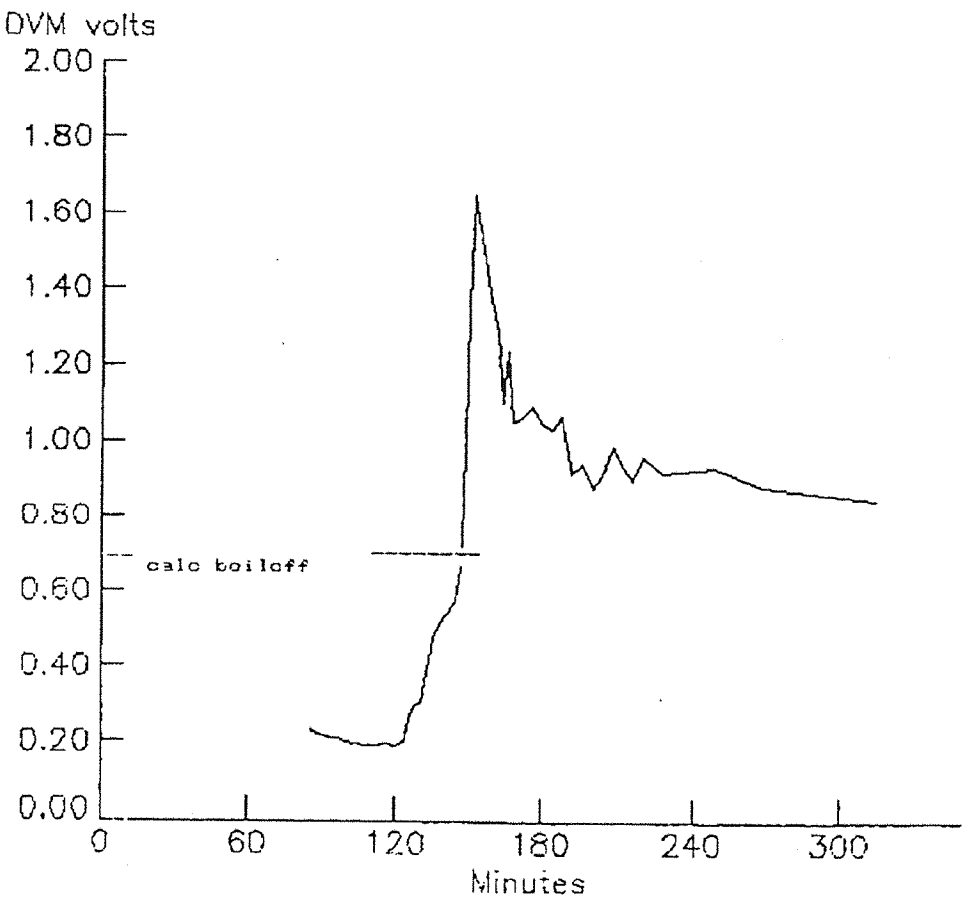

Fig. 37 Vapour Generation Record of Flow Visualisation

As the temperature of the lower layer increased the interface developed an oscillatory form with the greatest disturbances near the wall where boundary layer flow was evident. The boundary layer would intermittently move the layer vertically upwards and then fall back into the lower layer. The boundary layer separated from the wall at the interface and a small amount of material from the upper layer was entrained into the lower layer as evidenced by the movement of the interface upwards. The disturbances in the interface appeared to be the results of intermittent thermals or eddies incident on the underside of the interface though a wavy motion was evident and its wavelength was approximately of the order of a/5 though this figure should not be taken literally in view of the rather chaotic nature of the motions.

As the experiment progressed the wave motions in the interfacial region grew in amplitude and near 120mins in fig.37 convective motions were apparent in the upper layer. The rise in boiloff at this point is apparent. Convective motions in the upper layer developed strongly and the interfacial level fell slightly as liquid from the lower layer was now entrained into the upper layer. This is in contrast to the events in the saline-water system where the interface only moved upwards indicating that entrainment was occurring only from the underside of the interface. At this time the boundary layer plume from the lower layer into the upper region was clearly breaking and fluid was now entraining from the lower boundary layer into the upper layer by this mechanism. It can be seen from the boiloff record that the it now increased sharply and the peak of the boiloff occurred while layers were clearly visible.

The movements in the interface had grown in amplitude and in wavelength and were more in the form of wave motions. The downward jet formed by the upper layer convective flows played an important part in the entrainment process near the centre of the vessel and breaking waves could be seen in the interfacial region that was now subject to oscillations of a large amplitude, comparable to the depth of the liquid. The wavelength of these oscillations had lengthened to approximately the diameter of the vessel.

The boiloff at 180 minutes is below the peak level and several smaller peaks of vapour evolution correspond to major entrainments of the lower level into the upper layer. Final disappearance of the interface was not evident until 240mins into the experiment when it can be seen that the boiloff remained at an elevated level above the normal value associated with similar heating in an unstratified fluid.

Temperature Measurement Near the Interface

The temperatures taken near the interface could not utilise the change of level as the measurements near the surface had done. It was necessary to position the thermocouple near to the interfacial region with some judgement. Although the schlieren visualisation of the interface had revealed a very similar picture to the structures at the surface the temperature scans indicate some subtle differences. Fig.38 shows temperature measurements taken in a similar way to those at the surface with the thermocouple positioned some 5mm from the interfacial region. Its precise position is hard to define because of the diffuse nature of the interface.

It can be seen that the fluctuations in temperature are of longer timescale than those seen in the region below the liquid-vapour interface.

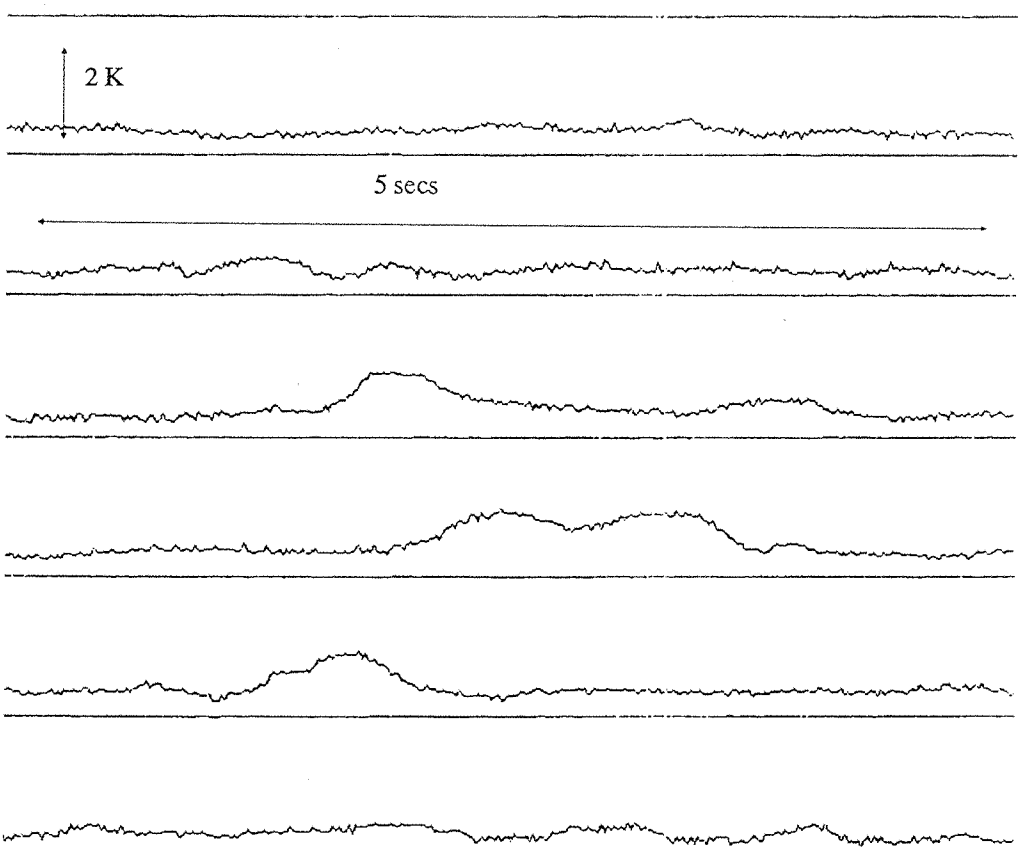

Fig. 38 Temperature Scans Near the Interfacial Region , 30s continuous.

Schlieren Imaging of the LIN/LIN-LAr Interface

The schlieren images of the liquid-liquid interface appeared qualitatively similar to those seen at the free surface, moreover the horizontal wavenumber of the streamers is very similar to that seen at the surface. The compositional gradients at the interface were not discernible since the refractive index change for low concentrations of LAr are much less than those due to temperature fluctuations. No compositional gradient would exist in the lower layer material and any effect due to horizontal compositional differences would only become apparent when large scale mixing is initiated between the layers. Once mixing starts at the interface the heat transport to the upper layer is sufficient for the onset of convective motions at the free surface which contribute to the image. The changes in the interfacial region during mixing could be observed using the perspex rod and the mixing processes appeared highly turbulent in the form of the central core of the upper layer shown in the prints included with this report.

The observations suggests strongly that both interfaces have great similarities and this confirms the conclusions of the previous section where the high-speed temperature measurements revealed an almost identical pattern to that seen at the surface.

Rollover Temperature Profiles

In the laboratory scale simulations of rollover the enhanced boiloff due to mixing at the interface had a characteristic pattern when compared to bubbles passing through the interface and surface layer. The temperature profiles clearly show the contrast between the two kinds of events. The results from bubbles are discussed in the next section.

In interfacial mixing the rise time of the boiloff is slow and in the visualisations of boiloff this is seen to be associated with entrainment of lower layer material into the upper layer. The temperature profiles demonstrate a commensurate increase in temperature of the upper layer as material passes from the lower layer into the upper layer and it appears that the surface structure controlling the boiloff remains intact. By contrast the passage of a bubble through the system increases the boiloff and lowers the temperature of the upper layer.

The rollover event seen in fig.39 demonstrates the time history of the temperatures in the upper and lower layers for an upper layer of LIN and a lower layer of 2% LAr in LIN v/v and a base only heating of 150W/m^2. The vessel was 50mm in diameter with a lower layer 10cm in depth and a 9cm upper layer. Figs.40-44 show details of this example event referenced in the main picture by letters 'A'-'E'. Each vertical segment is a 2s interval and 9 microthermocouples spanned the system.

It can be seen in fig.40 that a temperature difference of 2K had been established at the start of the measurements and that the temperature profile of the lower layer is quite uniform as shown by the relative smoothness of the top of the isometric view. There is some indication that the temperature of the upper layer fell slightly just at the end of fig.40 and from the fall in temperature of the lower layer it is apparent that interfacial heat transfer was substantial at this point, greater than the base heat inleak.

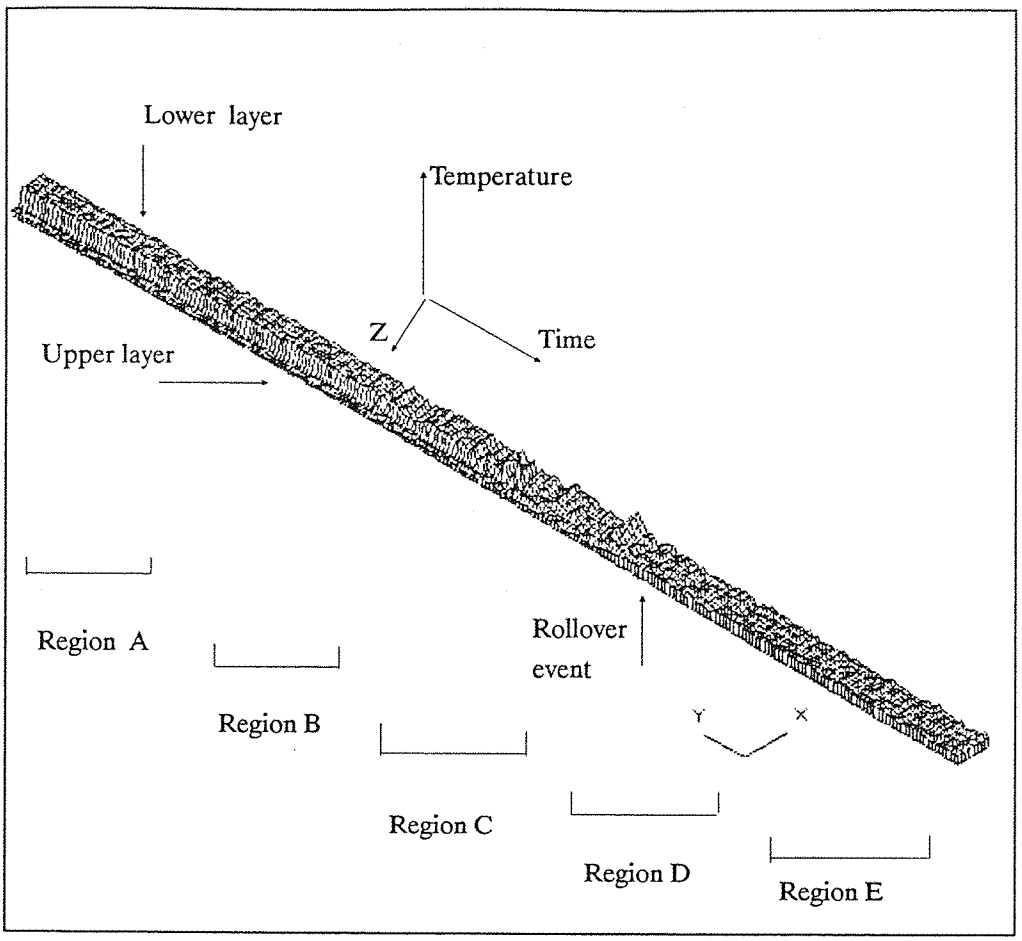

Fig. 39 Temperature Profile of Rollover in LIN/LAr (cra#1)

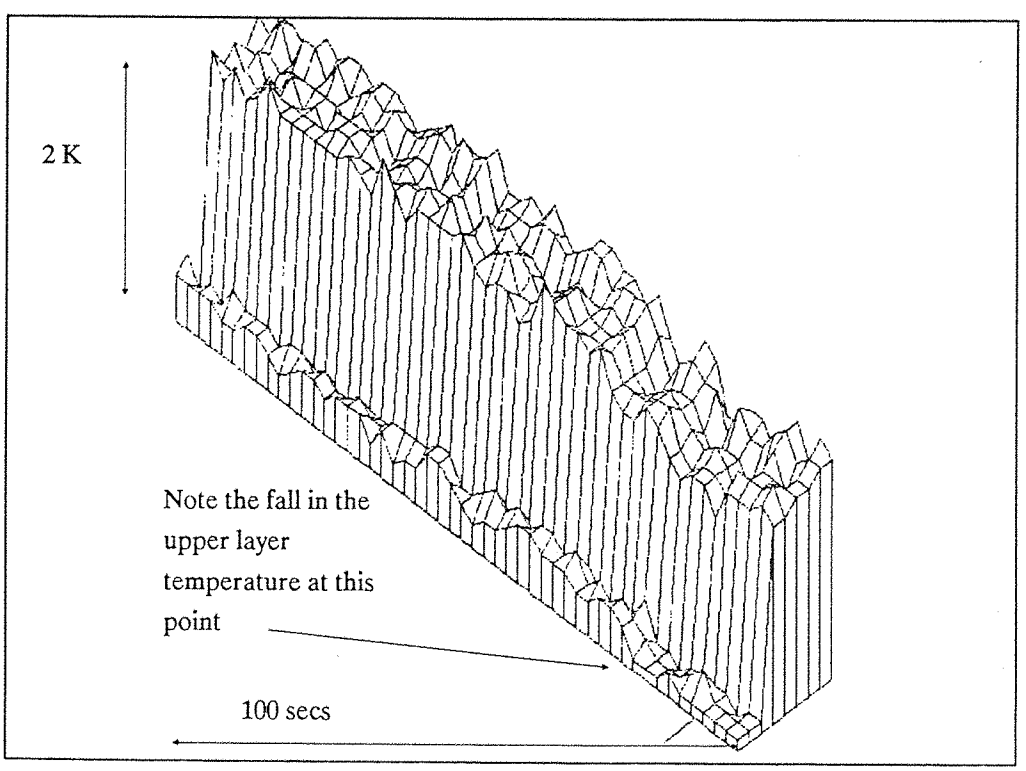

Fig. 40 Region 'A' Detail of LIN/LAr Rollover Event

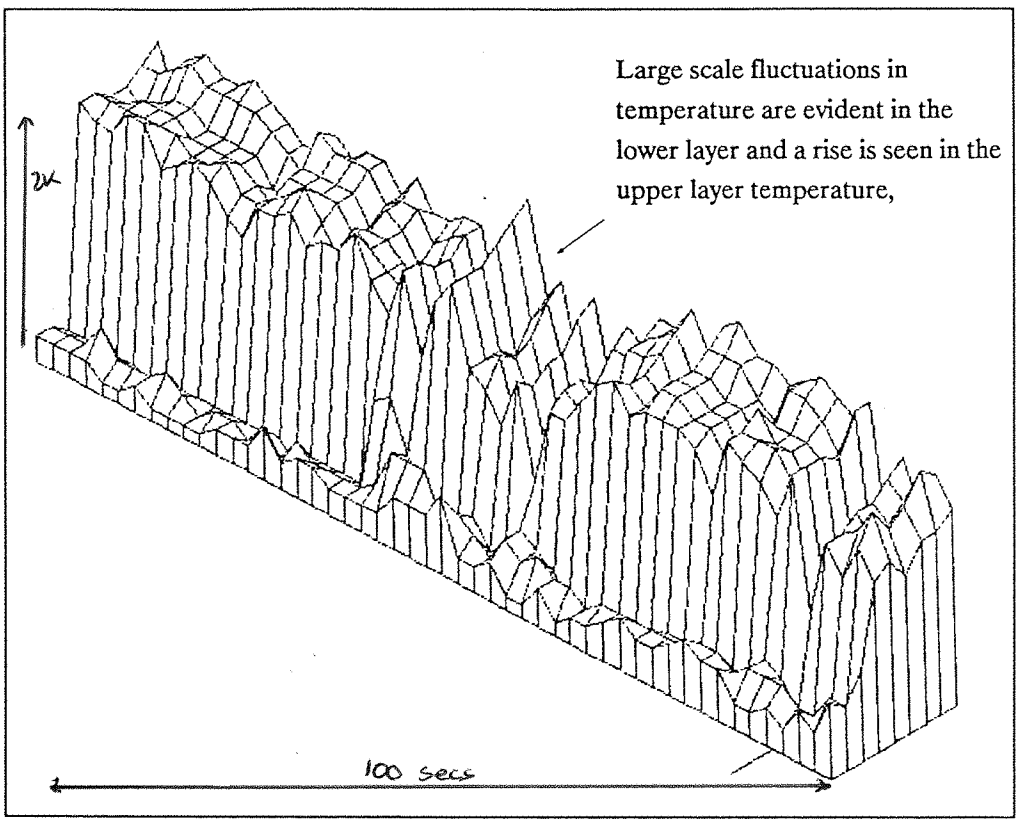

Fig. 41 Region 'B' of Rollover Event

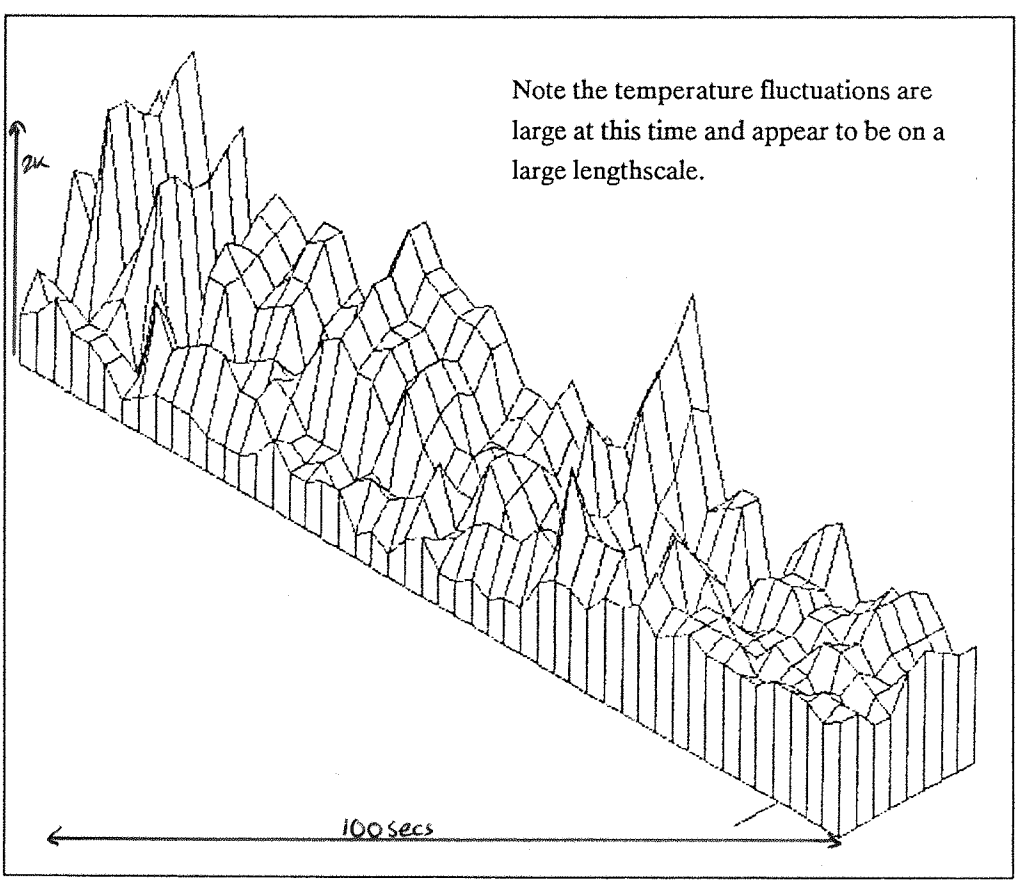

Fig. 42 Region 'C' of Rollover Event

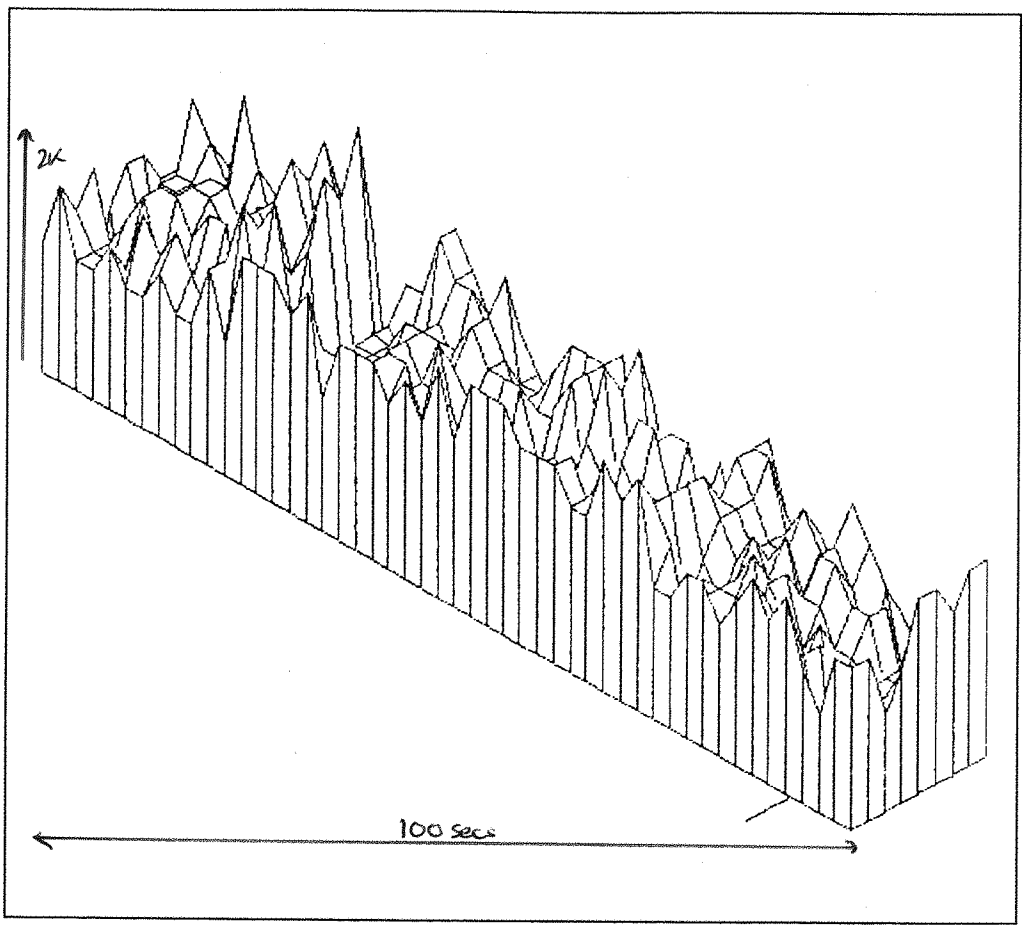

Fig. 43 Region 'D' of Rollover Event

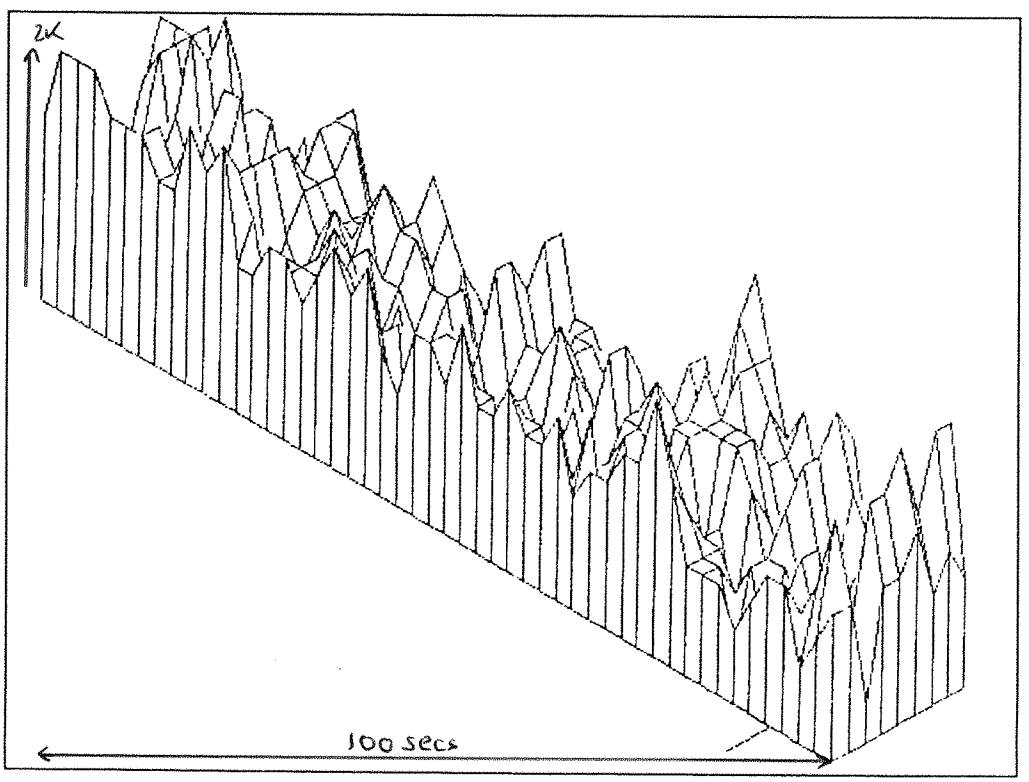

Fig. 44 Region 'E' of Rollover Event

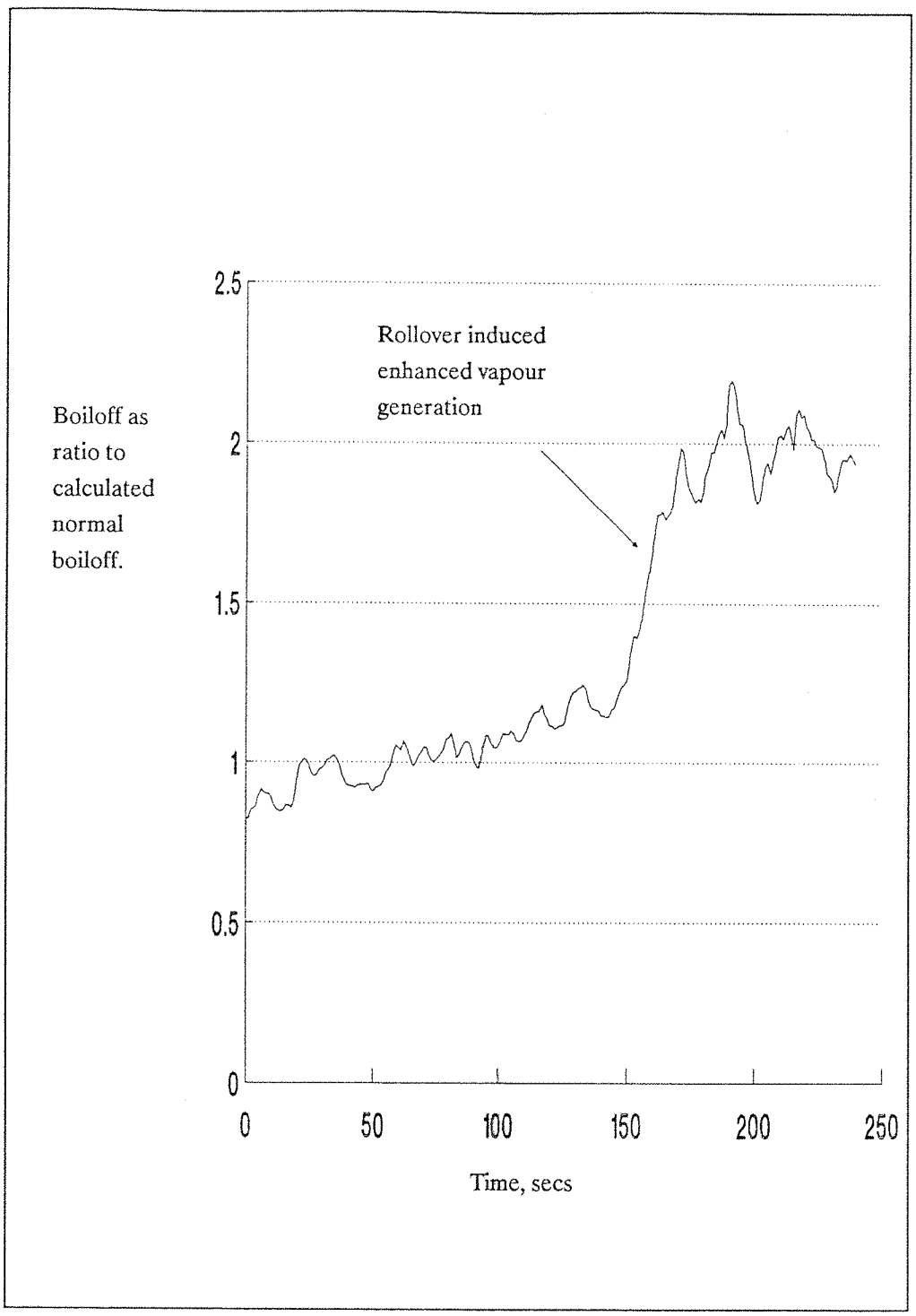

Fig. 45 Vapour Generation of LIN/LAr Rollover

In the centre of Region B the temperature fluctuations in the lower layer become more prominent and the temperature of the upper layer rises significantly. From the visualisation studies of rollover we can associate entrainment and mass transfer throughout Regions A and B.

In Region C the major mixing occurs with a pronounced elevation of the upper layer temperature. The boiloff at this point was at a maximum and there are major fluctuations in the temperature profile of both layers indicating that the mixing processes extended deep into that layer and upwards towards the surface. Despite the large scale mixing the highest temperature in Region C occurs after the rollover event, in fact ~60 seconds after large scale mixing processes are clearly present. It must be concluded therefore that large eddies of hot liquid are preserved during this phenomenon and that they are not subject to viscous mixing because of their size. In Regions D and E, which extend the observations by 100 seconds each, the large scale temperature fluctuations remain.

Bubbles Generated in the Lower Layer

Nucleate boiling in the lower layer of stratification was a persistent and unwelcome feature of the early experiments on stratified layers. An examination of the results from these events is of merit since the vapour bubbles did produce large boiloffs and had a characteristic signature in both the change of stratification and the vapour generation.

The incidence of a single vapour bubble was not sufficient to completely mix both the layers in the vessel. Liquid from the lower layer was entrained from the wake of the bubble into the upper layer causing the level of the interface to fall. A typical bubble event is shown in fig.46 where it is apparent that both the upper and lower layers were superheated prior to the event. Several features can be identified.

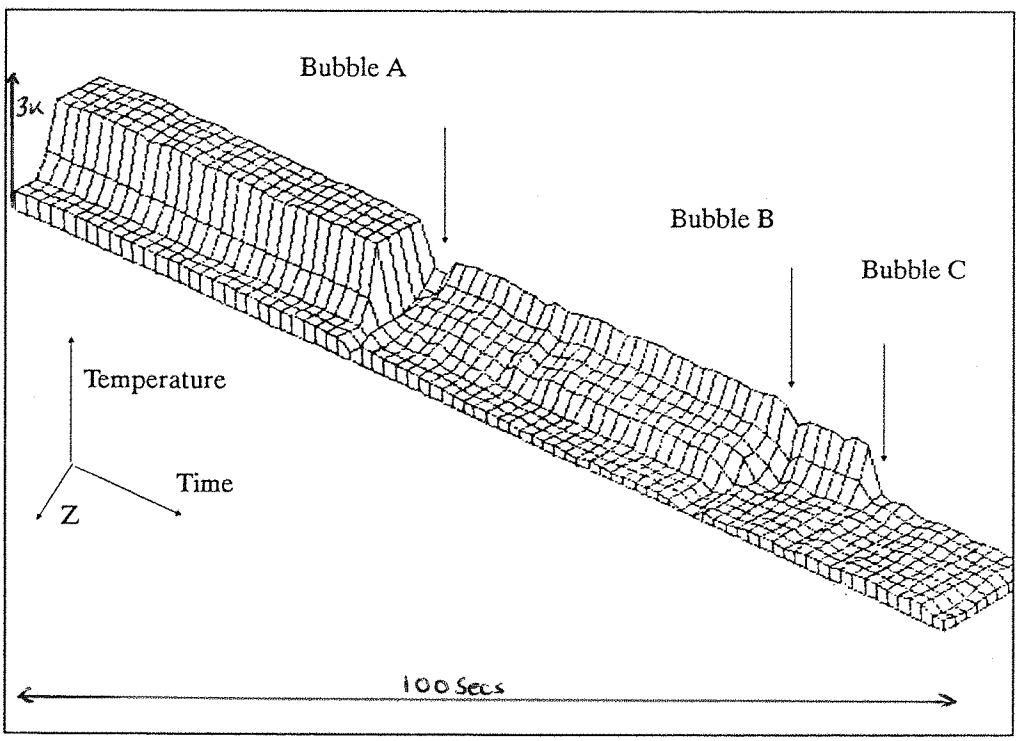

Fig.46 Temperature Profile of Bubble Event (rollover/data)

- The bulk temperature of the lower layer falls nearly uniformly and remains at a lower level.
- The temperature of the upper level also falls in an equivalent way.
- The interface moves downward (in this figure away from the reader)
- The temperature of both the upper and lower layers remain well below the temperatures prior to the vapour bubble incident for a considerable time, in excess of 100s in this example.

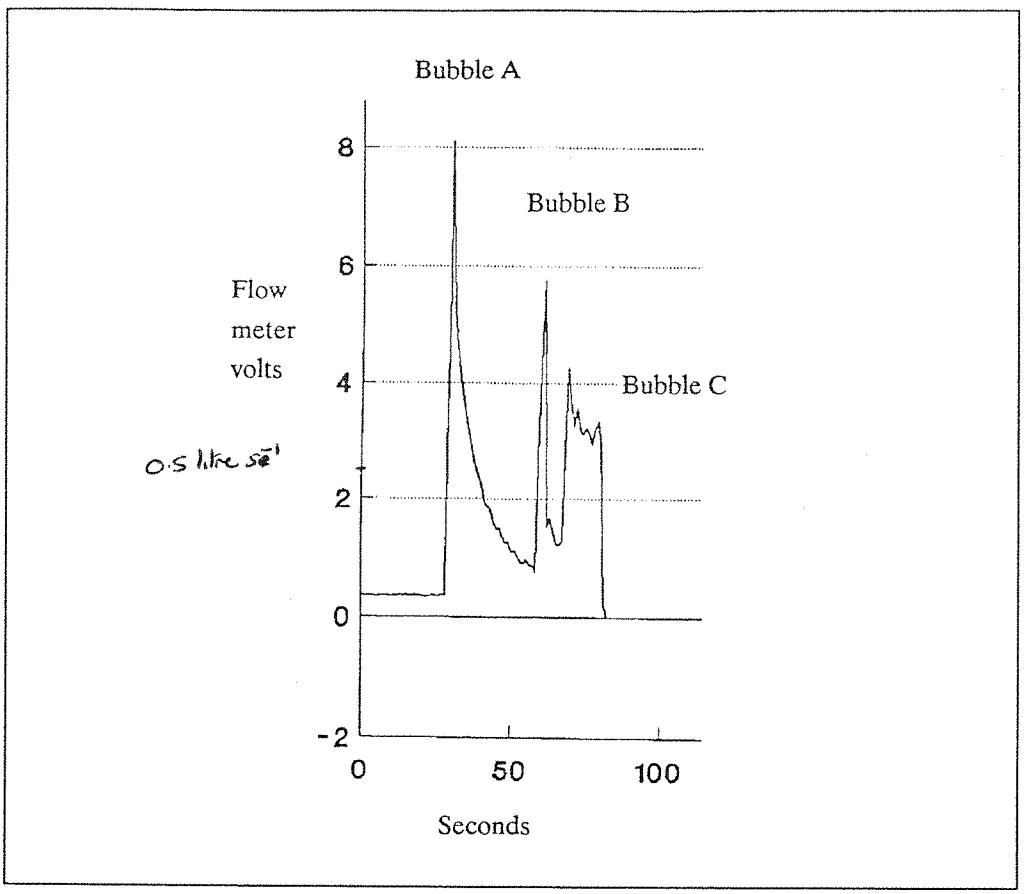

Fig. 47 Vapour Generation from Boiling in Lower Layer

The boiloff chart for a bubble event is shown in fig.47

The boiloff record shows the very rapid increase in vapour generation. The decline in boiloff is much slower and enhanced boiloff continues for some considerable time after the bubble event and comparing the temperature data in the previous figure it can be seen that the enhanced boiloff coexists with a lower bulk temperature. The conditions in the upper layer have deviated from the equilibrium values observed in single layer systems. In this thesis it has been demonstrated that the surface layer effectively controls the rate of vapour generation and this is discussed further in chapter 8. It must therefore be concluded that the passage of the bubble through the surface layer and the incidence of the turbulent wake of the bubble has changed the nature of the sublayer structure and that these changes persist for a considerable timescale.

8. DISCUSSION

ROLLOVER

The heat and solute transfer leading up to rollover instability is seen to be controlled by diffusion processes with a long timescale of the order of tens of hours. Models of rollover that use the enhanced heat and mass transfer rates of double-diffusive convection are equally successful at predicting the same timescale to the onset of EVG. The processes of mixing that occur during rollover are very much faster than those of diffusion being of the order of tens of minutes. Enhanced mass and heat transfer due to double-diffusive oscillatory instabilities within the layer may make a minor correction to the time taken for the densities to approach equality. It follows that the calculations of existing rollover models serve only to model the diffusive transfers and thus to calculate the time to the rollover instability.

The flow visualisation experiments described in this thesis have shown that entrainment mixing and boundary layer penetration are both important when the densities are nearly equal. The precise mechanism by which a given stratified system then mixes is dependent on the degree of sidewall heating and the velocity of the boundary layer. With small boundary layer flows the interfacial region may not be penetrated until the densities are equal. Conversely a high rate of boundary layer flow is observed to penetrate the interfacial region and transfer heat and mass by a mechanism of entrainment of the plume.

The hazard of rollover is the high EVG and what is needed is a correlation to predict the EVG during a rollover event. Unfortunately the experiments for this thesis have not provided such a correlation, but they do provide a good indication of what further experiments are needed. For example, the peak EVG estimated for the La Spezia incident is very much higher than the equilibrium vapour generation at the estimated bulk superheat. The peak rate of vapour generation was conservatively a factor of 200 times the normal boiloff rate for the tank allowing for the fact that only the mean rate of 1189 kg/hr over a 3hr period has been reported.

It is clear that the behaviour of the LNG at La Spezia, with an estimated 2-3K bulk superheat in the tank with heel and cargo, does not fall within the correlation of bulk superheat to rate of vapour generation presented in this thesis. The normal boiloff from the La Spezia tank corresponds to a bulk superheat of the order of 0.5K. The added cargo was ~2K hotter. A calculation, using the correlation presented in this thesis, from the average peak rate during the 3hr period of relief valve opening corresponds to a bulk superheat of 15K. It must therefore be concluded that the surface layer was not acting as the thermal impedance in the fluid, that the conducting region of the surface structure was absent and the LNG at La Spezia was not in the normal state of a stored cryogen.

SURFACE AND INTERFACIAL STRUCTURE

The schlieren observations reveal radially oriented structures, called streamers, in the surface whose number density increases with the rate of surface vapourisation. Near the wall of the vessel these streamers move around in the surface region only very slowly with time constants of the order of 10 seconds. As the streamer approaches the centre of the vessel it exhibits an oscillatory instability and in the central region the streamers form a turbulent zone with time constants of the order of 0.1 seconds. They have been identified as lines of cold fluid descending into the bulk.

The form of the streamers and the oscillatory mode of instability that they undergo as they approach the centre of the pool strongly indicate a radially inward directed flow in the surface structure and in the interfacial region.

Schlieren visualisation and temperature measurements of the liquid-liquid interface reveal a very similar structure to that seen at the liquid-vapour interface.

ENHANCED VAPOUR GENERATION

The sublayer structure has been shown to control the rate of vapour generation from the bulk liquid. In an equilibrium condition there is a correlation between the bulk superheat, above the surface saturation temperature, and the rate of vapour generation per unit area. In the sublayer immediately adjacent to the surface there exists a region supporting a high temperature gradient. The thickness of this region is related to the bulk superheat and the rate of vapour generation and the heat flow across it is controlled by conduction. It is this conduction mechanism which provides the major impedance to heat flow from the bulk leading to evaporation at the surface.

Any bubble generated in the liquid is observed to collapse the surface structure leading to enhanced vapour generation and the removal of superheat from the bulk. Furthermore, the ensuing release of superheat from the bulk has a time constant far greater than the passage of the bubble through the liquid. We can therefore conclude that the time constant for the formation of the sublayer is long or that the turbulence associated with the wake of the bubble is sufficiently energetic to collapse the temperature gradient. There is some evidence from the experimental studies of temperature profiles during rollover mixing that eddy formation at the interfacial region may also be sufficient to collapse the surface structure.

STABILITY OF THE SUBLAYER

In chapter 5 it was noted that the liquid-liquid interface may be stable to infinitesimal perturbations beyond the statically stable configuration but entrainment serves to mix the interfacial region when the densities become equal. The problem is then why the liquid-vapour sublayer is stable to entraining mechanisms beyond the limit of a stable density stratification. Specifically, why is the sublayer not entrained into the bulk by the convective processes incident upon it from the bulk?

We speculate that either:

- The entrainment mechanisms at low stability are suppressed.

- The entrainment of the sublayer does occur but reestablishment of the thermal gradient has a shorter timescale such that entrained liquid is replaced as rapidly as it is lost from the sublayer.

If the entrainment is suppressed then we expect the local Richardson number must be large indicating a high density gradient in the surface or that the vertical gradient of the horizontal velocity is vanishingly small. The latter would support the observations of ambient liquids referred to in chapter 3 and the behaviour of liquid balls resting on the surface of LIN in that the horizontal component of the velocity is maintained up to the true surface.

EDDIES AND THE SURFACE STRUCTURE

In chapter 3 it was shown theoretically that the surface layer should be less stable to large scale eddies incident upon it, the balance of gravitational and surface tension restoring forces occurring for eddies of length ~ 4mm in LIN. The results of the experiments indicate that the length scale of the eddies produced at the interface by mixing processes near the limit of a statically stable density stratification are of the order of the diameter vessel in laboratory scale simulations. There is also some evidence from the analysis of the simulation that the upper layer temperature did fall slightly near rollover. We must therefore question whether the eddies produced in larger vessels will retain scale lengths as large as the vessel and whether the surface sublayer will be less stable to large eddies. If this is indeed the case then a mechanism for the EVG from the La Spezia tank can be postulated that avoids invoking nucleate boiling, a mechanism rejected by tank operators.

The La Spezia event was characterised by high boiloff, 'sloshing' sounds reported from the vessel and an EVG timescale of over 3hrs. It is conceivable that mixing processes at the interfacial layer created large eddies which circulated in the vessel. These eddies were sufficient to collapse the sublayer when they reached the surface and indeed to

significantly distort the liquid surface which would account for the noises. The timescale for the dissipation of these eddies would be long since their size precludes viscous effects. Laboratory simulations in 8cm diameter dewars show that smaller eddies, of the order of 5cm, were evident from their effect on the temperature profile for more than 200secs. The lifetime of larger eddies, in larger vessels, is proportional to the square of their characteristic length as shown earlier. Such large scale eddies will have an extended lifetime and may play an important role in the vapour generation of the rollover process through their effect on the surface sublayer.

9. RECOMMENDATIONS

ON EXPERIMENTAL METHODS

The Dynamics and Stability of the Sublayer

The experimental simulations and measurements have shown the importance of the sublayer in controlling vapour generation in both stable and unstable systems. The sublayer itself is stable to most fluid flows incident upon it in this set of experiments. It has been seen that bubbles, formed from boiling in the bulk liquid, do have the capability to destroy the sublayer. This begs the question as to the stability of the sublayer to perturbations and this has implications beyond stratified systems to all cryogenic storage vessels and their vapour generation instabilities outlined in chapter 1.

It is recommended that an experimental investigation is performed to elucidate the conditions necessary and sufficient for bulk liquid flows to penetrate the sublayer and reach the liquid-vapour interface.

There has been considerable investigation of the response of interfaces to turbulence, normally from an oscillating grid, and the extension of these techniques may provide a sound foundation for the generation of known perturbations. Alternatively convection from a point source can be used, but this will introduce thermal gradients that will interfere with observations that rely upon measurement of temperatures. In chapter 3 it was shown that surface tension plays a less important role in the stabilisation of the surface to large eddies or plumes and therefore consideration must be given to scaling effects.

The schlieren observations detailed in chapter 7 show a wealth of features in the upper layers of the fluid and this experimental technique offers a way to observe the response of the sublayer. As explained in chapter 6 the illumination at a point on the screen is proportional to the horizontal temperature gradient. If the bulk liquid is allowed to reach the liquid-vapour interface through the sublayer the existing schlieren apparatus will be sufficient to observe breakdown of the structure. Perhaps a more useful variation on the schlieren observation technique would involve using stainless steel mirrors, angled at 45 degrees, to illuminate a section of the surface perpendicular to the surface and observe the sublayer directly.

A central question is how the bubble actually collapses the temperature gradient in the sublayer. Results in chapter 7 and their interpretation in chapter 8 suggest that it may be the turbulent wake of the bubble that is sufficient to break down the sublayer structure or perhaps to prevent re-establishment for a period of time after an opening has been created. This too can be observed with the proposed extension of the schlieren visualisation and high speed recording equipment.

As has been discussed in chapter 8 the Rayleigh-Benard picture of the sublayer is inappropriate. It seems that the failure of the large scale fluid flows from the bulk of the liquid to entrain the sublayer, or for billows in the sublayer to break and collapse the temperature gradient, there must be a function of the local Richardson number in the sublayer. Measurements of the horizontal velocity in the sublayer to obtain values of the Richardson number will clarify many of the uncertainties that have been discussed and the development of the laser-doppler anemometry system described in chapter 6 facilitate these measurements.

Turbulence Generation on Mixing

We know that the sublayer can be destroyed and, perhaps, modified in structure. The extension of our question to stratified systems then becomes: Can the conditions required to affect the sublayer be generated from mixing processes deep in the bulk of the liquid or from boundary layer penetrations at the liquid-liquid interface? It is clear that fluid flows generated from the mixing process at the liquid-liquid interface will have maximal effect at the surface sublayer if the densities of the layers are nearly equal and the plumes and thermals from the lower layer rise in an ambient density close to their own. The required investigations in the future are clearly to more marginally stable stratification. The technique of layer formation that has been developed is clearly adequate to form layers with only marginal differences in composition. The magnitude and nature of the heat inleak into the lower must be sufficiently slow so as not to perturb the interface into mixing at high stabilities. Clearly high boundary layer flows at the wall will induce mixing and should be minimised to observe the behaviour of the liquid-liquid interface close to marginal stability.

The proposed modified schlieren technique may also be used to observe the dynamics of the temperature gradient in the liquid-liquid interface as the resolution required precludes the use of microthermocouples.

ON HANDLING STRATIFIED LNG TANKS

The observed simulations in this study have not reproduced the effects seen at La Spezia but do demonstrate the danger of stratified LNG. Until further experiments reveal alternative mechanisms for superheat dumping, there remain the observations on the capability of vapour bubbles to rapidly destroy stratification. Faced with a potentially dangerous stratified LNG tank there are actions that could cause dumping of the total superheat of the tank contents with catastrophic results. Any attempt to introduce a submerged mixing device may promote nucleate boiling with consequent EVG and must be considered highly hazardous.

It has been seen that mixing of stratified layers can be achieved in a controlled manner without excess vapour generation of great magnitude through boundary layer penetration and mixing. This effect can be exploited if the boundary layer flow can be increased

locally on a small section of the tank circumference, to promote greater penetration into the upper layer. The boundary layer generated by wall heating has not caused rollover and catastrophic vapour generation on a short timescale. Therefore low flux wall mounted heaters near the base of the tank must be tested on a large scale with a view to inclusion as safety devices in LNG tanks. These heaters must not have the capacity to induce nucleate boiling and should be placed in the insulation space. A suitable heat flux to test would be a value equal to the basal heat flux. The success of boundary layer penetration in alleviating the stratification may be measured as the excess boiloff gas generated over the extra heat inleak due to the heaters.

REFERENCES

1 Chatterjee & Geist The effects of stratification on boil-off rates in LNG tanks. Pipeline & Gas Journal 199 40 (1972)

2 Germeles A model for LNG tank rollover. ACE 21 330 (1975)

3 Sarsten LNG stratification and rollover. Pipeline & Gas Journal 199 37 (1972)

4 Heestand, Shipman & Meader A predictive model for rollover in stratified LNG tanks. AICHE Journal 29 no 2 199-207 (1983)

5 Hashemi & Wesson Cut LNG storage costs. Hydrocarbon Process 117-120 (1971)

6 Atkinson, Beduz, Rebai & Scurlock Heat and evaporative mass transfer correlation at the liquid-vapour interface of cryogenic liquids Proc ICEC 10 (1984)

7 Sugawara, Kubota & Muraki Rollover test in LNG storage tank and simulation model. ACE (Colorado Springs) 29 805-811 (1983)

8 Chatterjee & Geist Spontaneous stratification in LNG tanks containing nitrogen. ASME Process Industries Division (1976)

9 Smith & Germeles LNG tank stratification consequent to filling procedures. Proc 4th INT. LNG conf. session IV paper 3 (1974)

10 Turner The Coupled Turbulent Transport of Salt and Heat Across a Sharp Density Interface. Int. J. Heat Trans. 8 759 (1965)

11 Turner Buoyancy effects in fluids. CUP (1973)

12 Bellus, Reveillard, Bonnaure & Chevalier. Essais au terminal de fos sur le comportment du LNG dans les grands reservoirs. LNG 5 paper 9 (1977)

13 Germeles Forced plumes and mixing of liquids in tanks. J. Fluid Mech. 71 Part 3 601-623 (1975)

14 Narusawa The problem of double-diffusive convection in large energy storage tanks. (1982)

15 Von Vilhelm Pruger Zeitschr. f. Physik vol 115 p202 (1940)

16 Berg, Acrivos & Boudart Evaporative convection. Chem. Engng. 6 61-123 (1966)

17 Pearson J. Fluid Mech. 4,225 (1958)

18 Nield J. Fluid Mech. 19,341 (1964)

19 Rebai, Rest & Scurlock Nature (1984)

20 Berg & Acrivos Chem. Eng. Sci. 20,737 (1965)

21 Berg PhD Dissertation University of California, Berkeley, Ca (1964)

22 Veronis On finite-amplitude instability in thermohaline convec tion. J. Mar. Res. 23,1 1-17 (1965)

23 Stern Tellus (1960)

24 Pellew & Southwell On maintained convective motion in a fluid heated from below. (1940)

25 Lorenz Deterministic nonperiodic flow. J Atmos Sci 20 130-141 (1963)

26 Moore, Toomre, Knobloch & Weiss Period-doubling and chaos in partial differential equations for thermosolutal convection. Nature 303 663-667 (1983)

27 Veronis Effect of a stabilising gradient of solute on thermal convection. J. Fluid Mech. 34 315-336 (1968)

28 Baines & Gill On thermohaline convection with linear gradients. J. Fluid Mech. 37 289-306 (1969)

29 Huppert. On the Stability of a Series of Double-Diffusive Layers. Deep-Sea Res. 18, 1005 (1971)

30 Goroff An experiment on heat transfer by overstable and ordinairy convection. Proc. Roy. Soc. A 254,537 (1960)

31 Takao & Narusawa Int. J. Heat & Mass Trans. 23, 1283 (1980)

32 Takao & Suzuki Prediction of LNG rollover. Gastech s6 p8 (1982)

33 Turner Int. J. Heat & Mass Trans 8,759 (1965)

34 Griffis & Smith Numerical & Physical Experiments in Double-Diffusive Convection: A lateral heat flux imposed on a vertical concentration gradient. NTIS PB80-205339 (1979)

35 Narusawa & Suzukawa Experimental study of double-diffusive convection due to uniform lateral heat flux. J. Fluid Mech. 113,387 (1981)

36 Nakano, Sugawara & Yamagata An experimental study on the mixing of stratified layers using liquified freon. Gastech (1982)

37 Cromwell T. Pycnoclines created by mixing in an aquarium tank. J. Mar. Res. 18, 73 (1960)

38 Turner The influence of molecular diffusivity on turbulent entrainment across a density interface. J. Fluid Mech. 33, 639 (1968)

39 Grigg & Stewart Turbulent diffusion in a stratified fluid. J. Fluid Mech. 15,174 (1963)

40 Long A theory of mixing in a stably stratified fluid. J. Fluid Mech. 84 113 (1978)

41 Fernando & Long On the nature of the entrainment interface of a two-layer fluid subjected to zero mean-shear turbulence. J. Fluid Mech. 151 21-53 (1985)

42 Wolanski & Brush Turbulent entrainment across stable density step structures. Tellus 27,259 (1975)

43 Dickinson & Long Oscillating-grid turbulence including effects of rotation. J. Fluid Mech. 126,315 (1983)

44 Baines & Turner Turbulent buoyant convection from a source in a confined region. J. Fluid Mech. 37,51 (1969)

45 Morton, Taylor & Turner Turbulent gravitational convection from maintained and instantaneous sources. Proc. R. Soc. A 234 1.1- 23 (1956)

46 Morton Forced plumes. J. Fluid Mech. 5 151-163 (1959)

47 Gebhart Heat Transfer. Tata McGraw-Hill (1971)

48 Beresford PhD Thesis, University of Southampton (1984)

49 Atkinson & Scurlock Cryogenics 25,7,393 (1985)

50 Maher & Vangelder Rollover and thermal overfill in flat bottom LNG tanks. Pipeline & Gas Journal 199 46-48 (1972)

51 Liang, Vidal & Acrivos Buoyancy-driven Convection in Cylindrical Geometries. J. Fluid Mech. 36 part 2 239 (1969)

52 Mani & Venart Proc. Int. Conf. LNG, London(1969),p171

53 Landau and Lifshitz, Fluid Mechanics. Pergamon Press 1987

54 Davies, Turbulence Phenomena. Academic Press 1972

55 Rayleigh, On convection currents in a horizontal layer of fluid when the higher temperature is on the under side. Phil. Mag (6) 32, 529-546 (1916)

56 Beduz, Rebiai & Scurlock. Thermal overfill and the surface vapourisation of cryogenic liquids under storage conditions. Advances in Cryogenic Engineering, vol 29 pp795 (1984)

57 Howard. Convection at high Rayleigh number. Proc. 11th Int. Cong. & App. Mech. Berlin (1964) pp1109-1115

58 Foster. Intermittent convection. Geophysical Fluid Dynamics. v2 (1971) pp201-217

59 Ahlers. Low temperature studies of the Rayleigh-Benard instability and turbulence. Phys. Rev. Lett. 33,1185

60 Koschmeider. Benard convection. Adv. Chem. Phys. 26,177-212

61 Prandtl. Essentials of fluid dynamics. London Blackie (1952)

62 Weyl. Analysis of optical methods (in Physical measurements in gas dynamics and combustion - Ladenburg, ed.) Princeton Univ. Press (1954)

63 Rebai. PhD Thesis, Southampton University (1985)

ACKNOWLEDGEMENTS

I am indebted to British Gas for a CASE award and to the S.E.R.C for a postgraduate grant which supported this research.

I wish to extend to all the members of the Institute of Cryogenics, past and present, my thanks for their help, their suggestions and, most of all for their friendship. In particular I wish to offer my special thanks to Dr Carlo Beduz, friend and colleague, and hope that we may have the opportunity to work together again.

May I thank Adrian Pickering for his hospitality, help and fellowship especially during the preparation of this thesis.

Professor R Scurlock has created a centre of research which is productive and encourages the best traditions of scientific work. This should be a sufficient accolade but in this case I wish to add my congratulations for more than this. The Institute is also a most enjoyable place to study. Professor Scurlock leads by example, encourages and guides us all. I am in his debt.

APPENDIX I

THE LIQUID NATURAL GAS STORAGE TANK

Tables 1,2 and figs 1, 2 give dimensions, structure and operating characteristics for typical LNG storage tanks. The figures show an 8000 m^3 (4000 ton) tank; included with the heat flux and flow data are values for a 50000m^3 vessel.

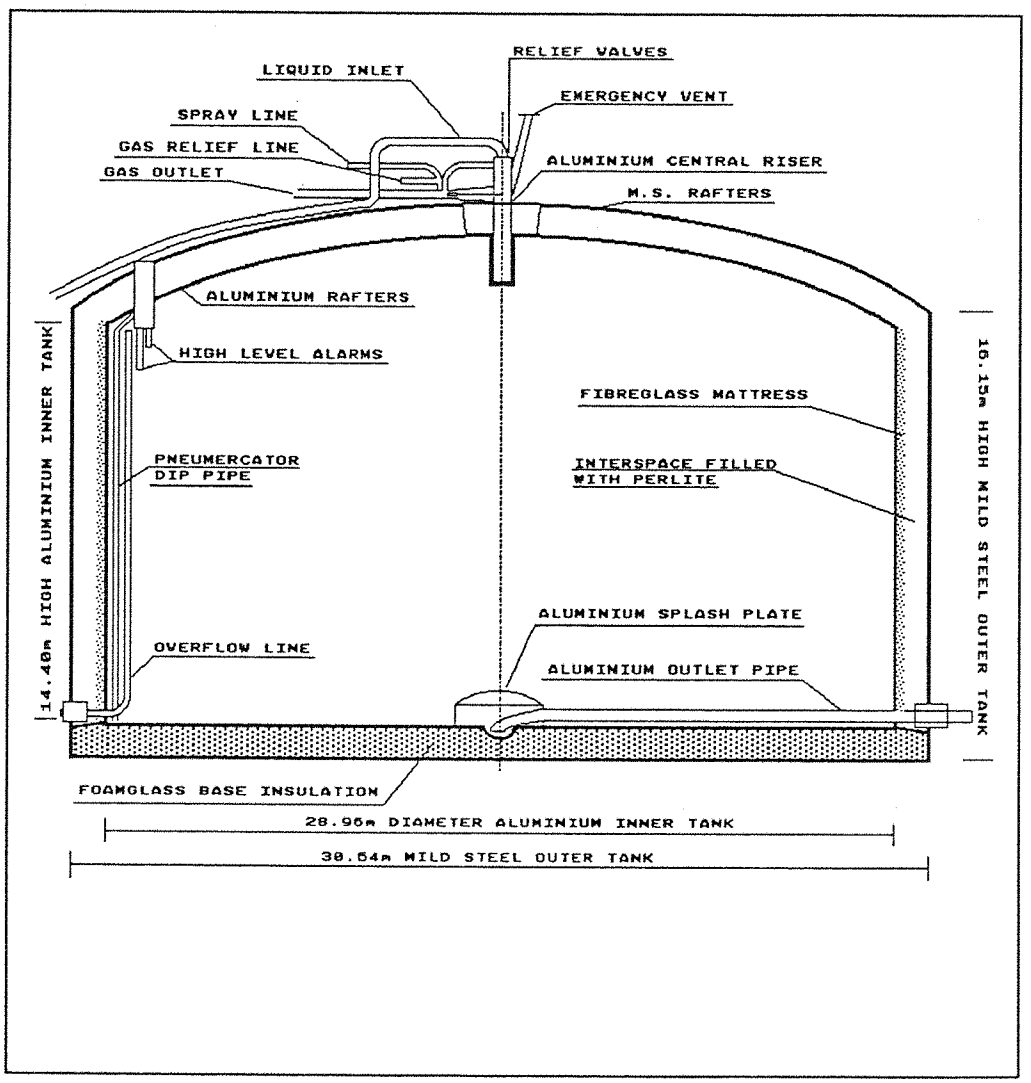

Fig. 48 4000 TON LNG Storage Tank

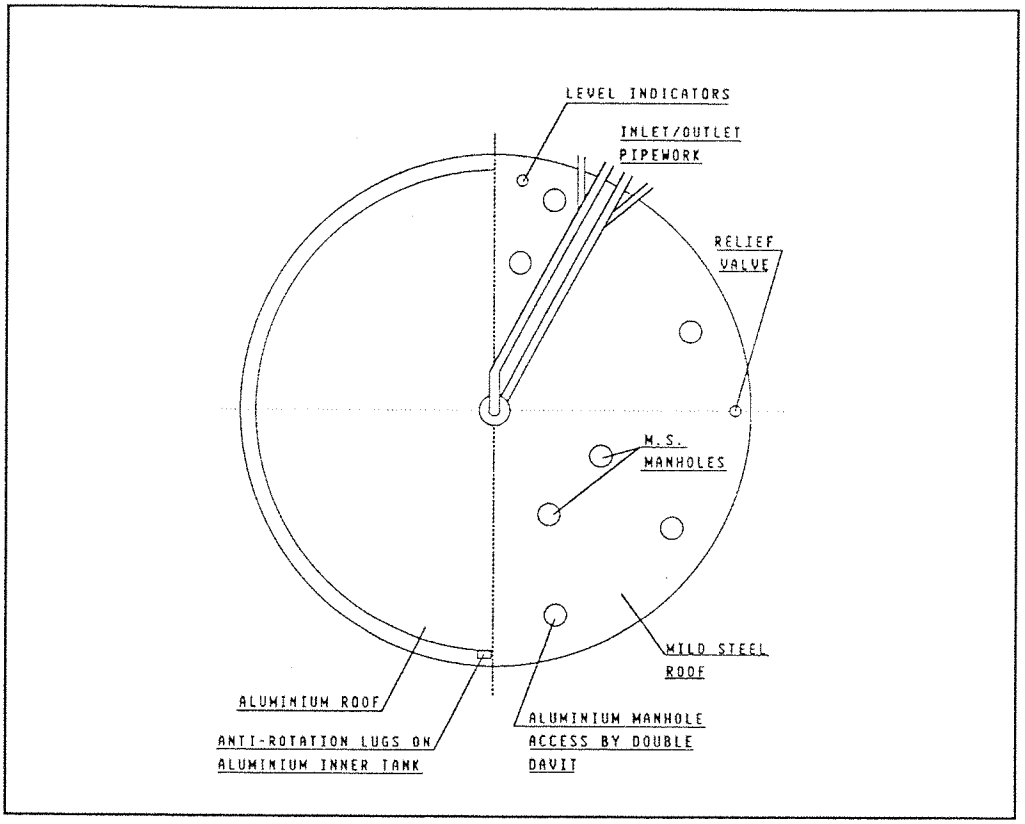

Fig. 49 Plan view of 4000 TON LNG Storage Tank

8000 cu m (4000 TON) tank filled to operational maximum level		
	heat flux (W/m^2)	heat flow (kW)
Base	15.3	10.0
Sidewall (liquid)	6.7	7.4
Sidewall (vapour)	5.2	1.0
Top Dome	3.3	2.3
Total		20.7

Table. 6 $8000m^3$ 4000 TON tank

50000 cu m tank filled to operational maximum level		
	heat flux (W/m^2)	heat flow (kW)
Base	13.0	22.0
Sidewall (liquid)	2.8	12.0
Sidewall (vapour)	2.7	0.5
Top Suspended Deck	5.7	9.4
Total		43.9

Table. 7 50000 m^3 tank

In addition to the equilibrium boiloff of gases there are non-equilibrium conditions which lead to changes in vapour evolution.

- Vapour may be displaced by addition of liquid.
- Liquid being added to the tank flashes as it falls to the tank pressure.
- Boiling of liquid as it enters a warm tank and this is rare unless the tank is nearly empty.
- Boiling caused by compositional differences between the cargo being added to the tank and an existing heel particularly when the cargo has a higher nitrogen content.
- Addition of a cargo of differing composition leading to a stratified load with the subsequent depression of boiloff.
- The mixing of a stratified system where layers away from the free surface are warmer and a have a higher density for compositional reasons. This is termed 'rollover'.

The potential for stratification increases in situations where the cargo is of different composition and where there is a high fill rate, for example whilst ship unloading. Peak shaving plants are less prone to layer formation as the tank is filled at a slow rate with a liquid of uniform composition. If the tank and feed LNG do differ it is now recommended practice to bottom fill the lighter feed and top fill the heavier. Figures 1 and 2 show an older tank without this capability.

LIQUID NATURAL GAS

LNG is primarily methane but it is a mixture. The composition varies according to the origin of the feed gas. The feed gas will also contain a number of less volatile components which have to be removed before liquefaction to avoid blockages in heat exchangers and other equipment by the separation of insoluble solids. The conditioning of the feed gas removes water, methanol, CO_2, odorants, H_2S and heavy hydrocarbons. In tables 9 - 11 the compositions and properties of some typical liquefied natural gases in use in Britain are listed.

	Methane	North Sea	Algerian	Libyan
Average Mol Wt.	16.04	16.41	18.52	22.87
Bubble Point K	111.6	110.6	111.9	112.2
Density at Bubble Point kg/m^3	422.4	431.6	468.7	533.5

Table. 8 LNG properties

	Methane	North Sea	Algerian	Libyan
N_2		0.5	0.36	0.9
CH_4	100.0	97.5	87.2	70.0
C_2H_6		1.8	8.61	15.0
C_3H_8		0.2	2.74	10.0
iso-C_4H_{10}			0.42	1.4
n-C_4H_{10}			0.65	2.1
C_5H_{12}+			0.02	0.6
Total	100.0	100.0	100.0	100.0

Table. 9 Composition of LNGs by %mol

Natural gas at 15 C 1013.25 mbar. Liquid at bubble point.				
	Methane	North Sea	Algerian	Libyan
Specific gravity gas relative to dry air	0.5547	0.5675	0.6410	0.7927
Vol Gas/Vol Liquid	621.4	621	597	549
Heat of Vapourisation kJ/kg	890.1	885.1	894.6	916.5

Table. 10 Natural gas properties

Boiloff Gas in equilibrium with LNG at Bubble Point 1013.25 mbar				
	Methane	North Sea	Algerian	Libyan
Nitrogen in boiloff %mol	0	9.6	8.2	21.8
Av Mol Wt. of boiloff	16.04	17.19	17.02	18.65
Density of boiloff	0.680	0.728	0.721	0.790

Table 11. Boiloff gases

The data was chosen to show the range of property values over the differing feed gas stocks. It can be seen that there are contexts where it is appropriate to consider LNG as pure methane and, conversely, where the composition of the mixture must be taken into account. In particular the molar percentage of nitrogen in the boiloff should be noted. The implications of this are discussed in the next section.

NITROGEN-RICH LNG

A high concentration of nitrogen in LNG complicates the preventive handling of potential stratification when loading cargo into a storage tank.

As can be seen in table 11 the boiloff gas from nitrogen-bearing LNG is rich in nitrogen as the most volatile component. As the LNG weathers the remaining LNG becomes less dense than the original load. High nitrogen fill added to an existing heel of originally identical LNG should therefore be top filled to induce mixing. This is particularly a problem in peak-shaving plants where the calorific value is diluted with nitrogen to provide the customer with a uniform product forcing a high nitrogen heel and feed. To avoid stratification the correct filling procedure is always to bottom fill with lighter feed and vice versa.

When fill is added there will be vapour generated as the high pressure liquid flashes to tank pressure. When the fill is richer in N_2 there is additional vapour as equilibrium is established between the mole fraction of nitrogen in the vapour and in the liquid. Over a long period of time the total vapour generated is the same whether the load mixes immediately or forms a layer but the maximum vapour evolution rate will differ depending on the mechanism by which the layer mixes into the bulk. If there is no mixing and a layer is formed there will be vapour evolution during filling and then further evolution as mixing or 'rollover' takes place. If mixing is done as filling is taking place there will be increased boiloff over an extended period of time as equilibrium is reached between the bulk and the vapour.

High-N_2 in a well mixed tank leads to the further potential problem of spontaneous stratification. As the warmed bulk liquid rises to the surface in the boundary-layer flow it flashes at the surface. In low-N_2 LNG the result is that the flashed portion is then more

dense and sinks into the bulk where it mixes. In contrast a high-N_2 LNG will become less dense as a result of flashing at the surface and the flashed liquid can remain at the surface giving rise to a surface layer. The density gradient at the liquid/liquid interface so formed may then be sufficient to suppress convective heat transfer across the interface and lead to a further superheating of the bulk and the conditions for 'rollover'.

PROPERTIES OF CRYOGENS

The properties of the cryogens used in this study are listed below

Fluid	Specific Heat C_p (kJ/kg K)	Viscosity μ (μPa s)	Thermal conductivity (mW/m K)	Prandtl number	Surface tension (mN/m)
Helium	4.48	3.563	27.2	0.587	0.093
Nitrogen	2.051	158	139.6	2.32	8.75
Argon	1.136	252	123.2	2.32	11.08
Methane	3.451	118	193.1	2.11	14.1
Oxygen	1.695	190	151.4	2.13	13.2

Table 12. Cryogenic liquid properties at saturation

Table 13shows fluid properties of liquids used in this study at saturation.

Fluid	Boiling Point at 1 atm (K)	Saturated Liquid Density (Kg/l)	Saturated Vapour Density (Kg/l)	Heat of Vapourisation (kJ/Kg	Critical Temp (K)	Critical Pressure (atm)	Critical Density (Kg/l)
Helium	4.2	0.125	0.0169	20.9	5.2	2.24	0.0697
Nitrogen	77.3	0.809	0.00461	199.0	126.2	33.6	0.3140
Argon	87.3	1.394	0.00577	162.0	150.8	48.0	0.5360
Methane	111.6	0.423	0.00181	512.0	190.6	46.0	0.1620
Oxygen	90.2	1.142	0.00448	213.0	154.6	49.8	0.4360

Table 13. Properties of selected cryogens

APPENDIX II

Paper 1. Presented at the International Cryogenic Engineering Conference, Helsinki August 1984[1].

Paper 2. Published in Cryogenics v25 pp393 July 1985

Paper 3. Presented at the International Cryogenic Engineering Conference, Berlin April 1986

1 A film of the schlieren results was included in the presentation.

The following published papers were included in the bound thesis. These have not been digitised due to copyright restrictions, but the links are provided.

M.C.M. Atkinson, C. Beduz, R.Rebiai and R.G. Scurlock (1984) "HEAT AND EVAPORATIVE MASS TRANSFER CORRELATION AT THE LIQUID-VAPOUR INTERFACE OF CRYOGENIC LIQUIDS." Presented at the International Cryogenic Engineering Conference, Helsinki August 1984.

https://doi.org/10.1016/0011-2275(85)90007-4

T.Agbabi, M.C.M.Atkinson, C.Beduz and R.G.Scurlock (1986) "CONVECTION PROCESSES DURING HEAT AND MASS TRANSFER ACROSS LIQUID/VAPOUR AND LIQUID/LIQUID INTERFACES IN CRYOGENIC SYSTEMS." Presented at the International Cryogenic Engineering Conference Berlin April 1986.